QUALITY OF THE JURASSIC-CRETACEOUS MIST MOUNTAIN FORMATION COALS, SOUTHERN CANADIAN CORDILLERA: RELATIONSHIPS TO SEDIMENTOLOGY AND COALBED METHANE POTENTIAL

by

SARAH JANE VESSEY

B.Sc. (Hons.), University of Canterbury, 1995

A THESIS SUBMITTED IN PARTIAL FULFILLMENT OF
THE REQUIREMENTS FOR THE DEGREE OF
MASTER OF SCIENCE

in

THE FACULTY OF GRADUATE STUDIES
Department of Earth and Ocean Sciences

We accept this thesis as conforming
to the required standard

THE UNIVERSITY OF BRITISH COLUMBIA

August 1998

In presenting this thesis in partial fulfilment of the requirements for an advanced degree at the University of British Columbia, I agree that the Library shall make it freely available for reference and study. I further agree that permission for extensive copying of this thesis for scholarly purposes may be granted by the head of my department or by his or her representatives. It is understood that copying or publication of this thesis for financial gain shall not be allowed without my written permission.

Department of Earth & Ocean Sciences

The University of British Columbia
Vancouver, Canada

Date 25 August 1998

DE-6 (2/88)

ABSTRACT

A detailed investigation of the Jurassic-Cretaceous Mist Mountain Formation in the southern Canadian Cordillera was undertaken to determine what, if any relationships exist between coal quality parameters, stratigraphic stacking, depositional environment and coalbed methane potential. In the Line Creek area, a shift in depositional environment within the Mist Mountain Formation is recorded as a change in abundance and lateral continuity of lithofacies. The lower part of the formation was deposited in an interdeltaic coastal plain environment and is typified by alternation of laterally extensive coal seams and thick, widespread channel sandstones. In the upper Mist Mountain Formation, channel sandstones are replaced by an increasing abundance of thin coal seams, floodplain and crevasse splay facies sediments. The upper unit was deposited in a distal alluvial-fluvial floodplain environment.

Coal seam geometry and quality data indicate that Mist Mountain Formation peat mires were not directly influenced by contemporaneous clastic sedimentation. The geometry of coal seams reflects the proximity of under- and overlying channel sandstones, but ash content and mineralogy of the coal do not parallel changes in thickness, proximity or composition of surrounding clastic sediments. Examination of lower unit characteristics suggests that peat mires developed only during breaks in clastic deposition; the upper unit coal appears to have formed in domed mires, raised above active clastic sedimentation.

Mist Mountain Formation coals are of suitable rank and composition to host significant coalbed methane reserves, but exploration to date indicates only limited volumes of gas. The coal is commonly sheared and oxidised, features which generally enhance the permeability of coal, yet the effect of these factors on coalbed methane potential is not understood. Results from this investigation indicate greater volumes of methane are adsorbed with increasing vitrinite content in the Mist Mountain Formation coals. Additionally, oxidised coals have decreased methane adsorption capacity. The effects of maceral composition and oxidation on methane adsorption overshadow the effect of shearing. Groundwater is likely to travel preferentially through sheared and oxidised coal due to increased permeability, facilitating

methane desorption and escape from the coal. It is probable that a combination of decreased adsorption due to oxidation and leakage of methane from sheared and oxidised zones account for the low volumes of methane in Mist Mountain Formation coals.

TABLE OF CONTENTS

LIST OF FIGURES

LIST OF TABLES

ACKNOWLEDGEMENTS

This research would not have been possible without the support, help and patience of a number of people. Firstly, my deepest thanks to my supervisor, Dr. Marc Bustin for his guidance, advice and sense of humour throughout my time at The University of British Columbia. Thanks also to my supervisory committee, Dr. Kurt Grimm and Dr. Paul Smith for their interest and suggestions.

Access to all data and outcrop was provided by Line Creek Resources Limited. The staff at Line Creek were extremely helpful and accommodating throughout my research, but I especially want to thank Ted Hannah for giving so freely of his time and his excellent advice and patience. Thanks also to Lynn Taylor of the Elkview Coal Corporation, for arranging access to Elkview Mine and answering my numerous questions. Special thanks to Barry Ryan of the B.C. Geological Survey, for his help in getting me started on my research, and especially for critically reviewing my thesis.

Financial support for my research was provided by the UBC Department of Earth and Ocean Sciences, The Geological Society of America, and the Natural Sciences and Engineering Research Council of Canada. Many thanks to the UBC geology staff and technicians for their support and sample preparation, often at short notice. Thanks also to Mati Raudsepp for his help on the SEM. A number of students assisted me in the field and laboratory and put up with my "kiwisms" including Jayna Houston, Leslie Zednai, and Taby Alvandkoohi. Discussions with Raphael Wust were very helpful and his assistance with XRD analyses is much appreciated.

Finally, I'd like to extend my deepest gratitude to my husband, James Pope, without whose undivided support, encouragement and assistance this thesis would never have eventuated.

Chapter 1

Introduction.

Chapter 1

Introduction.

1.1. – INTRODUCTION

Coal quality parameters such as seam geometry, maceral composition, ash content and mineralogy determine the mineability and utility of a coal. Knowledge of how these parameters can be expected to vary with changes in clastic sedimentology is useful in both coal exploration and mining. Variation in coal quality parameters is commonly believed to reflect changes in depositional environment during peat accumulation and has been used to construct depositional models for ancient coal deposits. Post-depositional processes such as deformation and oxidation also influence coal quality and therefore are important parameters in determining coal utilisation.

Two aspects of coal quality in the Late Jurassic-Early Cretaceous Mist Mountain Formation of the southern Canadian Cordillera are investigated in this thesis. Chapter 2 attempts to relate coal quality to stratigraphic stacking and depositional environment of the Mist Mountain Formation and examines the applicability of depositional models. Chapter 3 investigates the effect of maceral composition, shearing and oxidation on the ability of coal to adsorb and retain economic quantities of methane. It is hoped that this study will lead to improved understanding of the causes and effects of variation in coal quality.

1.2. – THE EFFECT OF SEDIMENTOLOGY AND DEPOSITIONAL ENVIRONMENT ON COAL QUALITY

Coal has been identified with sediments from most terrestrial depositional environments in both ancient and modern settings. However, almost all economic coal deposits are found in association with meandering river, deltaic and shoreline depositional environments (McCabe, 1987). Many depositional models of coal-bearing strata are based on Fisk's (1960) work on modern Mississippi delta sediments. In such depositional models, peat mires are envisaged to form in close proximity to active fluvial and deltaic sedimentation and are influenced by local clastic sedimentation. The geometry and quality of coal seams is therefore commonly expected to reflect the proximity of peat mires to active clastic sedimentation at the time of accumulation.

McCabe (1984) was among the first to question the validity of the early depositional models for coal-bearing strata. He proposed that thick, low ash coal is only likely to accumulate in areas removed from active clastic sedimentation, either in domed mires raised above clastic activity or during a hiatus in clastic sedimentation. Despite McCabe's arguments (1984, 1987, 1991), much modern literature still accepts that economic coal may accumulate in close proximity to active clastic sedimentation.

Numerous studies have examined relationships between coal measure sedimentology and coal quality parameters and correlated these relationships to depositional environment. Relationships between coal seam geometry and sedimentology are well documented (for example: Flores, 1981; Weisenfluh and Ferm, 1984; Ferm and Staub, 1984; Levey, 1985; and Kirschbaum and McCabe, 1992). However, evidence for sedimentological control on coal quality parameters, especially ash content is commonly lacking and relationships are often inferred by association rather than confirmed by direct systematic observation (for example: Horne et. al., 1978).

With conflicting ideas in the literature (Fisk's versus McCabe's depositional models), associations between coal quality and clastic sedimentology need to be re-examined. Relationships between these two parameters need to be established, and if present, variation with changing depositional environments must be documented. If relationships between coal quality and clastic sedimentology are not present, many of the basic assumptions made by geologists will need to be revised, and many coal deposits re-interpreted.

A shift in depositional environment in the Mist Mountain Formation is accompanied by changes in coal quality and geometry, lateral continuity and abundance of lithofacies. This variation means the Mist Mountain Formation stratum are ideal to investigate relationships between coal quality, sedimentology and depositional environment.

1.3. – THE EFFECT OF COAL QUALITY ON COALBED METHANE POTENTIAL

Not only is coal a potential source of natural gas, it also acts as a reservoir because gas can adsorb to the large internal surface area of coal. Gas is produced during the thermal and biogeochemical alteration of coal and may be present in economic quantities depending on features such as thickness, current depth of burial and rank of the coal (Rightmire, 1984). Since the early 1980's there has been interest in coalbed methane (CBM) as an economically viable, alternative source of natural gas. Interest in the CBM potential of the Mist Mountain Formation coals quickly developed as production increased in the USA. Despite its apparent suitability as a CBM reservoir, preliminary investigations indicate that the Mist Mountain Formation contains only limited CBM resources (Dawson and Clow, 1992).

Mist Mountain Formation coal is commonly sheared and oxidised, but the effect of these features on methane adsorption and retention is unknown. Shearing and oxidation can be related to the quality of the coal; sheared coal commonly has a high ash content and will oxidise more rapidly than unsheared coal (Bustin, 1982); in addition, oxidation decreases the coking ability of coal. Feng et. al. (1984) noted that

sheared coal releases more methane at a faster rate than unsheared coal. Subsequent work has failed to follow up these results and it remains unclear if Mist Mountain Formation coal has low coalbed methane content because shearing and oxidation reduce the adsorption potential of the coal or other factors. Shearing and oxidation may also enhance methane leakage from the coal. Establishing the cause of the low methane content in Mist Mountain Formation coal has obvious economic implications that could be applied to other low gas coal around the world.

1.4. – STRUCTURE OF THE THESIS

This thesis is presented as two stand-alone papers, which may be read without reference to preceding chapters. Chapter two investigates relationships between coal quality parameters and sedimentology. The primary objectives of this chapter are to:

a) document lateral and vertical variation in facies and coal quality parameters such as seam geometry, thickness, ash content and mineralogy, sulphur content and maceral composition of the coal;
b) interpret sedimentological factors influencing those quality parameters mentioned above and;
c) determine the depositional environment of the Mist Mountain Formation coal and if possible, relate quality parameters to depositional controls.

Chapter three investigates the gas adsorption capacity of the Mist Mountain Formation coal. Specifically this chapter:

a) compares the effect of maceral composition, shearing and oxidation on the gas adsorption capacity of coal and;
b) determines if shearing and oxidation affect the methane adsorption capacity of the coal enough to account for low volumes of gas encountered in the Mist Mountain Formation.

By combining investigations of coal quality and coalbed methane potential of the Mist Mountain Formation, a better understanding of factors influencing the mineability and quality of the coal will be obtained.

1.5. – REFERENCES CITED

Bustin, R.M. 1982, The effect of shearing on the quality of some coals in the Southeastern Canadian Cordillera: CIM Bulletin, v. 75, p. 76-83.

Dawson, F.M. and Clow, J.T. 1992, Coalbed methane research: Elk Valley Coalfield, In the Canadian Coal and Coalbed methane Geoscience forum: Parksville, BC, p. 57-71.

Feng, K.K., Cheng, K.C. and Augsten, R. 1984, Preliminary evaluation of the methane production potential of coal seams at Greenhills Mine, Elkford, British Columbia: CIM Bulletin, v. 77, p. 56-61.

Ferm, J.C. and Staub, J.R. 1984, Depositional controls of mineable coal bodies, *in* Rahmani, R.A. and Flores, R.M. eds. Sedimentology of coal and coal-bearing sequences, Volume 7: International Association of Sedimentologists Special Publication: Oxford, Blackwell Scientific Publications, p. 241-274.

Fisk, H.N. 1960, Recent Mississippi River sedimentation and peat accumulation, C.r.4 Congre l'avancement des etudes de stratigraphie et de geologie du Carbonifere, Volume 1: Heerlen, p. 187-199.

Flores, R.M. 1981, Coal deposition in fluvial paleoenvironments of the Paleocene Tongue River Member of the Fort Union Formation, Powder River area, Powder River Basin, Wyoming and Montana: SEPM Special Publication, v. 31, p. 169-190.

Horne, J.C., Ferm, J.C., Caruccio, F.T. and Baganz, B.P. 1978, Depositional models in coal exploration and mine planning in Appalachian region: AAPG Bulletin, v. 62, p. 2379-2411.

Kirschbaum, M.A. and McCabe, P.J. 1992, Controls on the accumulation of coal and on the development of anatomised fluvial systems on the Cretaceous Dakota Formation of southern Utah: Sedimentology, v. 39, p. 581-598.

Levey, R.A. 1985, Depositional model for understanding geometry of Cretaceous coals: major coal seams, Rock Springs Formation, Green River Basin, Wyoming: AAPG Bulletin, v. 69, p. 1359-1380.

McCabe, P.J. 1984, Depositional environments of coal and coal-bearing strata, *in* Rahmani, R.A. and Flores, R.M. eds. Sedimentology of coal and coal-bearing sequences, Volume 7, International Association of Sedimentologists Special Publication.

McCabe, P.J. 1987, Facies studies of coal and coal-bearing strata, *in* Scott, A.C. ed. Coal and coal-bearing strata: recent advances, Geological Society Spec. Pub. 32, p. 51-66.

McCabe, P.J. 1991, Geology of coal; Environments of deposition, in Gluskoter, H.J., Rice, D.D. and Taylor, R.B. eds. Economic Geology, Boulder, Colorado, Geological Society of America, The Geology of North America, v. P-2.

Rightmire, C.T. 1984, Coalbed methane resources, *in* Rightmire, C.T. Eddy, G.E., and Kirr, J.N. eds. Coalbed methane resources of the United States, Volume 17, AAPG studies in geology series, p. 1-13.

Weisenfluh, G.A. and Ferm, J.C. 1984, Geological controls on deposition of the Pratt seam, Black Warrior Basin, Alabama, USA, *in* Rahmani, R.A. and Flores, R.M. eds. Sedimentology of coal and coal-bearing sequences, Volume 7, Special publication of the International Association of Sedimentologists, p. 317-330.

Chapter 2

Sedimentology of the Coal-bearing Mist Mountain Formation, Line Creek, Southern Canadian Cordillera: Relationships to Coal Quality.

Chapter 2

Sedimentology of the Coal-bearing Mist Mountain Formation, Line Creek, Southern Canadian Cordillera: Relationships to Coal Quality.

2.1. - ABSTRACT

A detailed sedimentological investigation of the Jurassic-Cretaceous Mist Mountain Formation in the southern Canadian Cordillera was undertaken to determine what, if any sedimentological factors control coal quality and seam geometry. In the Line Creek area, the Mist Mountain Formation is divisible into two units based on abundance and lateral continuity of facies. The lower unit consists of laterally extensive coal seams alternating with thick, widespread channel sandstones interspersed with crevasse splay and floodplain facies sediments. The lower unit was deposited in an interdeltaic coastal plain environment protected from marine incursion by beach ridge-dune sandstones of the underlying Morrissey Formation. The upper unit of the Mist Mountain Formation was deposited in a distal alluvial-fluvial floodplain environment and has similar facies as the lower unit. Coal seams and channel sandstones are less laterally continuous and thinner than their counterparts in the lower unit. Channel sandstones decrease in number and thickness up-section, and are replaced by an increasing abundance of coal seams, floodplain and crevasse splay facies sediments.

Seam geometry and ash data indicate that clastic sedimentation had only limited influence on peat (coal) accumulation in the Mist Mountain Formation. While the geometry of coal seams reflects the proximity of under- and overlying channel sandstones, neither ash content nor mineralogy of the coal reflects changes in thickness, proximity or composition of surrounding clastic sediments. The Mist Mountain Formation peat mires were thus not directly influenced by fluvial activity. Characteristics of the lower unit suggest peat mires developed only during breaks in clastic deposition, whereas upper unit coal appears to have formed in domed mires contemporaneous with clastic sedimentation. The vitrinite

content of the coal increases up section at the expense of semifusinite, reflecting an increase in the proportion of arborescent vegetation in the mire with time and a lower susceptibility to fires. The sedimentology of the Mist Mountain Formation can only be used to predict coal seam geometry and quality parameters on a regional scale because the peat mires developed away from the influence of clastic sedimentation.

2.2. - INTRODUCTION

The Mist Mountain Formation of the Jurassic-Cretaceous Kootenay Group is the major coal-bearing sequence of the southern Canadian Rocky Mountains containing up to 17 major and numerous minor coal seams. These coastal plain and fluvial sediments have been the focus of numerous stratigraphic and sedimentological studies due to economic interest in the high to low volatile bituminous coal (Gibson, 1985; Dunlop and Bustin, 1987; Grieve, 1989; Bustin and Dunlop, 1992; Grieve, 1993). Much of this work has been completed at a regional scale and little attempt has been made to predict either coal mineability or quality at the scale of mining operations.

Sedimentological studies of coal measures may be useful in prediction of coal seam geometry, thickness and quality. Notable early work includes Horne et. al. (1978), Flores (1981, 1983) and Levey (1985), who document relationships between sedimentology, coal distribution and coal seam geometry in the Appalachians, Montana and Wyoming. Although relationships between coal seam geometry and sedimentology are well documented, actual evidence for sedimentological control on coal quality parameters, especially ash content, is commonly lacking and relationships are often inferred rather than established. Geological data from the Mist Mountain Formation is sparse because outcrop is generally poor and detailed subsurface data limited to areas enclosed by mining and exploration leases. Hence, the Line Creek mine site in the Elk Valley Coalfield (Fig. 2.1) is an ideal location to investigate relationships between sedimentology, coal quality and mineability of coal.

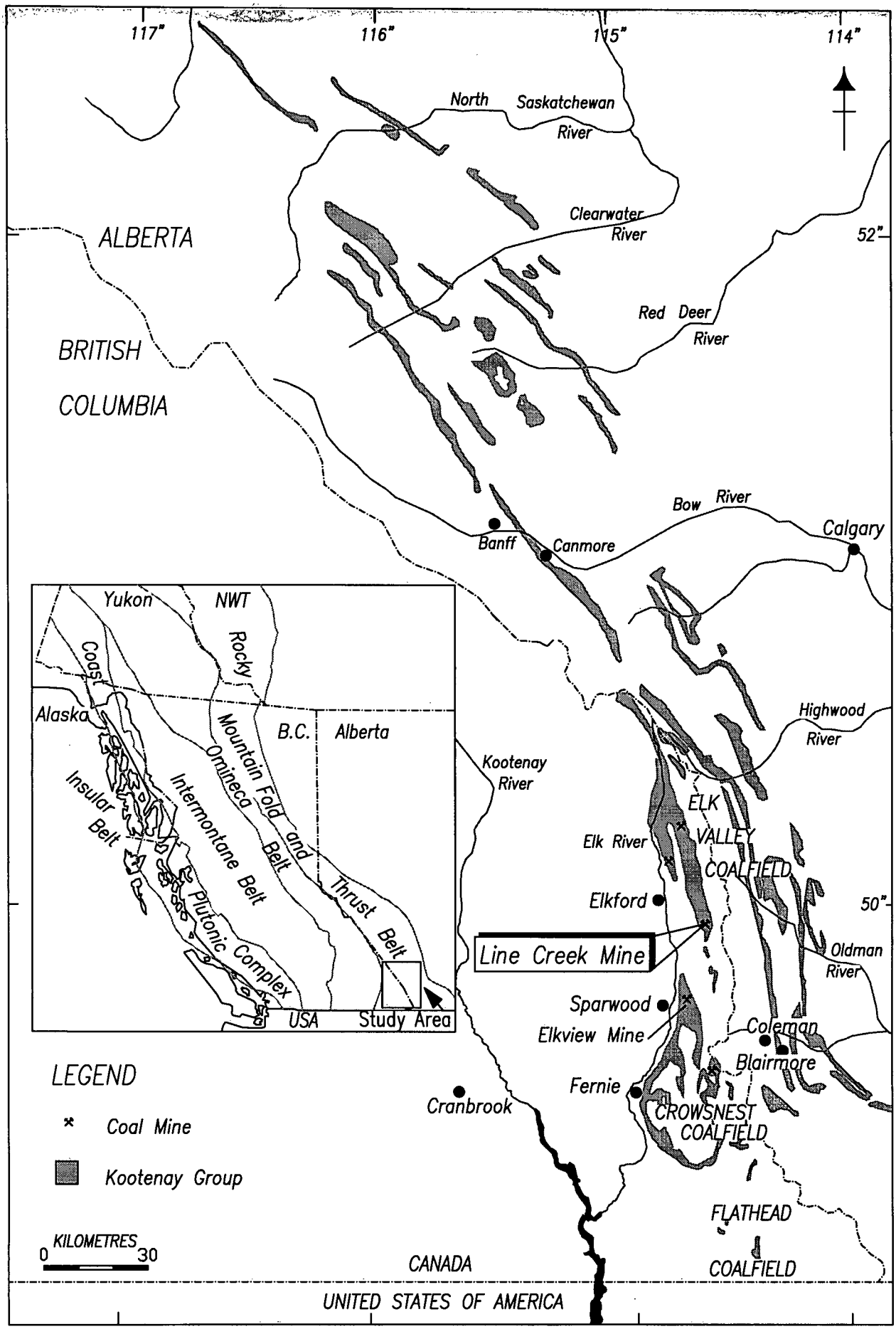

Figure 2.1 – Location map of the study area showing outcrop of the Kootenay Group (modifed from Gibson, 1985).

In this study, relationships between sedimentology and coal quality are examined with a view to determining the depositional factors influencing the geometry and quality of coal seams. In particular, this study:

a) documents facies associations within the Mist Mountain Formation;

b) investigates lateral and stratigraphic variation in coal seam geometry, ash content and mineralogy, sulphur content and maceral composition of major coal seams;

c) interprets sedimentological factors controlling coal seam geometry, ash content and mineralogy, sulphur content and maceral composition; and

d) interprets the original peat-forming environments of the coal and relates quality parameters to these depositional controls.

2.3. - PREVIOUS WORK

Dawson (1886) first described coal-bearing strata in southeastern British Columbia and southwestern Alberta and named the rocks the Kootanie Series. Economic interest in the coal in the early twentieth century led to a number of geological investigations of the region. Leach (1912) renamed the Kootanie Series the Kootenay Formation and Beach (1943) defined the thick lower sandstones of the Formation as the Moose Mountain Member. Newmarch (1953) named the upper sandstone rich strata the Elk Formation. Norris (1959) divided the Kootenay Formation into the Moose Mountain, Adanac, Hillcrest and Mutz Members. Gibson (1977; 1979) elevated the Kootenay Formation to Group status with three formations which in ascending order are the Morrissey Formation encompassing the Moose Mountain and underlying Weary Ridge Members, the Mist Mountain and Elk Formations. This classification is in current usage (Fig. 2.2).

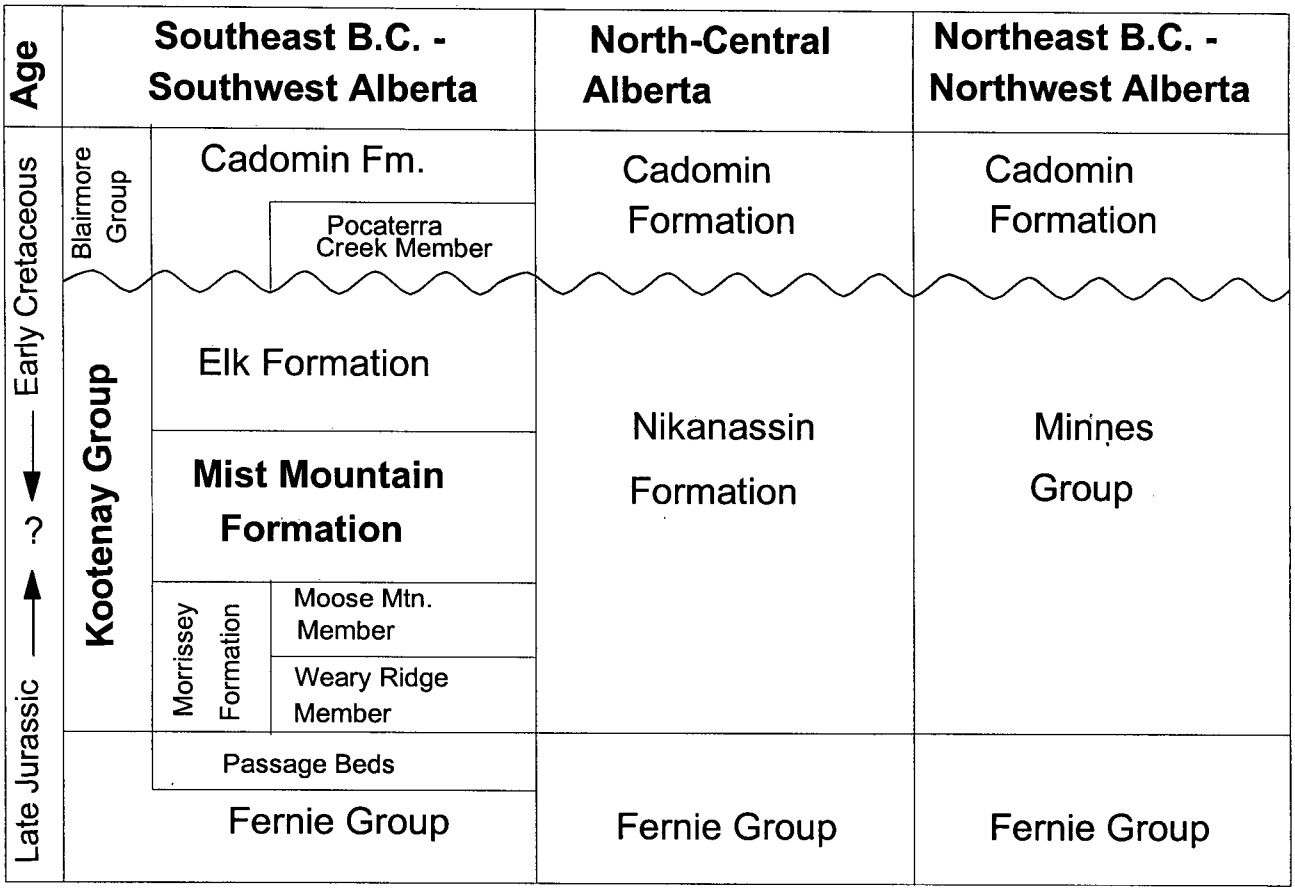

Figure 2.2 - Nomenclature of the Kootenay Group and its relationship to adjacent strata (modified from Gibson and Hughes, 1981).

More recent regional investigations of Mist Mountain Formation stratigraphy and depositional environments include Jansa (1972), Gibson & Hughes (1981), Gibson (1985), Hughes & Cameron (1985), Pearson & Grieve (1985) Grieve (1989) and Grieve (1993). On a local scale Donald (1984), Dunlop and Bustin (1987) and Bustin and Dunlop (1992) have completed stratigraphic and sedimentological studies in the Eagle Mountain region, north Elk Valley Coalfield. Cameron (1972) and more recently Mastalerz & Bustin (1997) have investigated petrology of Mist Mountain Formation coal.

2.4. - REGIONAL GEOLOGY

The Kootenay Group is a Late Jurassic-Early Cretaceous nonmarine sequence in the southeastern Canadian Cordillera. This group has been mapped throughout the Rocky Mountain Front Ranges and Foothills extending from approximately the United States border to the North Saskatchewan River (Fig. 2.1). Towards the north, the Kootenay Group grades laterally into the marine-nonmarine sediments of the Nikanassin Formation (Gibson, 1985).

Marine sandstones, siltstones and shales of the Late Jurassic Fernie Formation conformably underlie the Kootenay Group, whereas Early Cretaceous Cadomin Formation conglomerates and sandstones disconfomably overlie the Kootenay strata (Fig. 2.2; Gibson, 1985). The Kootenay Group thickens from an erosional eastern edge near Beaver Mines, Alberta to a maximum thickness of 1100 metres near Fernie, British Columbia.

Tectonic loading by thrust sheets and later sediment loading during the Columbian (Late Jurassic to Late Cretaceous) and Laramide (Late Cretaceous to Tertiary) orogenies caused deposition and subsequent deformation of clastic wedges in a foredeep that extended from Alaska to New Mexico (Stott, 1984). The Kootenay Group forms part of the oldest of three clastic wedges that make up this foredeep sequence. Deposition of the Kootenay and associated strata were the result of Late Jurassic uplift of the Omineca Crystalline belt (Fig. 2.1). Deposition was punctuated by several periods of regional regression and transgression. The Fernie Formation was deposited in an inland Fernie Sea (Fig. 2.3), and a major regression led to deposition of the Kootenay Group. Deposition occurred in an elongate trough, parallel to the rising Omineca Crystalline Belt and, later the rising thrust sheets of the Rocky Mountains (Stott, 1984). The Fernie Sea retreated to the north, resulting in northward progradation of the Kootenay Group into the marine-non-marine Nikanassin Formation.

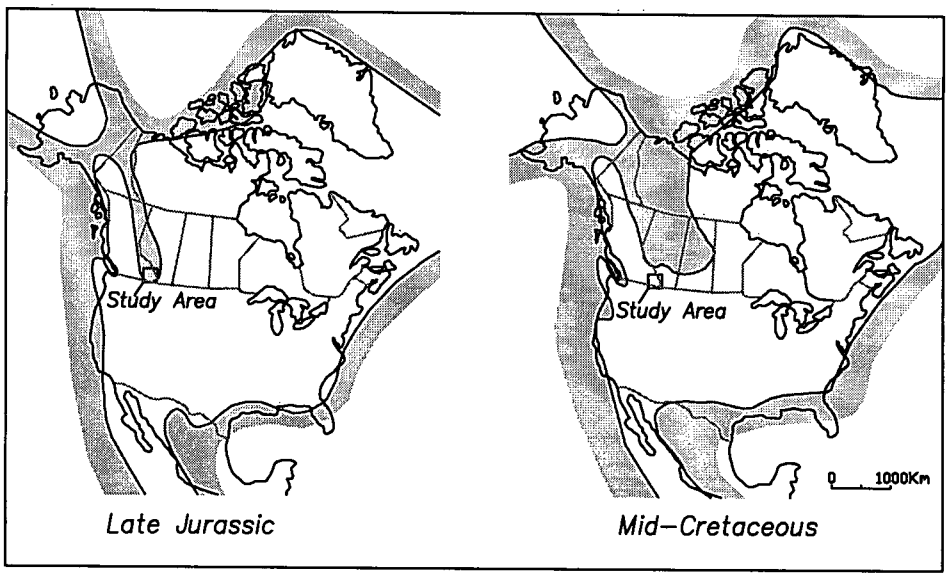

Figure 2.3 – Jurassic–Cretaceous seas of North America. Shading represents ancient ocean margins (modified from Bustin and Smith 1989).

During the Late Cretaceous-Tertiary Laramide Orogeny the Kootenay Group was compressed into broad, upright to overturned, concentric folds which are cut by thrust and tear faults as well as younger extensional faults (Bustin and Smith, 1993). Extensive shearing and structural thickening and thinning of coal seams are associated with this deformation.

The Mist Mountain Formation conformably overlies the Moose Mountain Member of the Morrissey Formation (Fig. 2.4). The Moose Mountain Member is interpreted as backshore, beach-ridge and dune deposits of a wave dominated delta (Gibson & Hughes, 1981; Gibson, 1985; Hughes & Cameron, 1985; Dunlop & Bustin, 1987). The lower part of the Mist Mountain Formation has been interpreted as a delta-interdeltaic coastal plain deposit and the upper part as an upper delta-alluvial plain deposit (Dunlop & Bustin, 1987). Alluvial fan-braided plain deposits of the Elk Formation conformably overlie the Mist Mountain Formation (Gibson, 1985). The contact between the Morrissey and Mist Mountain Formations is placed between the resistant quartzose sandstones of the Moose Mountain Member and the recessive coal bearing strata of the Mist Mountain Formation (Gibson, 1985). The contact between the Mist Mountain and Elk Formations is defined at the base of the first sandstone or conglomerate overlying the uppermost major coal seam of the Kootenay Group (Gibson, 1985).

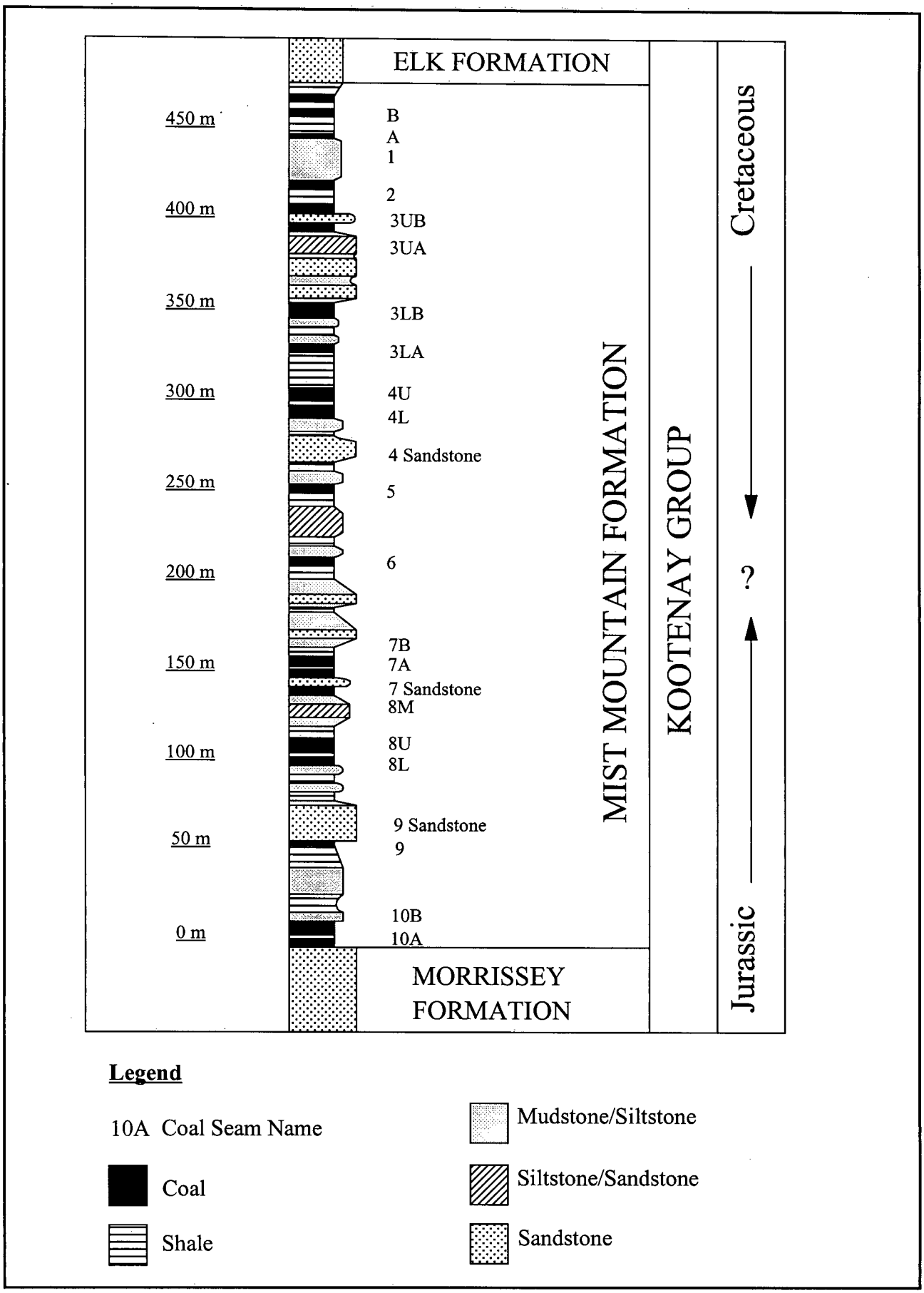

Figure 2.4 - Generalised stratigraphic section of the Line Creek area showing coal seam and sandstone nomenclature utilised in this study.

2.5. - METHODS AND DATA

Information for this study was derived from outcrop, drill core and geophysical logs from 115 drill holes. Palinspastic locations of the drill holes were determined by removing the effects of deformation using detailed structural cross sections provided by Line Creek Resources Ltd. The eastern edge of the map area (Fig. 2.5) was used as a base point for removing all deformation. The palinspastic map provided a base for all cross-sections and maps used in this study.

Stratigraphic columns were compiled for core and outcrop data. Descriptions of drill core were at a decimetre scale and included grain composition, size, sorting and colour as well as notes on sedimentary, biogenic and primary structures, including bedding orientation. Drill core descriptions and geophysical logs were used to construct eleven stratigraphic cross-sections, two fence diagrams, isopach maps for major coal seams and sandstone bodies and isoash maps for major coal seams. Line Creek Resources Ltd. supplied ash and washability data for drill core. Maceral content of the coal was determined by point counting 64 polished pellets under oil immersion microscopy. Three hundred points were counted for each pellet using standard procedures (Bustin et. al., 1985) . X-ray diffraction and scanning electron microscopy were used to determine clay mineralogy.

2.6. - LOCAL GEOLOGY AND STRATIGRAPHY

The Line Creek mine site includes two north-south trending ridges separated by the Line Creek valley (Fig. 2.6). The Mist Mountain Formation at Line Creek is up to 590 metres thick and consists of interbedded sandstone, siltstone, mudstone, carbonaceous shale, coal and rare conglomerate. Coal seams occur throughout the succession. Major seams are numbered from 10A at the base through to 1 near the top (Fig. 2.4). Above seam 1, coal seams are referred to successively by the letters A to D. Channel sandstones are numbered with reference to the coal seams they are associated with. For example, the channel sandstone that occurs below 7 seam is named 7 sandstone.

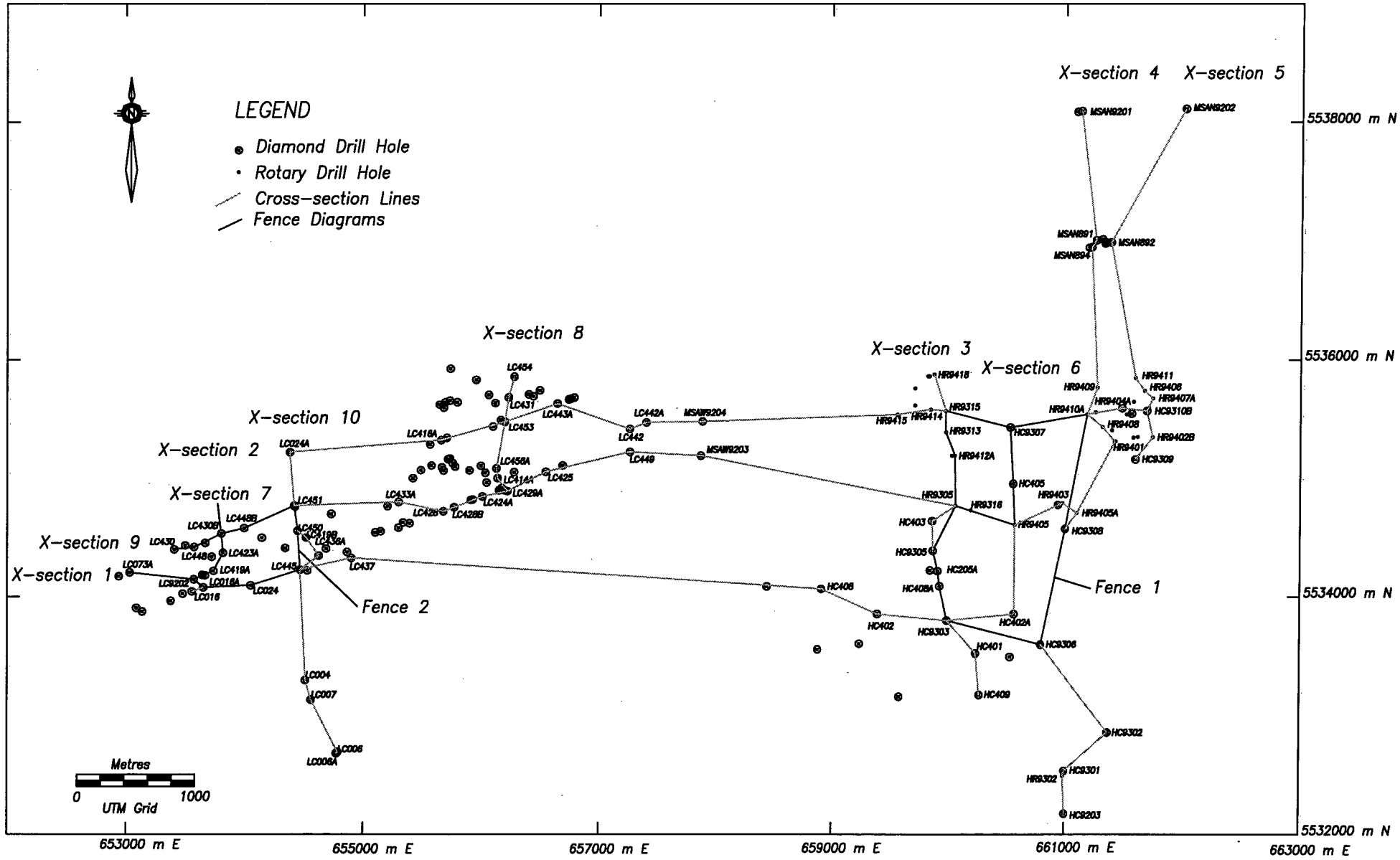

Figure 2.5 – Palinspastic map of the Line Creek area showing location of drill holes, cross-sections and fence diagrams.

The dominant structural feature of the Mist Mountain Formation at the Line Creek mine site is the Alexander Creek Syncline. The syncline axis trends through the eastern slope of Line Creek Ridge, so strata west of the axis is east dipping (Fig. 2.6) whereas Horseshoe Ridge is on the west dipping eastern limb (Fig. 2.6). The major fault passing through Line Creek is the Ewin Pass Thrust. The fault trace is mapped through the Line Creek River Valley and cuts the Alexander Creek Syncline south of the study area. North of Line Creek on Mt. Michael, the Mist Mountain Formation has been thrust over the Elk Formation by the Ewin Pass Thrust. Vertical throw of the Ewin Pass Thrust at Mt. Michael is approximately 600 metres and lessens toward the south (Grieve and Fraser, 1985). At the mine site scale, smaller structures associated with the Ewin Pass Thrust and numerous other thrusts are important geological controls. Small-scale deformation features include drag folds, overturned zones, thickened and sheared coal seams. The eastern limb of the Alexander Creek syncline is characterised by low-angle west dipping reverse faults and the western limb by high-angle east dipping reverse faults.

The Mist Mountain Formation reaches its maximum preserved thickness at Line Creek west of the Ewin Pass Thrust, and is thinned by erosion to approximately 250 metres at the southern end of Line Creek Ridge. East of the Ewin Pass Thrust, only the lower 430 metres of the formation are exposed.

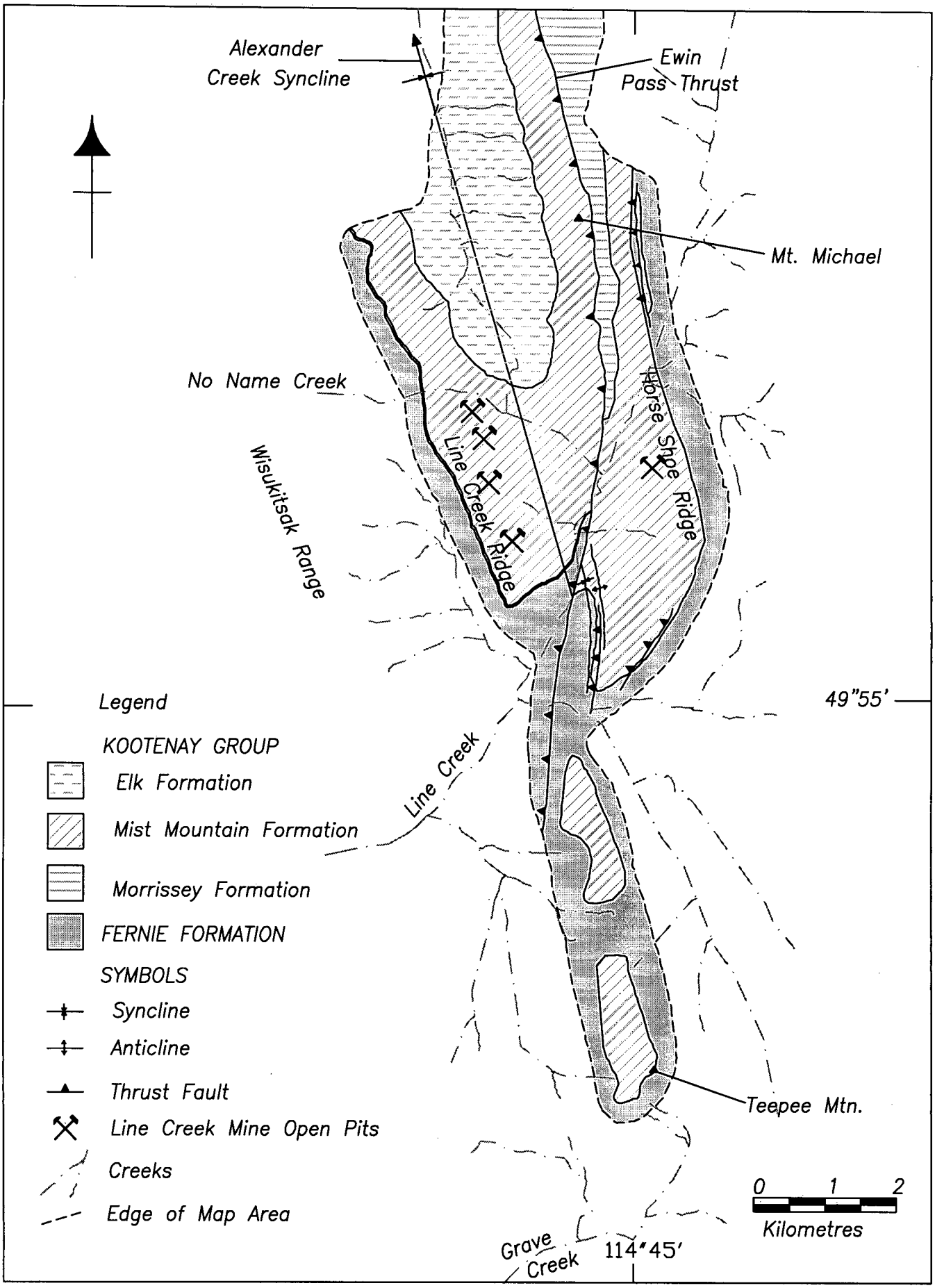

Figure 2.6 – Geological map of the Line Creek region of the Elk Valley Coalfield (modified from Grieve and Fraser, 1985).

2.7. - FACIES AND INTERPRETATION

In the Line Creek area sediments of the Mist Mountain Formation are divisible into four lithofacies; channel, crevasse splay, floodplain and organic rich facies. General characteristics of these facies are summarised and interpreted below.

2.7.1. - CHANNEL FACIES

The channel facies consists of dark grey to 'salt and pepper', fine to very coarse grained quartzose litharenites and rare granular litharenites and conglomerates. Channels occur either as single tabular to lenticular bodies up to 12 metres thick, or in stacks of channels up to 40 metres thick. The channel facies may extend laterally on a scale of kilometres. Individual channels within stacks are commonly separated by thin mudstone intervals, up to 10 centimetres thick. Typically, the channel facies have an erosional base with conglomeratic lag deposits and rip-up clasts of mudstone, siltstone or coalspar (Fig. 2.7). The channels fine upwards, from very coarse or coarse sandstone to medium or fine sandstone. Prominent sedimentary structures include planar and trough cross bedding in sets 0.5 to 1 metre thick and ripple cross-lamination. Other features include convolute bedding and rare carbonaceous partings.

The sedimentary structures, lateral continuity, fining up nature and the presence of lag deposits suggests the channel facies represent point bar deposits of meandering streams (Miall, 1996). Channel sandstones commonly have gradational upper contacts with crevasse splay and floodplain facies sediments, indicating a gradual transition from point bar to floodplain environments.

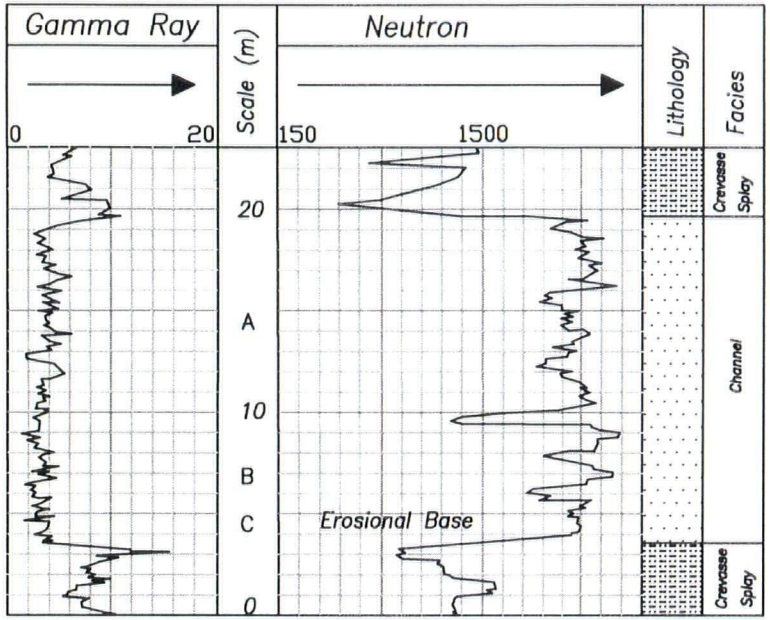

LEGEND (Figures 2.7, 2.8, 2.9 & 2.10)

- Sandstone
- Sandstone/Siltstone
- Siltstone/Mudstone
- Carbonaceous Mudstone
- Coal

Figure 2.7 – Sediments, log signature and sedimentary structures of the channel facies of the Mist Mountain Formation at Line Creek.

A – Cross–bedding in fine and medium grained sandstone in the 9 channel sandstone at Line Creek Coal Mine. Cross–bedding is common throughout channel facies sediments at Line Creek.

0 5 10cm

B – Rip–up clasts at the base of a sandstone unit in drill hole HC 9309. Rip–up clasts consist of siltstone and mudstone from the underlying unit.
Rip–up clasts are common at the base of channel facies units at Line Creek.

0 1 2cm

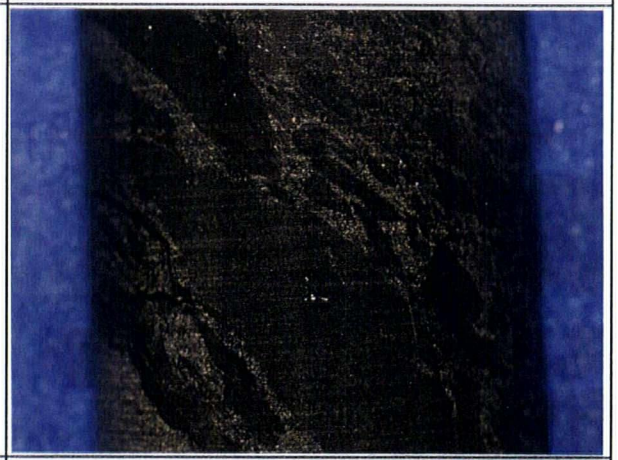

C – Lag conglomerate at the base of a sandstone unit in drill hole LC 413. Conglomerates are not common at Line Creek, but when present, they occur at the base of channel facies units.

0 1 2cm

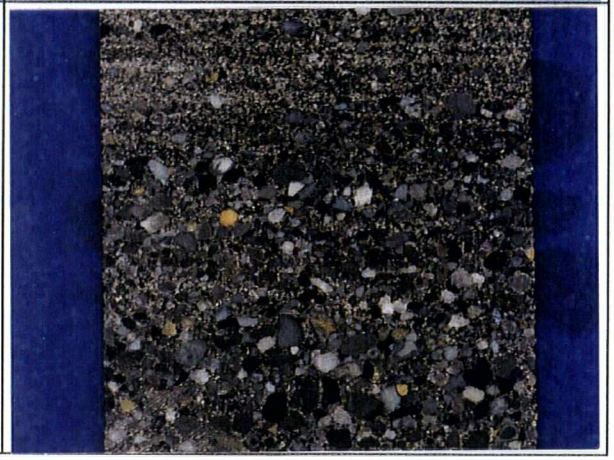

2.7.2. - CREVASSE SPLAY FACIES

The crevasse splay facies consist of light to dark grey siltstone to medium grained quartzose sandstone and rare mudstone. Both fining and coarsening upward sequences occur in units up to 3 metres thick. Fining up units have erosional or planar bases marked by rip-up clasts of underlying sediment and coalspar and grade up from medium to fine grained sandstone at the base to very fine sandstone or siltstone. The coarsening up units have gradational or planar bases and range from siltstone or silty sandstone at the base, to fine or medium grained sandstone. Dominant sedimentary structures within both fining and coarsening upward units are trough and planar cross bedding in sets up to 0.5 metres thick in sandstone, and ripple cross-lamination in siltstone. Other features include flaser bedding, parallel lamination, convolute bedding, coalspar and rare carbonaceous partings (Fig. 2.8).

The sedimentary structures and grain size of the fining up units are indicative of crevasse splay and crevasse channel deposits. Distal crevasse splay deposits commonly fine up from very fine sandstone to mudstone and may lack lag deposits and rip up clasts, due to their increased distance from active river channels during deposition (Miall, 1996). Coarsening up units occur as a result of progradation of crevasse splays into standing bodies of water (Horne et. al., 1978). The crevasse splay facies commonly occurs as a gradational unit between the channel sandstone and floodplain facies but also as stacks of interbedded fining and coarsening up deposits, especially close to channel sandstone bodies. Levee deposits are not evident but may be indistinguishable from crevasse splay deposits in outcrop.

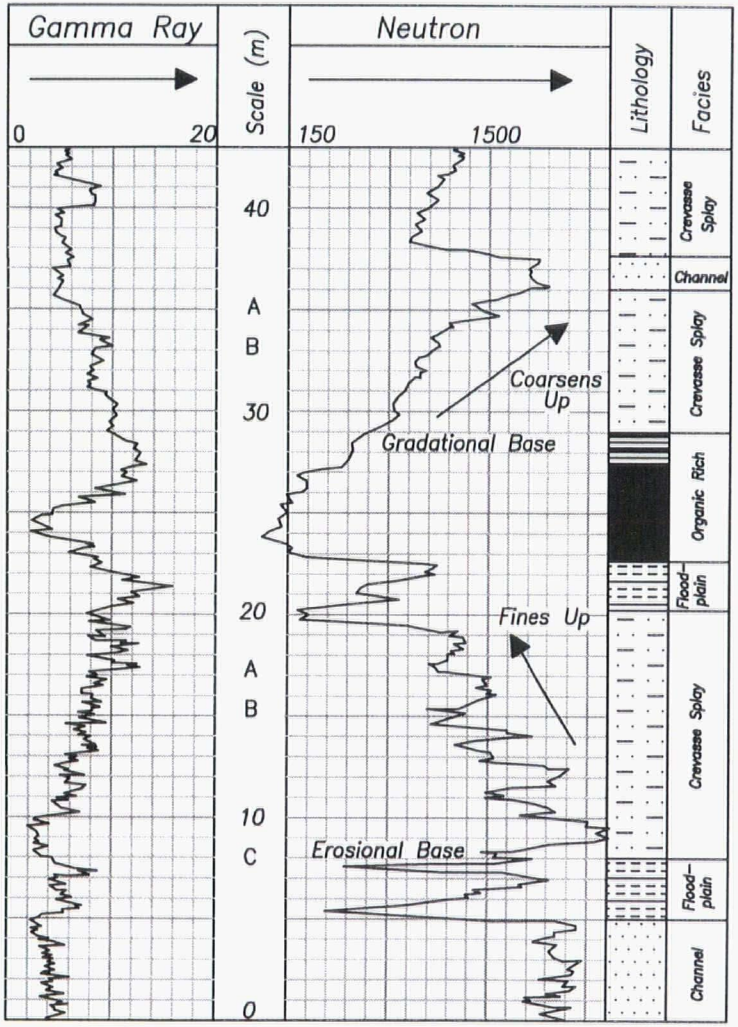

Figure 2.8 – Sediments, log signature and sedimentary structures of the crevasse splay facies of the Mist Mountain Formation at Line Creek.

A – Cross laminated siltstone and fine sandstone in drill hole HC 9309. Cross laminated siltstone and sandstone are common through out crevasse splay facies sediments at Line Creek.

0 1 2cm

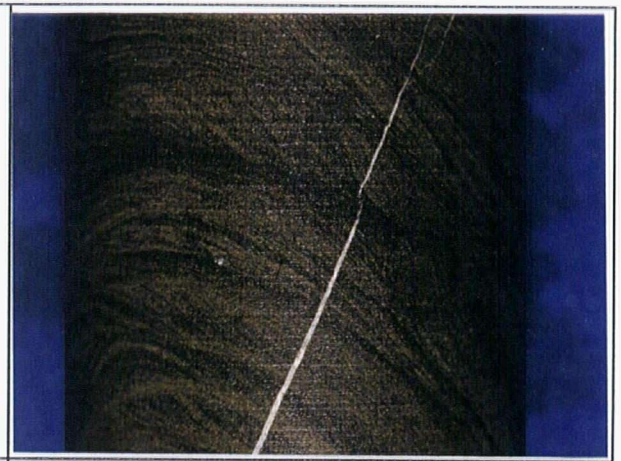

B – Flaser bedding in mudstone and siltstone/sandstone in drill hole HC 9305. Flaser bedding is common in crevasse splay facies sediments at Line Creek.

0 1 2cm

C – Load casting of cross laminated siltstone and sandstone into the underlying mudstone and siltstone of drill hole HC 9305. Load casting is common where crevasse splay facies overlie floodplain facies sediments.

0 1 2cm

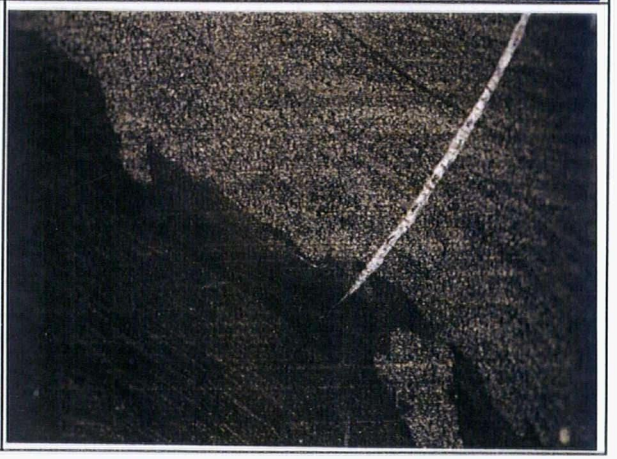

2.7.3. - FLOODPLAIN FACIES

The floodplain facies consists of interbedded and interlaminated medium to dark grey quartzose siltstones, mudstones and rare fine sandstones. Parallel lamination is the dominant sedimentary structure in siltstone but ripple cross-lamination, convolute bedding, wavy lamination and massive siltstone are also common. Mudstones are often massive but sedimentary structures, where present, include parallel to wavy lamination, convolute bedding and rare bioturbation. Alternations between mudstone and siltstone vary from a metre to millimetre scale with interlaminated units often exhibiting mud-draped ripples and flaser bedding (Fig. 2.9). Carbonaceous partings, coalspar and roots occur throughout the floodplain facies.

The sedimentary structures, presence of carbonaceous partings and bioturbation suggests low energy deposition as distal crevasse splays and suspension deposition on a river floodplain (Miall, 1996). The floodplain facies are commonly interbedded with crevasse splay deposits suggesting clastic rather than coal-forming environments predominated in distal floodplain regions during times of fluvial activity.

2.7.4. - ORGANIC RICH FACIES

The organic rich facies contains coal and carbonaceous mudstone and shale that are commonly interbedded with each other and share gradational contacts (Fig. 2.10). Carbonaceous mudstones are dark grey to brown-black and massive with abundant plant fragments and rootlets. Carbonaceous shales are black and consist of finely macerated plant material. Coal is the most abundant of the organic rich units, forming seams up to 20 metres thick. Lateral continuity is variable, some seams extending kilometres, others only metres. Thicker seams commonly split into multiple plies. Rank of the coal varies from high to low volatile bituminous and the sulphur content is less than 1%. Macroscopically, the coal is weakly to intensely tectonically sheared, which partially to completely obscures original textures. Where texture is observable, the coal consists of bright vitrain bands (up to 10cm thick) in moderately bright to dull

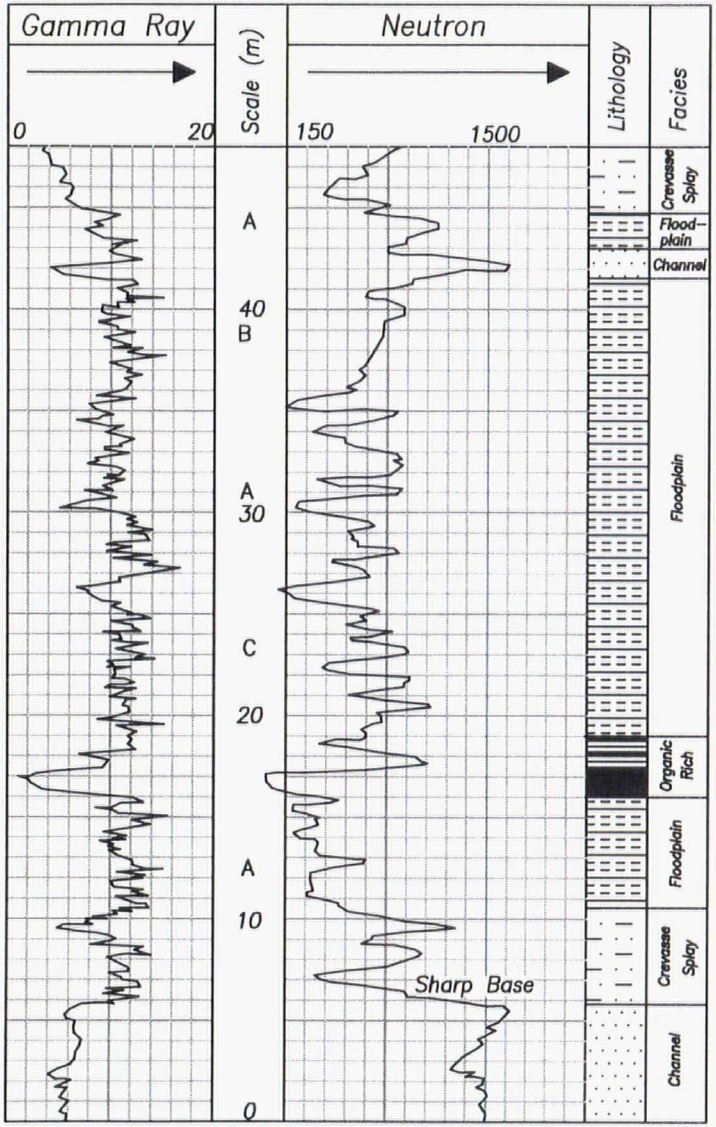

Figure 2.9 – Sediments, log signature and sedimentary structures of the floodplain facies of the Mist Mountain Formation at Line Creek.

A – Interbedded mudstone and siltstone in drill hole HC 9305. Interbedded mudstone and siltstone are common throughout floodplain facies sediments at Line Creek.

0 1 2cm

B – Convolute bedding in mudstone and siltstone from drill hole HC 9309. Convolute bedding is common in floodplain facies sediments at Line Creek, especially where overlain by channel and crevasse splay sediments.

0 1 2cm

C – Bioturbation in mudstone and siltstone from drill hole HC 9305. Burrows are infilled with fine sandstone. Bioturbation occurs only rarely in floodplain facies sediments at Line Creek.

0 1 2cm

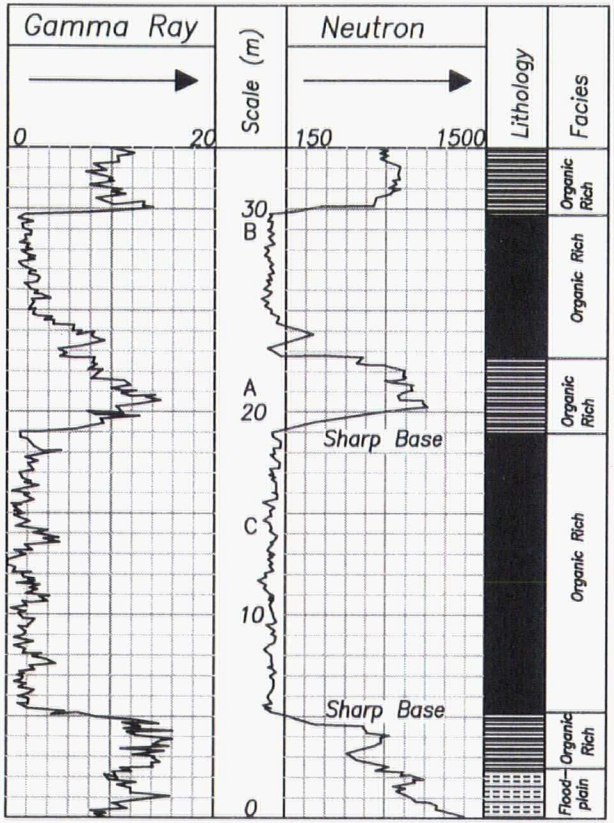

A – Massive carbonaceous shale with coaly partings and bedding planes from drill hole HC 9395. Carbonaceous shale is common in coal partings and immediately above and below coal seams at Line Creek.

0 1 2cm

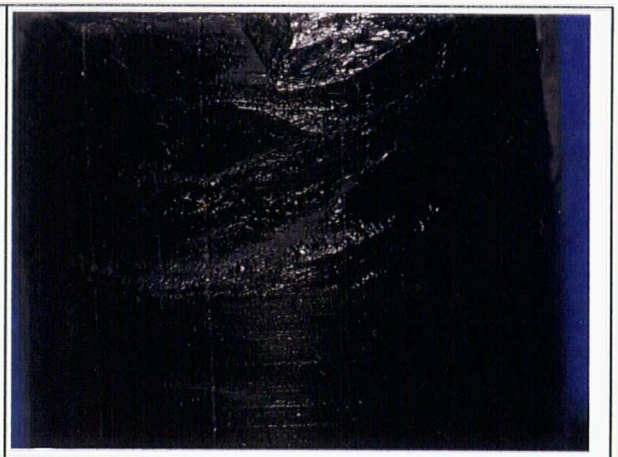

B – 4U coal seam at Line Creek Coal Mine. Bright coal grades up to argillaceous coal which has a sharp contact with the overlying cross–laminated siilstone and sandstone. This is typical of coal seams at Line Creek.

0 5 10cm

C – Sheared zone at roof of 6U coal seam at Line Creek Coal Mine. Note unsheared coal at bottom left corner and sharp upper contact between sheared coal and mudstone in top right corner of photograph. Sheared zones are common in coal seams at Line Creek.

0 20 40cm

Figure 2.10 – Sediments, log signature and sedimentary structures of the organic rich facies of the Mist Mountain Formation at Line Creek.

durain. Microscopically, vitrinite is the dominant maceral, but the coal ranges from semifusinite rich at the base to semifusinite poor at the top of the formation.

Rooted carbonaceous mudstone and shale generally underlie coal seams, indicating that the coal is autochthonous and peat deposition started slowly in response to anaerobic conditions and terrestrialisation. Partings are generally thin carbonaceous mudstone or shale beds, less than 3 centimetres thick. Coal seams often grade up into argillaceous coal and carbonaceous shale, except where eroded by channel sandstone and crevasse splay facies. Erosion indicates peat deposition was halted abruptly by an influx of clastic sediments, probably during flooding events. Gradational upper contacts of coal seams suggest gradual flooding of the peat mires terminated peat deposition.

2.8. - UNIT DESCRIPTIONS AND DEPOSITIONAL ENVIRONMENTS

The Mist Mountain Formation at Line Creek Coal Mine can be divided into two informal units based on the abundance and lateral continuity of constituent sedimentary facies. The lower unit extends from the base of the Mist Mountain Formation to the top of 7 seam and the upper unit is the interval from the top of 7 seam to the top of the formation (Figs. 2.11, 2.12 and 2.13).

2.8.1. - THE LOWER UNIT

The lower unit of the Mist Mountain Formation (Fig. 2.14) consists of laterally extensive coal seams alternating with thick, widespread channel sandstones interspersed with crevasse splay and floodplain facies sediments (Figs. 2.15, 2.16 and 2.17). These features suggest the lower unit was deposited in an interdeltaic coastal plain environment. Coal seams in the lower unit average 4.5 metres thick, have an average raw ash content of 26% and an average sulphur content of 0.5% (Table 2.1). The low ash content of the coal suggests limited clastic influx into mires at the time of peat accumulation. The low sulphur content of the coal indicates peat mires on the coastal plain were protected from marine incursion

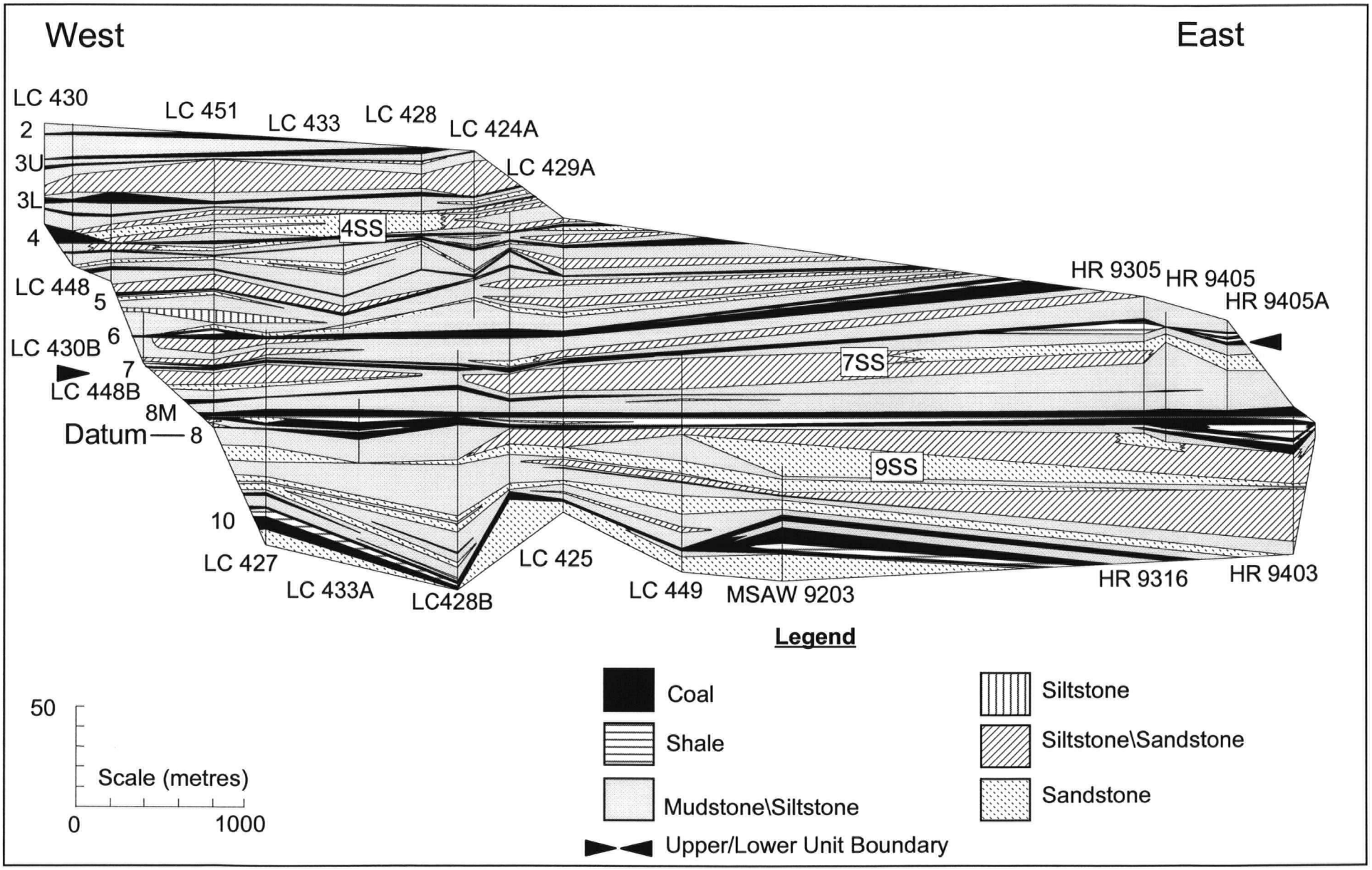

Figure 2.11 - Stratigraphic cross section 1. The Mist Mountain Formation at Line Creek. Refer to figure 2.5 for location of cross section.

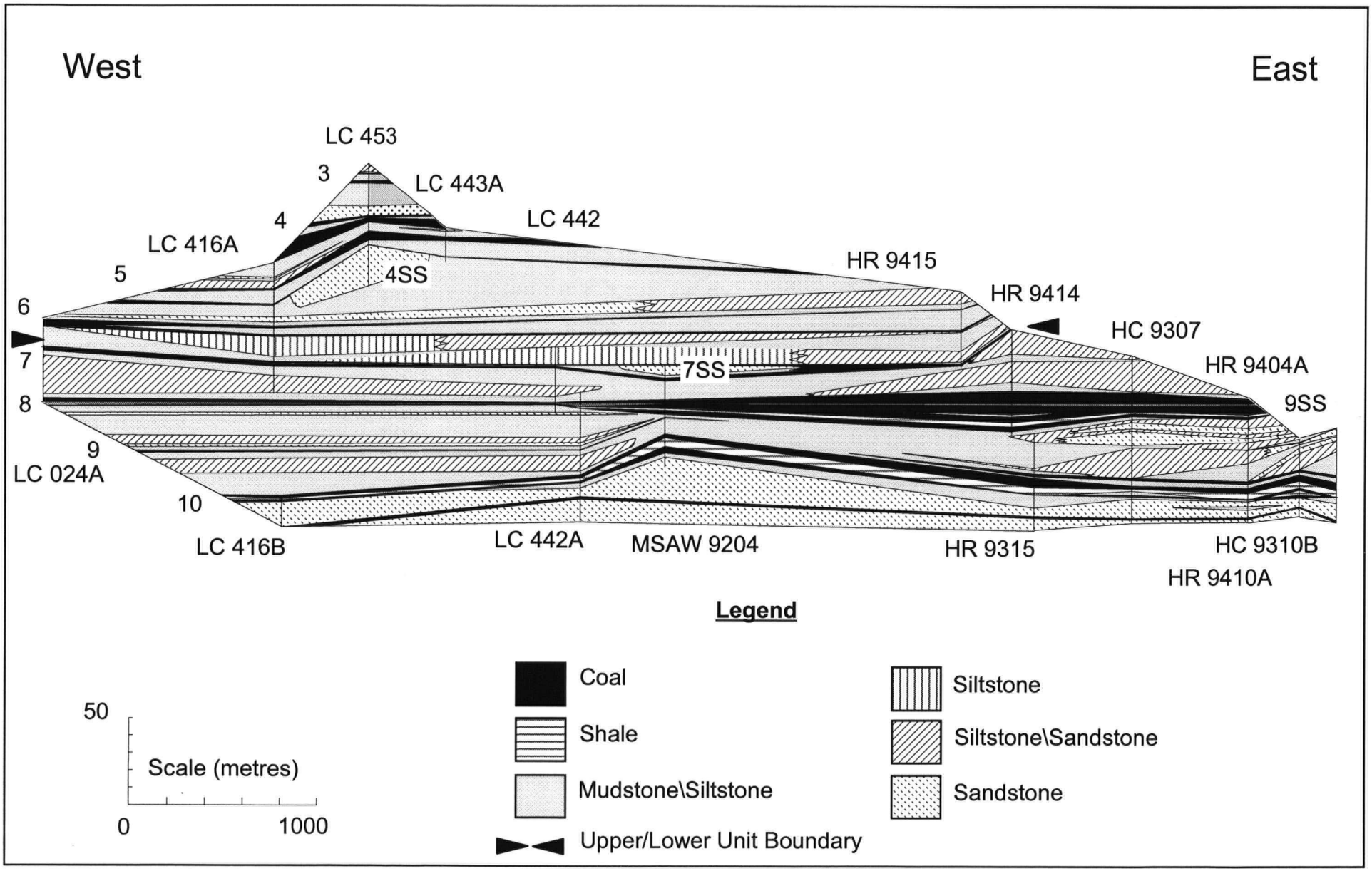

Figure 2.12 - Stratigraphic cross section 2. The Mist Mountain Formation at Line Creek. Refer to figure 2.5 for location of cross section.

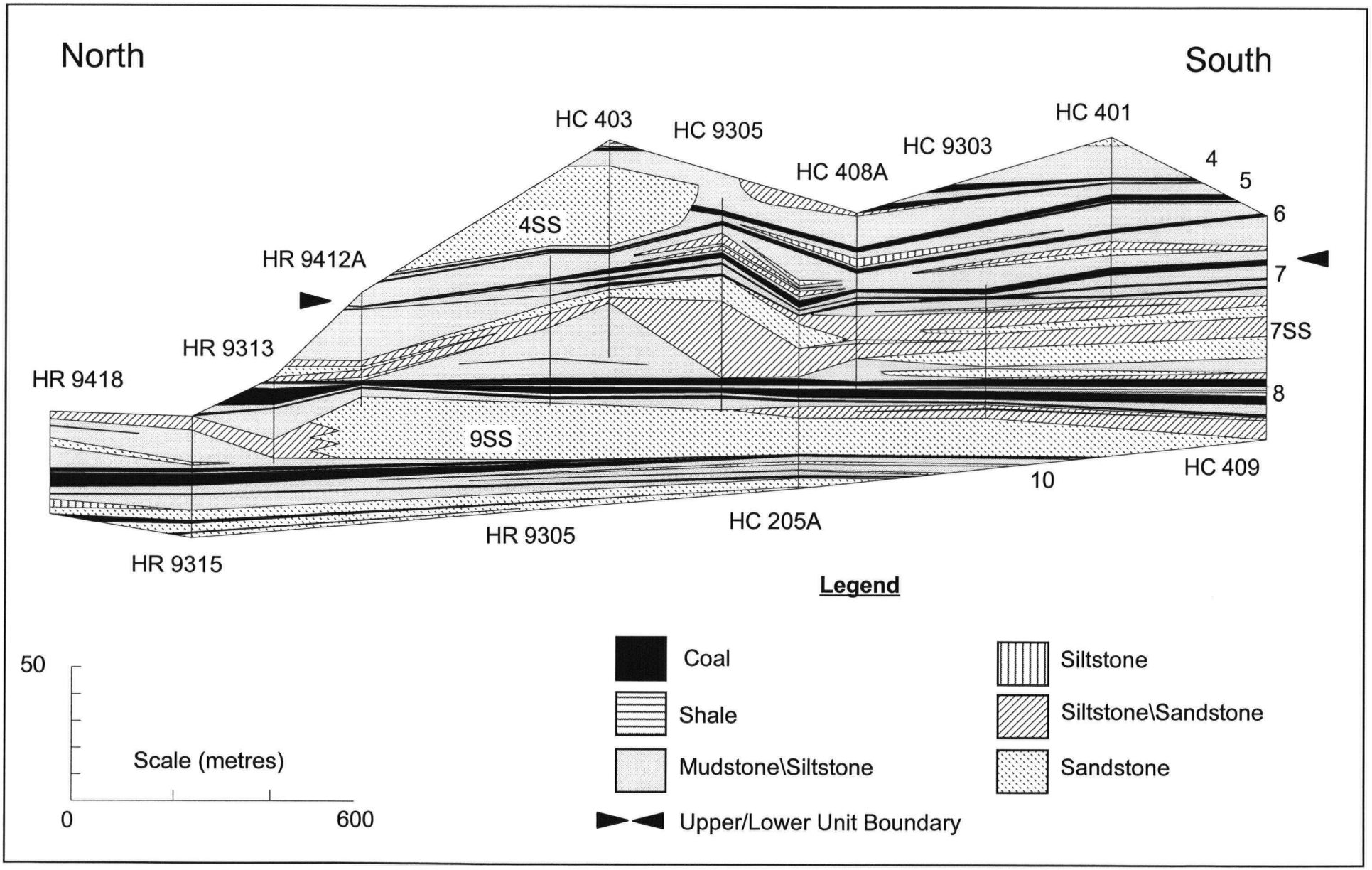

Figure 2.13 - Stratigraphic cross section 3. The Mist Mountain Formation at Line Creek. Refer to figure 2.5 for location of cross section.

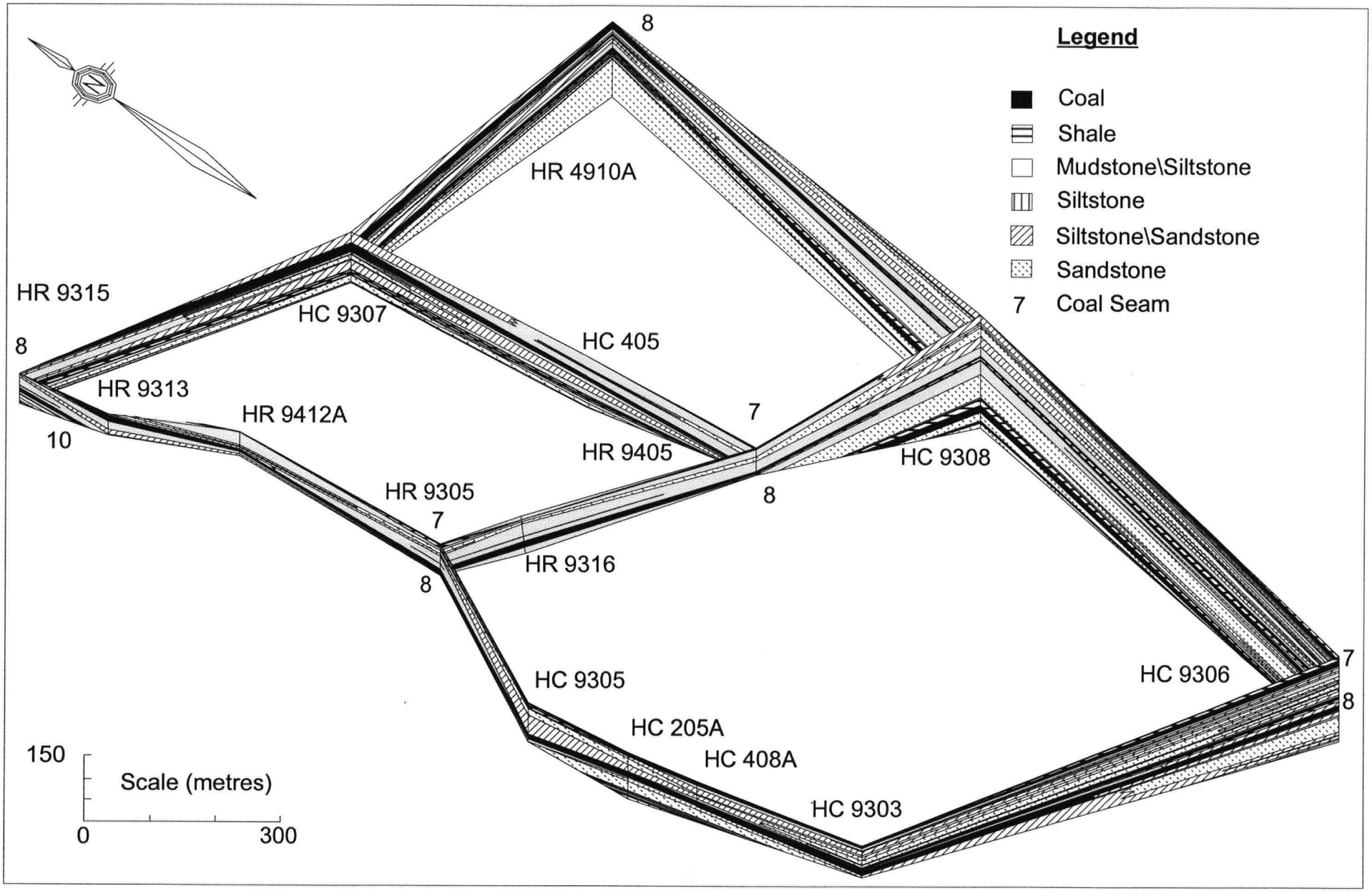

Figure 2.14 - Fence Diagram of the lower unit of the Mist Mountain Formation at Line Creek. Refer to figure 2.5 for location of Fence 1.

(Williams and Keith, 1963), probably by the beach ridge-dune sandstones of the underlying Morrissey Formation.

Seam Name	Average Seam Thickness (m)	Average Raw Ash Content (%)	Average Sulphur Content (%)	Number of Samples
7C	4.4	26.7	0.55	19
7B	4.1	24.9	0.69	49
7A	3.3	22.5	0.49	65
8M	3.7	28.2	0.53	28
8U	8.3	24.1	0.34	73
8L	6	33.9	0.41	60
8R	3.4	30.6	0.51	43
9	2.2	32.3	0.44	33
10C	4.4	17.1	0.41	35
10B	7.3	27	0.36	57
10A	2.6	23.9	0.52	59
AVERAGE	4.5	25.9	0.48	47

Table 2.1 – Average Seam Thickness, Raw Ash and Sulphur Content of Coal Seams Within the Lower Unit of the Mist Mountain Formation at Line Creek.

In the western half of the study area, 10 seam rests directly and conformably on top of Moose Mountain Member sandstones. Ten seam is split into two plies, which are separated by up to 8 metres of organic rich facies sediments. In eastern regions of the study area, up to 40 metres of floodplain, crevasse splay and channel facies sediments occur between 10 seam and the underlying Moose Mountain Member. The 10 sandstone occurs within these intervening sediments throughout most of the eastern part of the study area and is up to 20 metres thick. The nature of 10 seam suggests it is diachronous. In the east and northern part of the study area, 10 seam is split into 3 plies. Ten seam is capped by floodplain sediments, which coarsen up to crevasse splay and channel facies of the 9 sandstone. Nine sandstone is up to 40 metres thick and has partially to completely eroded 9 seam within much of the study area. Where 9 seam has escaped erosion, it generally occurs as a single seam but locally splits into two thin plies.

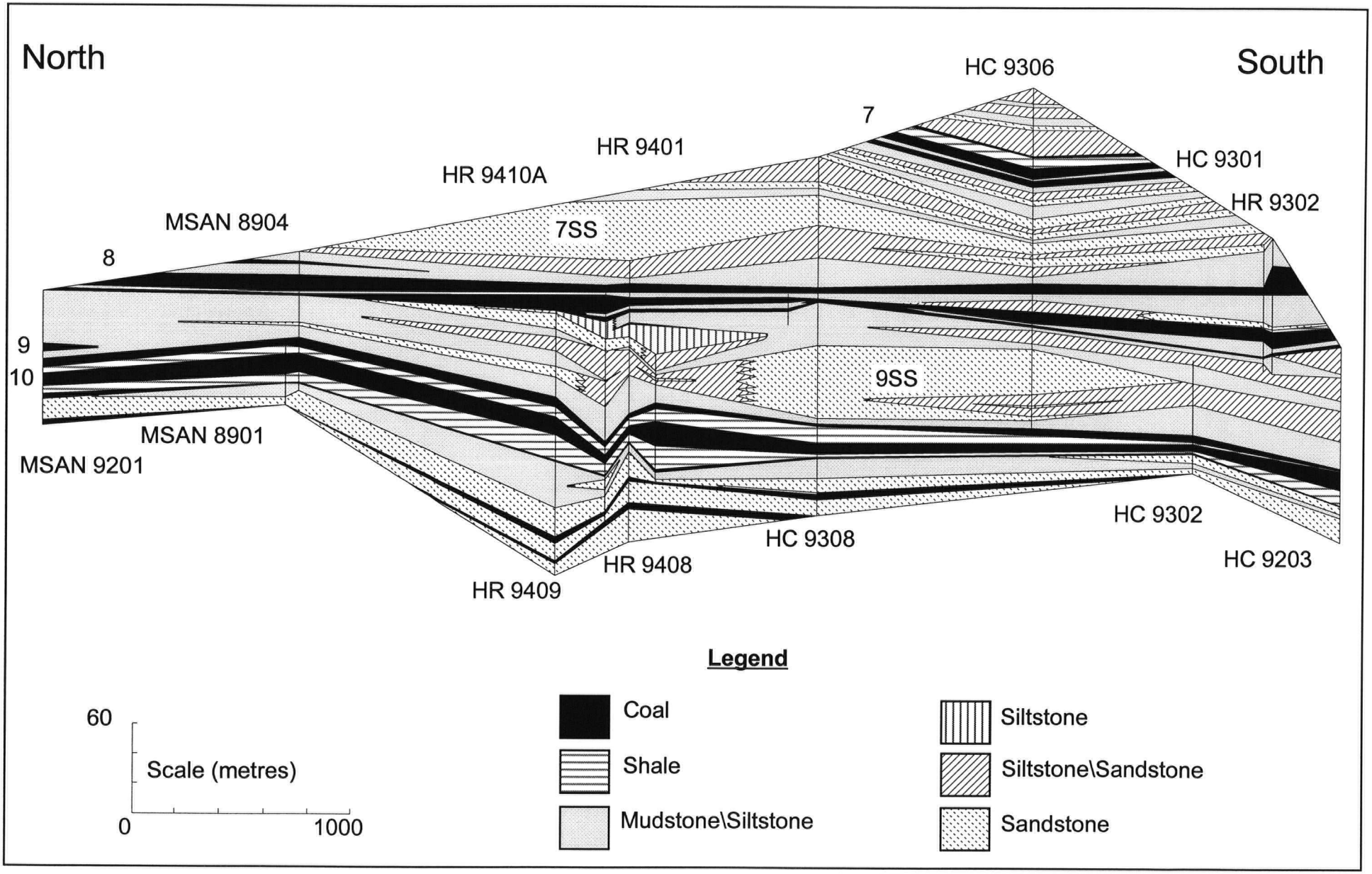

Figure 2.15 - Stratigraphic cross section 4. The lower unit of the Mist Mountain Formation at Line Creek. Refer to figure 2.5 for location of cross section.

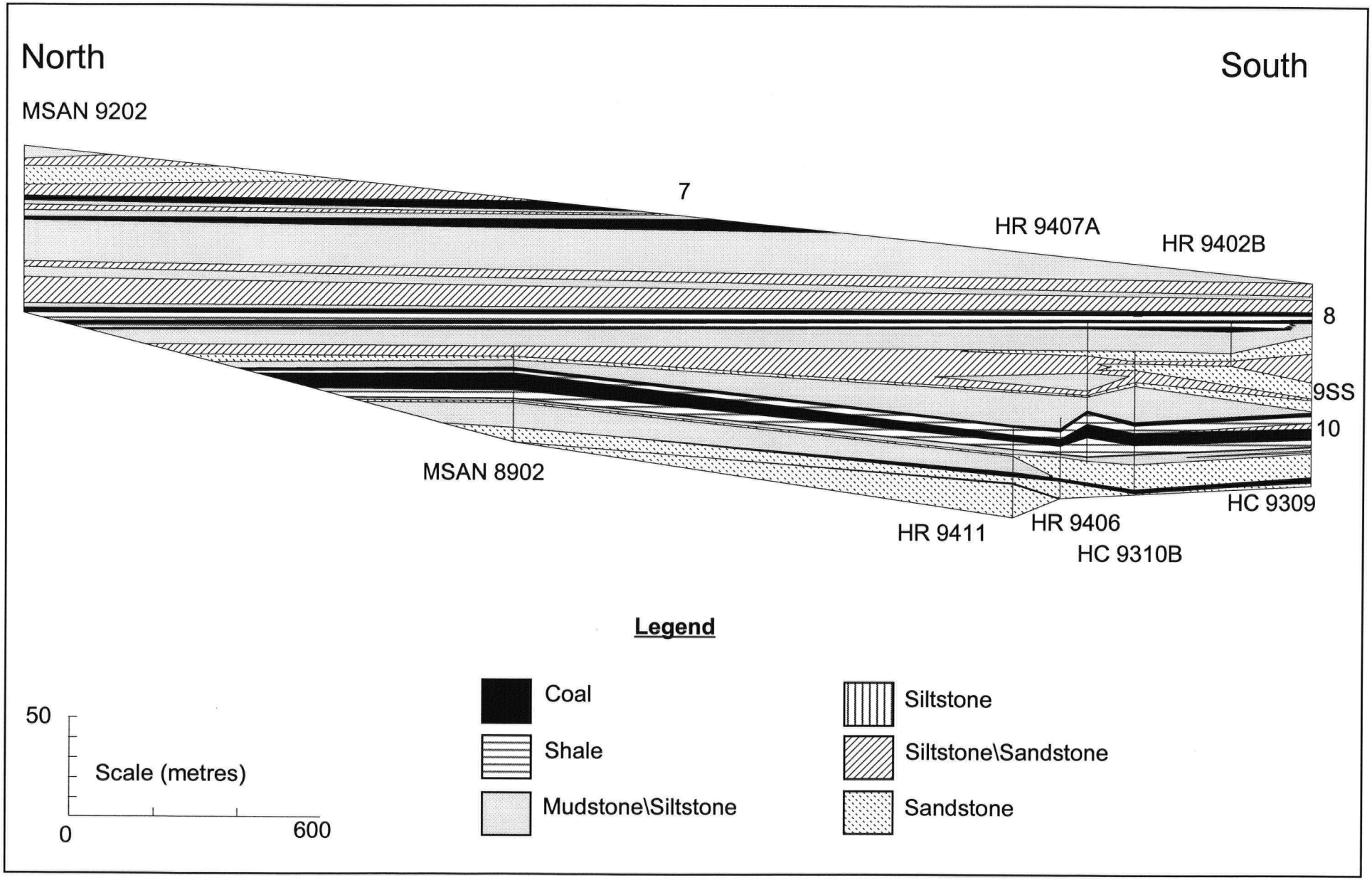

Figure 2.16 - Stratigraphic cross section 5. The lower unit of the Mist Mountain Formation at Line Creek. Refer to figure 2.5 for location of cross section.

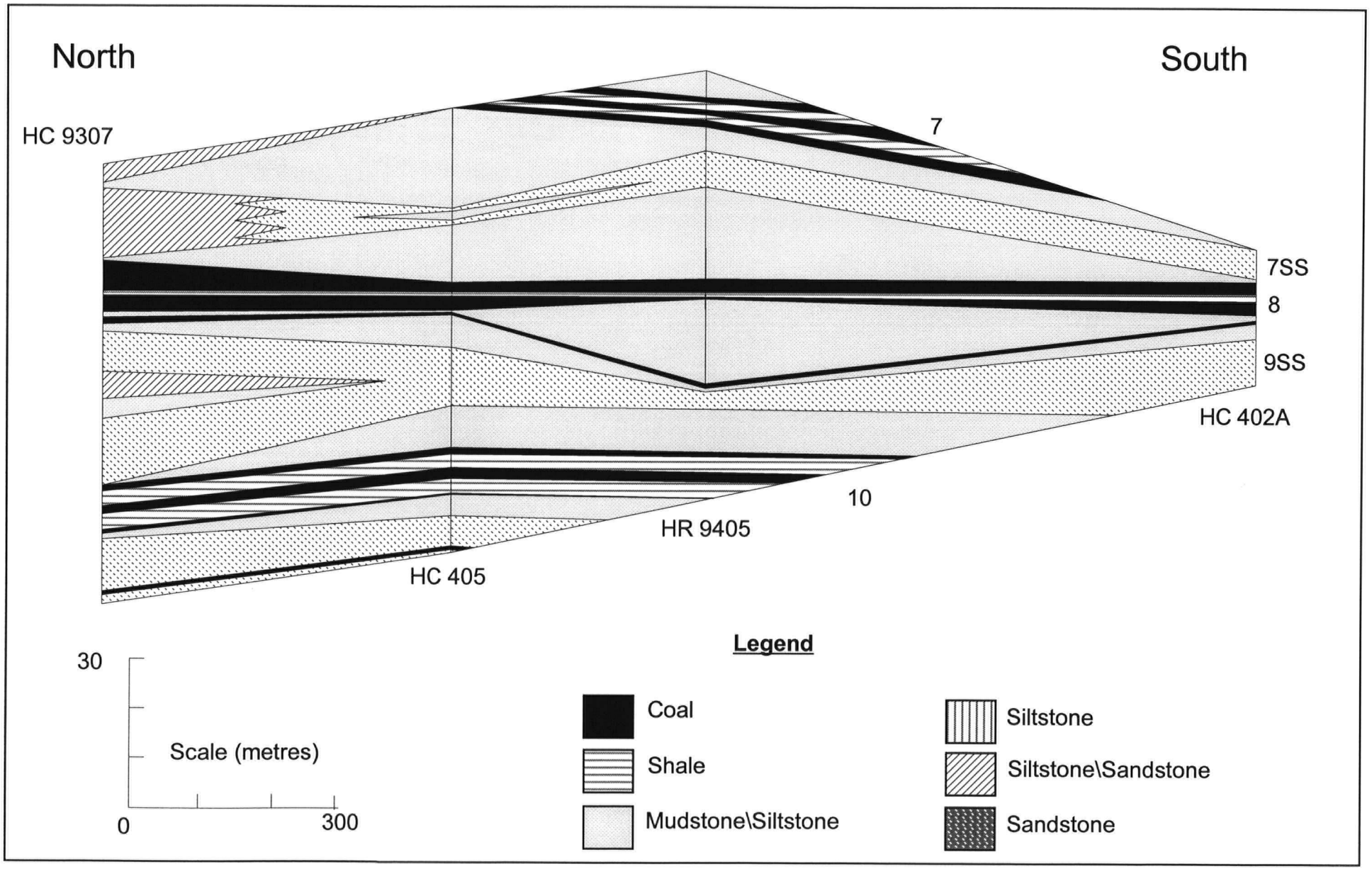

Figure 2.17 - Stratigraphic cross section 6. The lower unit of the Mist Mountain Formation at Line Creek. Refer to figure 2.5 for location of cross section.

Nine sandstone is separated from the overlying 8 seam by up to 30 metres of floodplain and crevasse splay facies sediments. Eight seam is a thick, laterally continuous seam that splits into three plies. The uppermost ply of 8 seam averages 8.3 metres thick and is the thickest individual ply within the Mist Mountain Formation. Partings are floodplain and organic rich facies sediments, from 1 to 20 metres thick. In the western half of the study area, a thin marker (8M) seam occurs 1 to 10 metres above 8 seam. Throughout the study area, up to 30 metres of floodplain and crevasse splay facies sediment occur between 8 seam and 7 sandstone channel facies, which is up to 40 metres thick. Seven sandstone fines upward to crevasse splay and floodplain facies sediments. The uppermost facies of the lower unit is 7 seam, which occurs up to 20 metres above 7 sandstone. Seven seam is laterally continuous and splits into 3 plies that are separated by up to 8 metres of floodplain and organic rich facies sediments.

2.8.2. - THE UPPER UNIT

The upper unit of the Mist Mountain Formation (Fig. 2.18) consists of the same facies as the lower unit, however they are generally less laterally continuous and thinner than their counterparts in the lower unit (Figs. 2.19 and 2.20). Rapid lateral variation in coal seam and parting thickness is also common, with thickness changes of up to 10 metres occurring in the space of tens of metres laterally. Both channel sandstones and coal seams decrease in thickness and lateral continuity, however the abundance of coal seams increases while channel facies decreases. Upper unit coal seams average 2.5 metres thick, have an average raw ash content of 28% and an average sulphur content of 0.6% (Table 2.2). Locally coal seams thicken significantly. The ash and low sulphur content of the coal suggests they were protected from clastic influx and marine incursion during peat accumulation. These characteristics of the upper unit suggest a distal alluvial floodplain depositional environment.

Up to 40 metres of floodplain, crevasse splay and minor channel facies sediments separate each coal seam in the upper unit. Four sandstone is the only laterally continuous channel sandstone in the upper unit. Four sandstone occurs between 4 and 5 seams, averages 11 metres in thickness, and locally has

completely eroded 5 seam and parts of 6 seam. A number of minor channel sandstones also occur through out the unit, they are generally less than 8 metres thick and are not laterally continuous.

Seam Name	Average Seam Thickness (m)	Average Raw Ash Content (%)	Average Sulphur Content (%)	Number of Samples
A	2.2	-	-	5
1	1	-	-	7
2U	3	-	0.41	18
2L	1.2	-	-	9
3UB	2.2	-	0.68	27
3UA	2	-	-	30
3LB	3.9	30.5	0.52	32
3LA	2.9	34.1	0.58	32
4U	6.1	27.5	0.55	39
4L	2.3	26.9	0.83	35
5U	1.8	20.9	0.67	32
5L	1.7	-	-	24
6U	3	30.1	0.64	41
6L	2.4	-	0.51	33
AVERAGE	2.5	28.3	0.6	26

Table 2.2 – Average Seam Thickness, Raw Ash and Sulphur Content of Coal Seams Within the Upper Unit of the Mist Mountain Formation at Line Creek.

Six seam is commonly split into 2 plies, whereas splitting in 5 seam occurs only locally. Four seam sits above 4 sandstone, and often splits into 2 plies. The upper ply is the thickest of the upper unit, averaging 6.1 metres, and is separated from the lower ply by up to 25 metres of carbonaceous mudstone, floodplain and crevasse splay facies sediments. Above 4 seam, facies are less laterally continuous than lower in the unit. Three seam is split into an upper and lower bench, both of which commonly have 2 plies. Much of the succession above 3 seam has been eroded or mined at Line Creek, but where present, the strata are similar to the rest of the upper unit. Sandstones of the Elk Formation conformably overlie D seam.

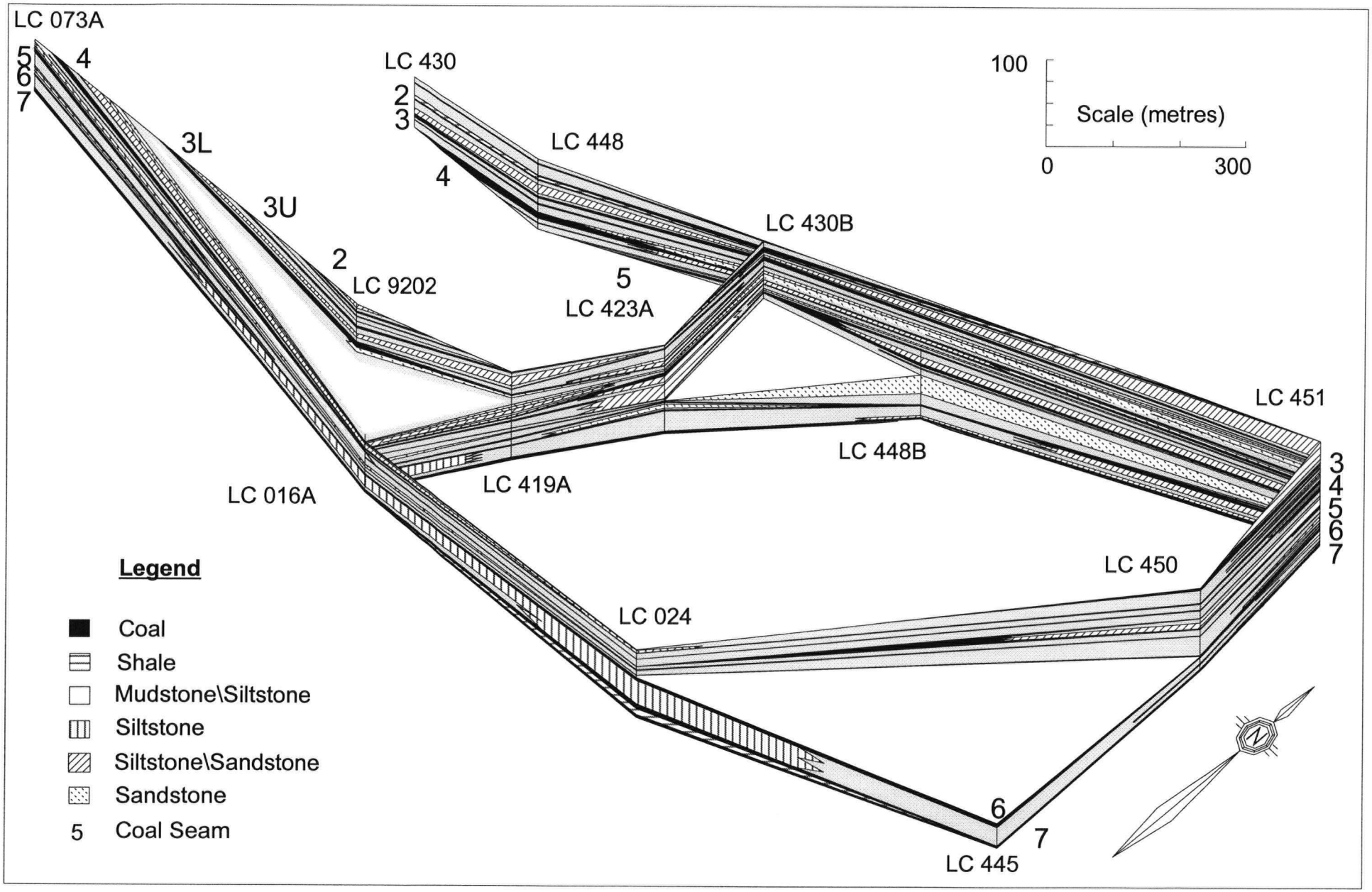

Figure 2.18 - Fence diagram of the upper unit of the Mist Mountain Formation at Line Creek. Refer to figure 2.5 for location of Fence 2.

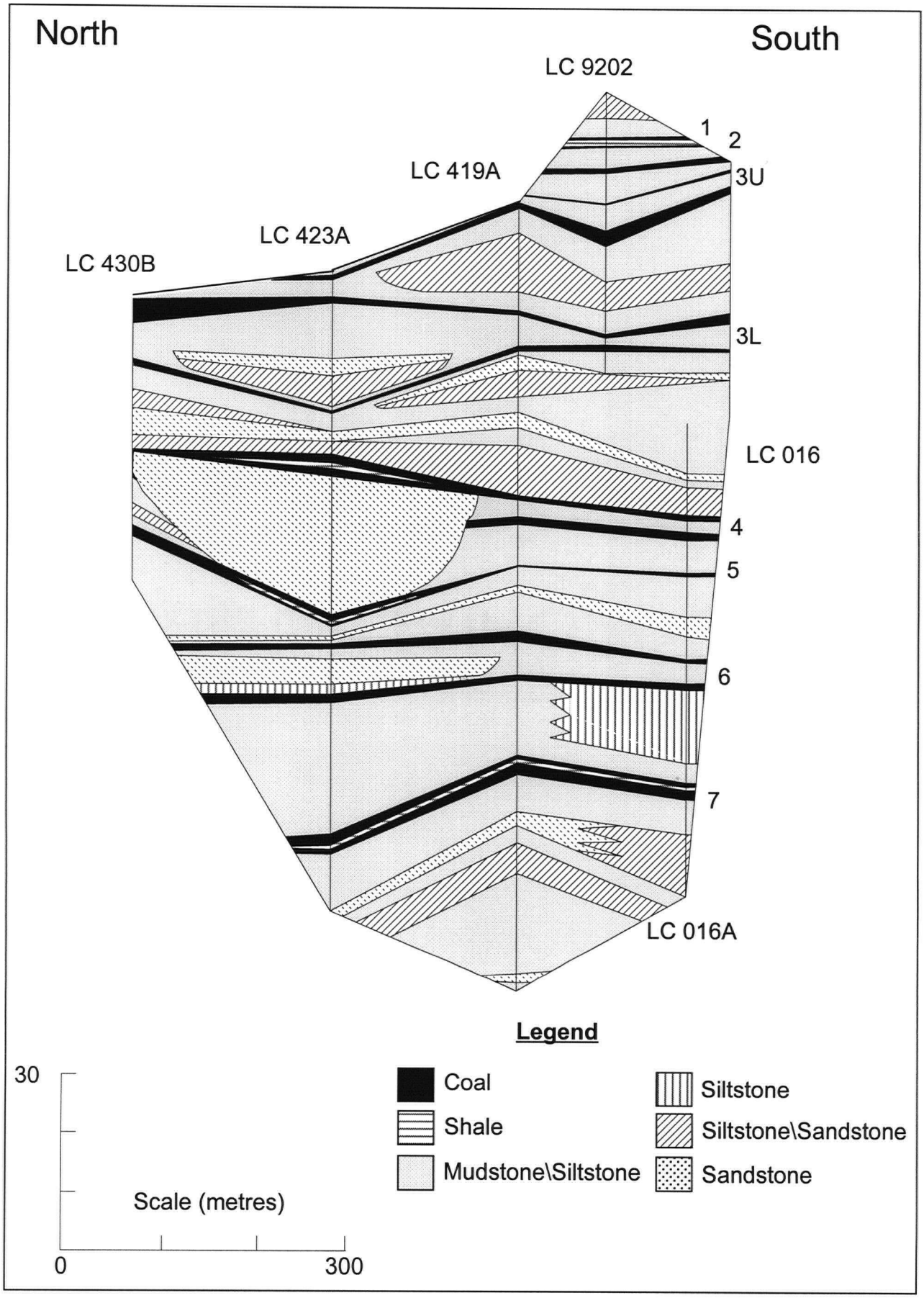

Figure 2.19 - Cross section 7. The upper unit of the Mist Mountain Formation at Line Creek Refer to figure 2.5 for location of cross section.

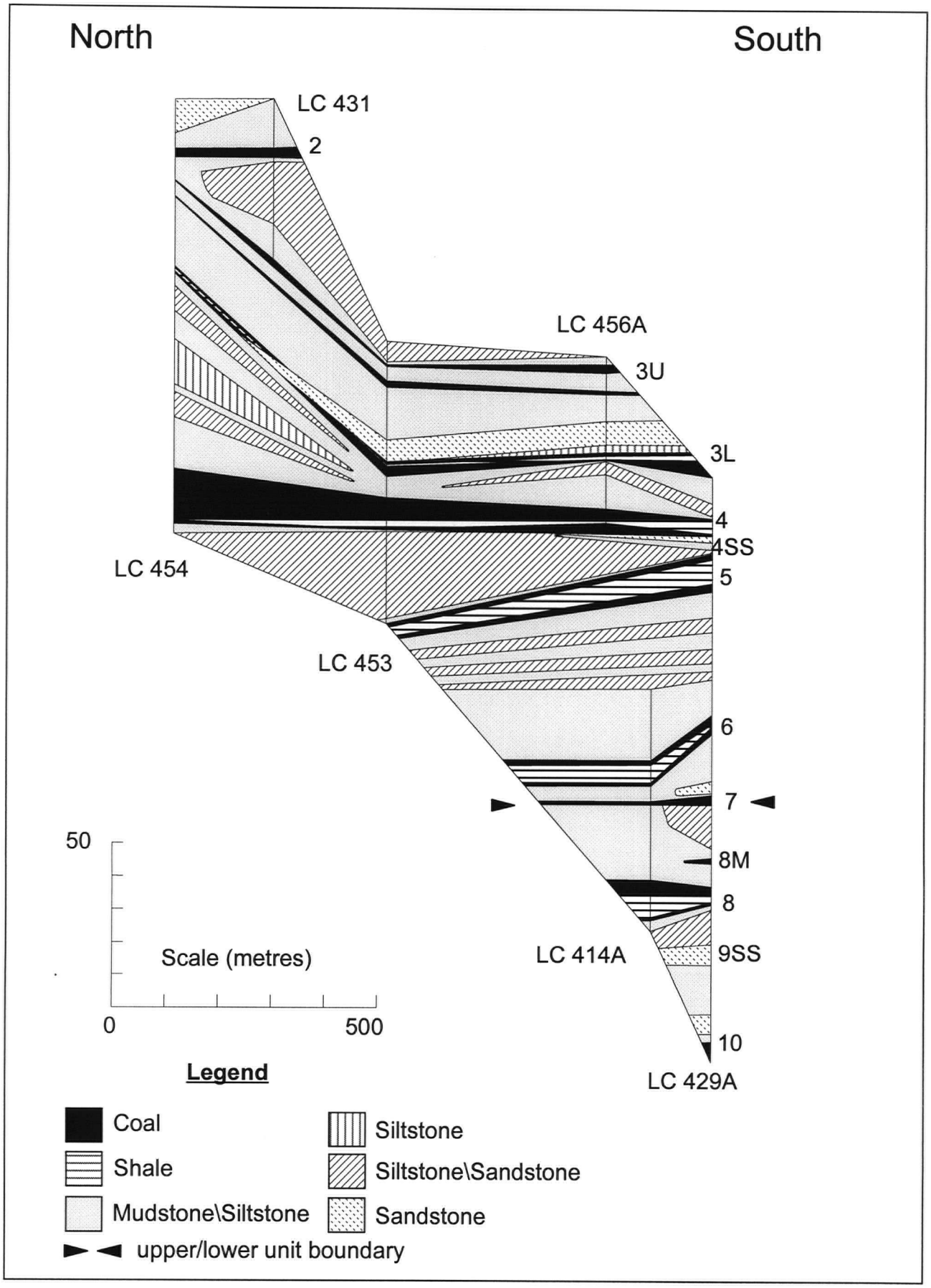

Figure 2.20 - Stratigraphic cross section 8. The upper unit of the Mist Mountain Formation at Line Creek. Refer to figure2. 5 for location of cross section.

2.9. - RELATIONSHIPS BETWEEN COAL QUALITY PARAMETERS AND SEDIMENTOLOGY AT LINE CREEK

The change in depositional environment between the lower and upper units of the Mist Mountain Formation has affected the overall geometry and sulphur content of coal seams at Line Creek but has had little influence on abundance or mineralogy of the coal ash. Seams in the coastal plain (lower) unit are thick and laterally extensive while those in the fluvial plain (upper) unit are more numerous but generally thinner and less laterally continuous. Localised changes in coal seam geometry occur, and may be related to the sedimentology of the coal measures, these include seam splitting, erosion and differential compaction. The ash content and ash mineralogy of the coal does not correlate with the sulphur content or sedimentology of the Mist Mountain Formation coal. The vitrinite content of the coal increases up section.

2.9.1. - DEPOSITIONAL CONTROLS ON SEAM THICKNESS

2.9.1.1. - Partings between Seams

Splitting of coal seams into multiple plies is an important feature of Mist Mountain Formation coal. Splitting is often abrupt and the change in parting thickness rapid. The abrupt nature of the splitting is often undetected in widely spaced drill holes and may cause problems during mining. All seams in the lower unit split into two or three major plies, and the number of partings increase toward the east. Lower unit plies tend to be laterally continuous over 100-1000's of metres (Fig. 2.21). Seams within the upper unit often split into discontinuous thinner plies that are only continuous on a scale of 10-100's of metres (Fig. 2.21). Partings in the lower unit generally consist of floodplain sediments whereas in the upper unit, crevasse splay facies sediments and occasionally small channel sandstones occur. Contacts between coal and overlying partings are generally sharp or erosional. The lateral continuity of partings in the lower unit suggests splitting was driven by a regional control, such as increases in subsidence rates towards the centre of the basin (Fielding, 1987). In contrast, the less laterally continuous partings of the upper unit

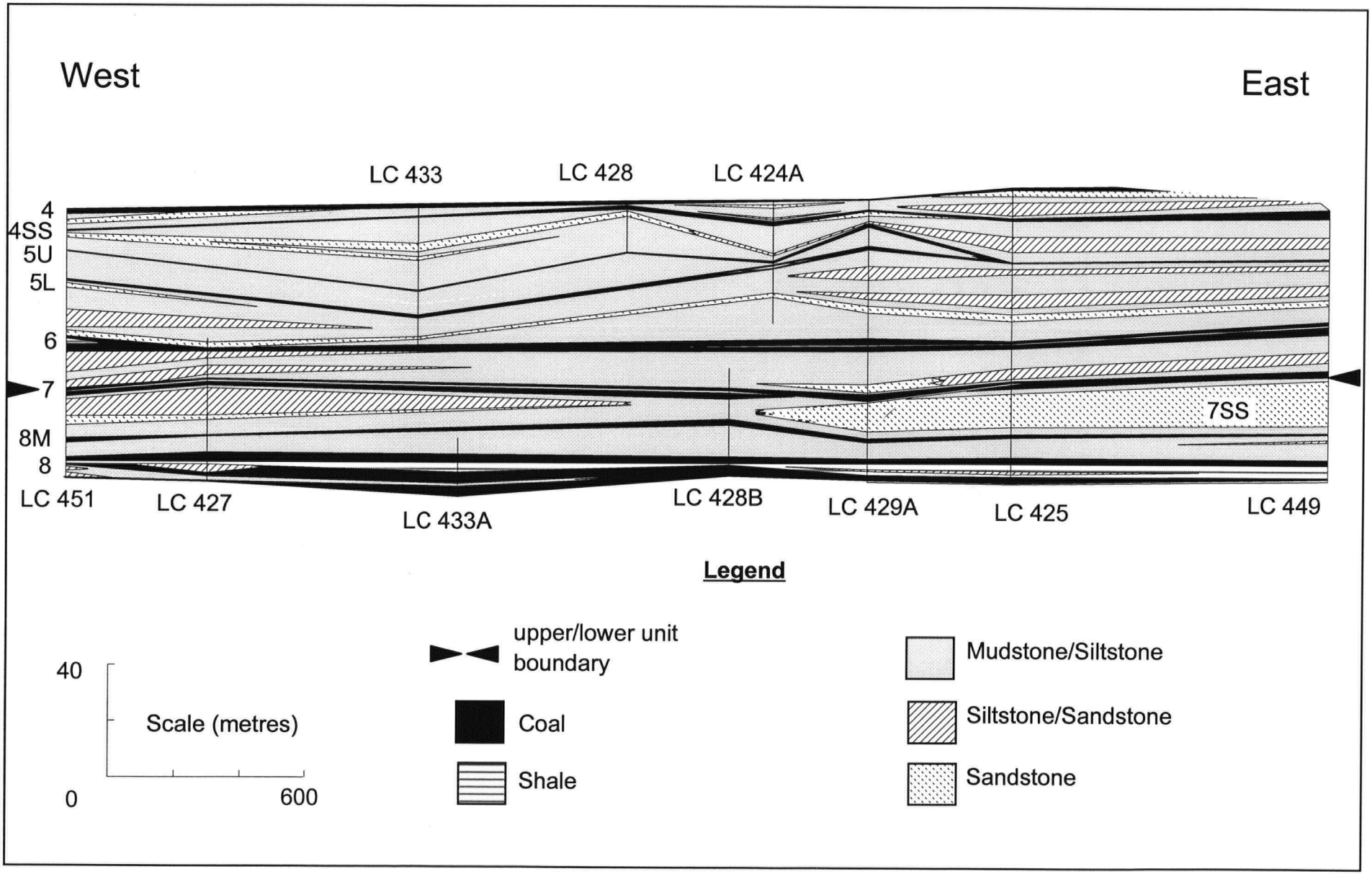

Figure 2.21 - Stratigraphic cross section 9. Variation in seam splitting between the upper and lower units of the Mist Mountain Formation at Line Creek. Refer to figure 2.5 for location of cross section.

were probably controlled by more localised factors such as differential compaction and/or contemporaneous fluvial sedimentation (Fielding, 1987).

2.9.1.2. - Erosion

Erosion of coal by overlying sediments has affected the geometry of coal seams in the Mist Mountain Formation. Channel sandstones and crevasse splays have erosional contacts with underlying coal while floodplain facies have gradational contacts. Where channel sandstones overlie coal seams, erosion has often completely to partially removed the coal. For example, 9 seam has been removed from large regions of the study area by 9 sandstone, and both 5 and 6 seams have been locally eroded by 4 sandstone. (Fig. 2.22a) Erosion by crevasse splays is limited to localised removal of the upper portions of seams (Fig. 2.22b). Termination of peat deposition by crevasse splay or floodplain facies sediments indicates flood related sedimentation, whereas erosion by channel sandstones suggests a fundamental change from peat to fluvial sedimentation, often with a hiatus between the two modes of deposition.

2.9.1.3. - Differential Compaction

Differential compaction plays two opposite roles in determining coal seam and parting geometry at Line Creek, depending on local depositional conditions. Where the floodplain is amenable to peat accumulation, less compactable areas such as above channel sandstones form topographic highs. These raised areas have less accommodation space than more compressible areas, so are subjected to less peat accumulation and clastic deposition (also see Bustin and Dunlop, 1992). An example is seam 8R, which thins from an average of 3.6 metres away from the 9 sandstone, to average 1.5 metres directly above the sandstone (Fig. 2.23a). On the other hand, if the floodplain is low-lying, areas that are less compacted, such as those underlain by mudstone and siltstone, will be more likely to accumulate thick deposits of peat. Low-lying peat mires will also be prone to flooding and clastic deposition (Bustin and Dunlop, 1992). Seams that thicken where they overlie channel sandstones include the 10A seam, which thickens from an average 1.8 metres away from 10 Sandstone, to 4.1 metres where it directly overlies the sandstone.

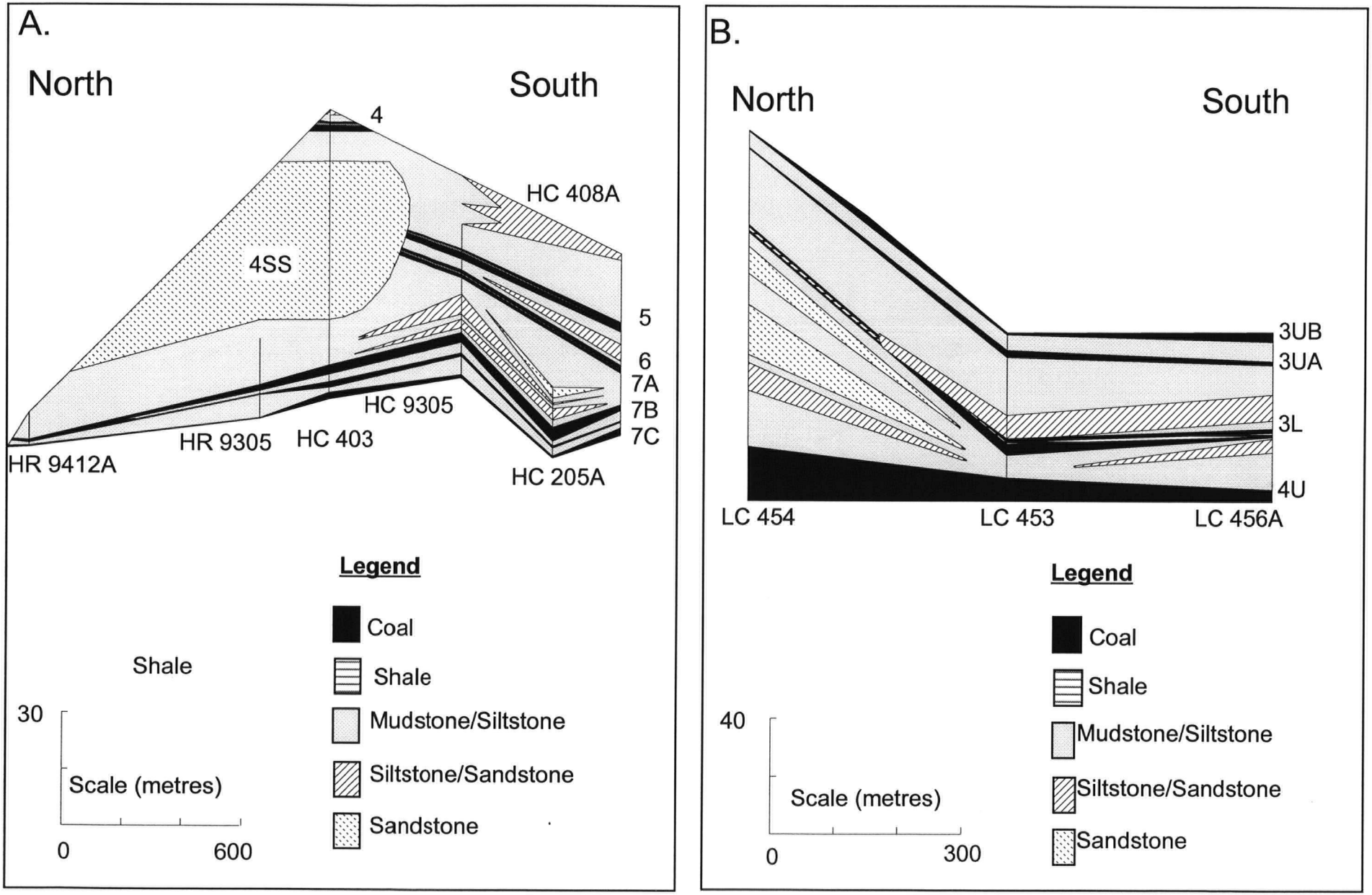

Figure 2.22 - Stratigraphic cross sections illustrating erosion of coal by a) - channel sandstones (cross section 3) and b) - crevasse splays (cross section 8). Refer to figure 2.5 for location of cross sections.

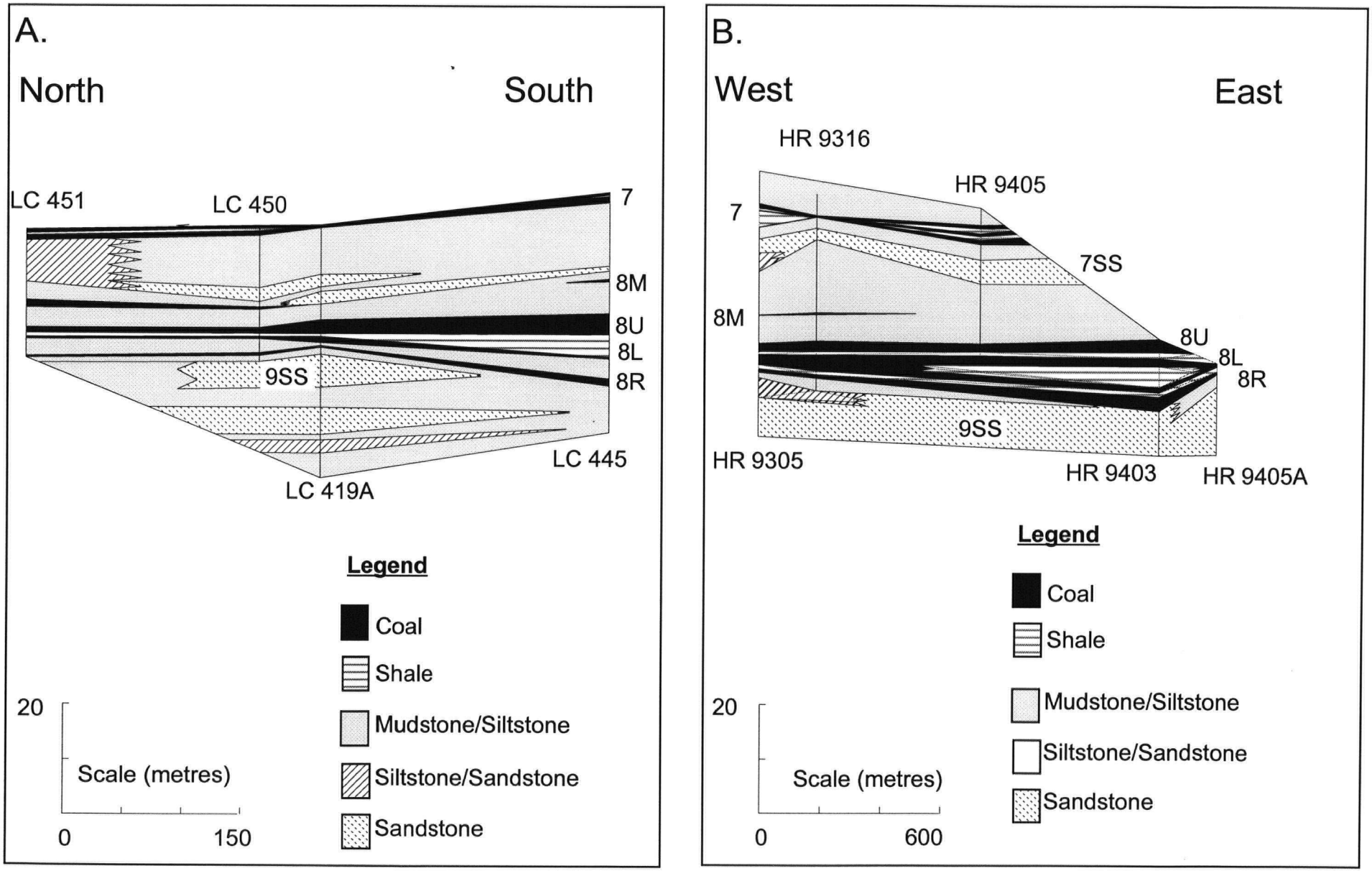

Figure 2.23 - Stratigraphic cross sections illustrating variation in coal seam thickness over channel sandstones. a) - 8 seam and partings thin directly over 9 sandstone (cross section 10). b) - 8 seam and partings thicken directly over 9 sandstone (cross section 9). Refer to figure 2.5 for location of cross sections.

Differential compaction is a localised effect because seams such as 8 seam, thicken and thin over channel sandstones in different parts of the study area (Fig. 2.23). Differential compaction is also reflected in seam partings. Partings may either thin or thicken where coal seams directly overlie channel facies sediments (Fig. 2.23) or they may disappear completely (Fig. 2.24). Haszeldine (1989) suggests that the effects of differential compaction are over-stated in the literature. He proposes coal seam thickness is more likely to be controlled by compaction of much thicker sedimentary units than just the facies directly underlying the seam. However in this study, large changes in coal thickness can be correlated to the lithology of underlying sediments.

2.9.2. – DEPOSITIONAL CONTROLS ON ASH MINERALOGY AND ABUNDANCE

2.9.2.1. – Ash Mineralogy

The ash mineralogy of the Mist Mountain Formation coal at Line Creek consists largely of quartz, kaolinite, illite and mica. Minor variation occurs in the trace mineral content of the coal, which includes smectite, vermiculite and interstratifed mica-vermiculite. An authigenic origin for the mineral matter would explain the lack of relationships between ash content and sedimentology in the Mist Mountain Formation. However, scanning electron micrographs (Fig. 2.25) show the grains have mechanically abraded edges, which indicates a detrital origin. Mineralogy of the Line Creek coal does not vary significantly with increasing ash content. This suggests the amount of clastic material entering the mires varied, but the source was constant throughout deposition.

2.9.2.2. - Ash Content

Ash content of Mist Mountain Formation coal at Line Creek does not reflect the proximity of channel sandstones (Fig. 2.26), nor is there a relationship between seam thickness and ash content (Fig. 2.27). There is variation in the ash content patterns of plies within a seam. The ash content pattern of plies within some seams are alike, suggesting there was a depositional or diagenetic control on the ash content of the coal. However, other seams show no relationships. For example, by plotting the ash content of two

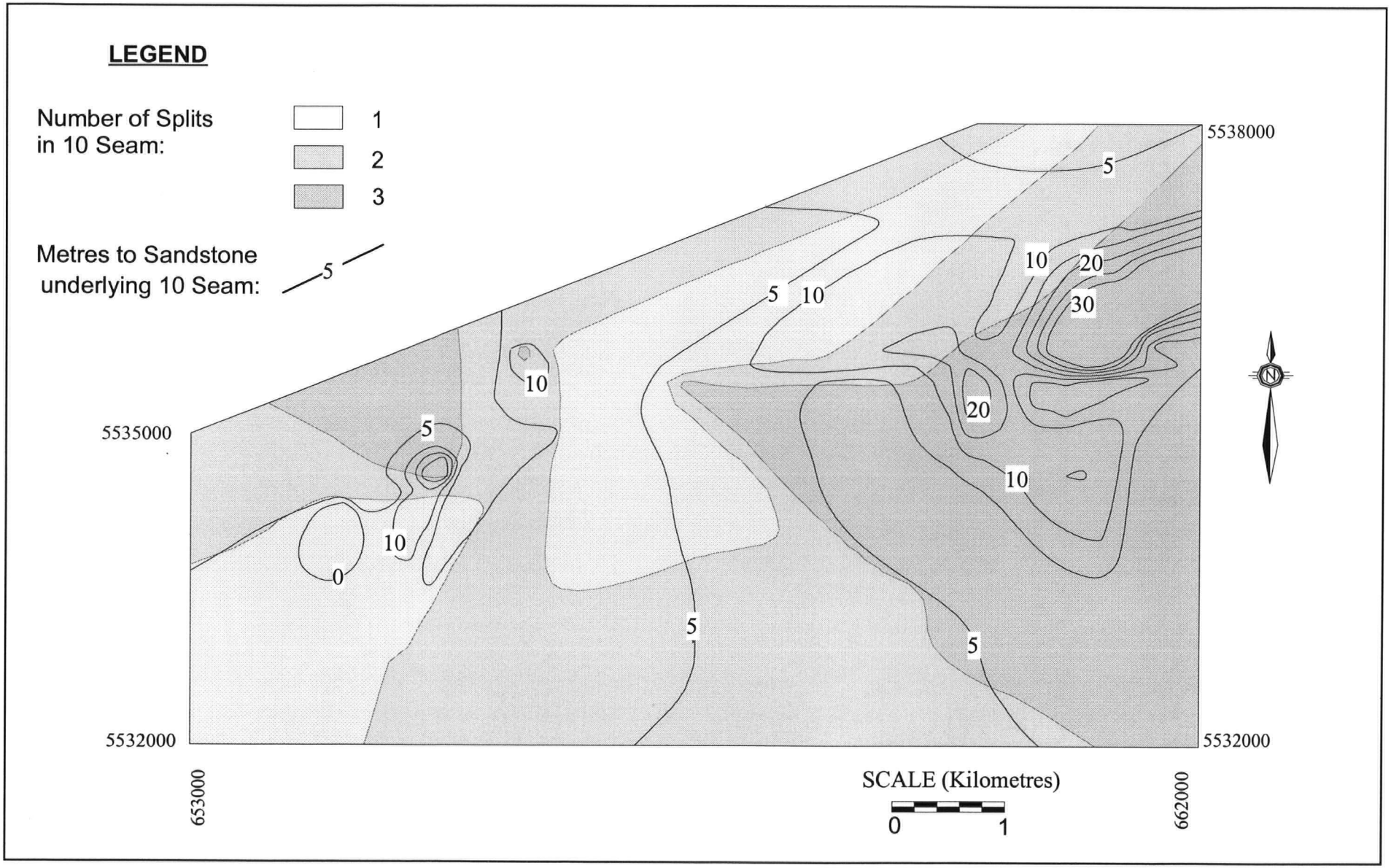

Figure 2.24 - Isopach map illustrating a weak correlation between the number of plies in 10 seam and the distance between 10 seam and underlying sandstone. The number of plies tends to increase with increasing distance from the underlying sandstone.

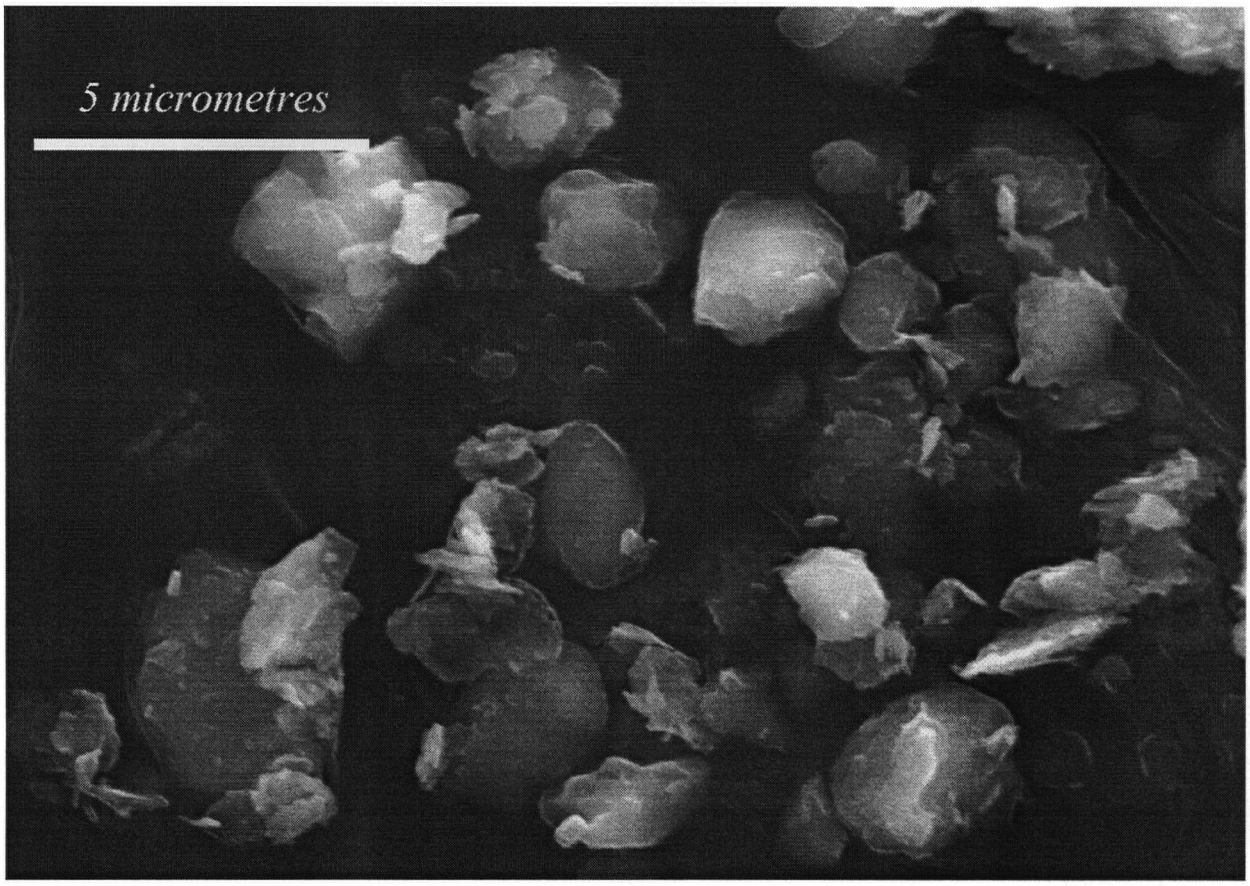

Figure 2.25 - Scanning electron micrograph of detrital quartz grains in 6 Seam at Line Creek.

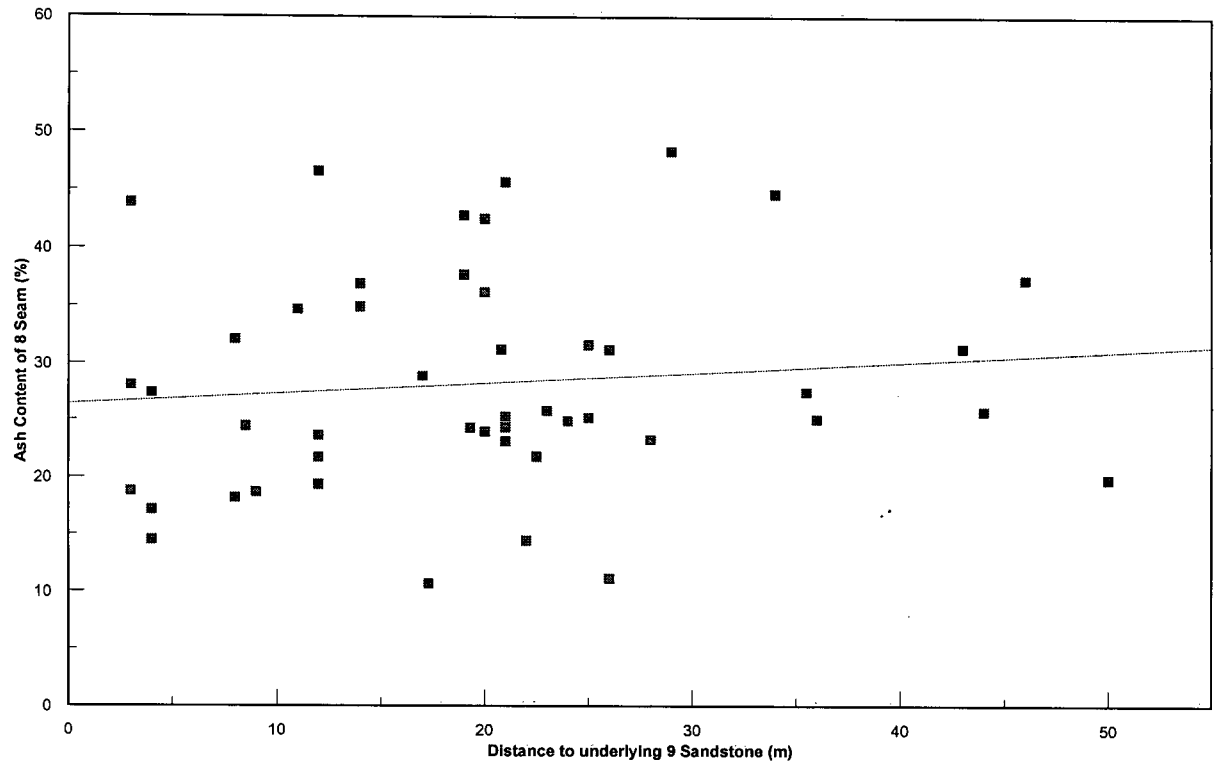

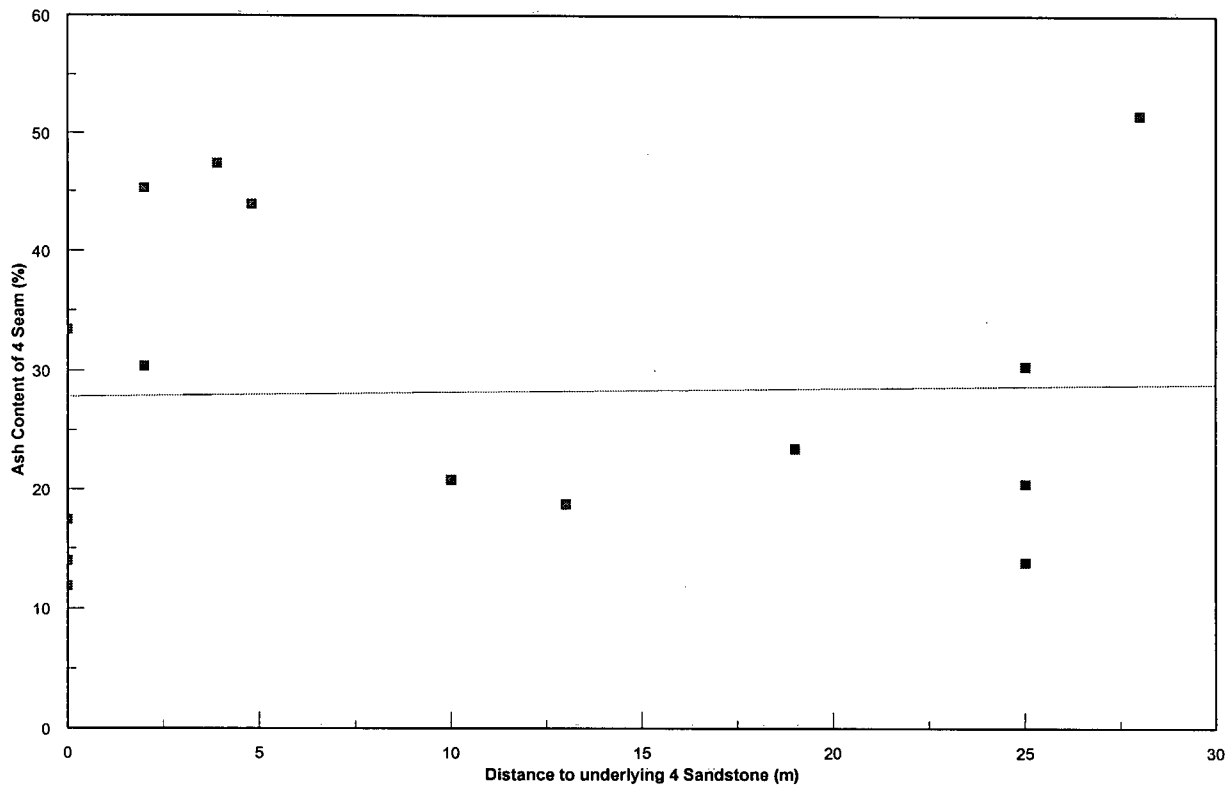

Figure 2.26 - Cross plots illustrating the lack of correlation between ash content and distance to underlying channel sandstone for a) - 8 seam and 9 sandstone, b) - 4 seam and 4 sandstone.

plies from the same seam at corresponding locations, the plies A and B of 7 seam have similar patterns of increasing ash content, but plies U and L of 8 seam show no relationship. (Fig. 2.28).

Relationships between ash content and seam partings are variable throughout the Line Creek area. The ash content increases toward clastic partings in some seams, but not in others (Fig. 2.29). At least two types of parting deposition are required to explain this variation. Firstly, a gradual introduction of clastics into the peat mire and an equally slow return to peat deposition would result in ash content increasing around partings. On the other hand, an abrupt transition from peat to clastic deposition would not be reflected in the ash content around partings. The abrupt transition may occur by either deposition of peat halting due to drying out or inundation of the peat mire prior to clastic influx, or erosion of the peat by incoming sediment during a flood event with no filtering down of clastics into the underlying peat.

2.9.3. - DEPOSITIONAL CONTROLS ON SULPHUR CONTENT

The sulphur content of all coal seams at Line Creek averages 0.5% (Fig. 2.30) and no individual seam contains greater than 1.0% sulphur. In general, the thicker the seam, the less sulphur it contains (Fig. 2.31). Thick coal seams of the lower unit tend to have less sulphur than the thinner seams of the upper unit (Tables 2.1 & 2.2 and Fig. 2.30). However, ash content does not significantly correlate with the sulphur content of the Mist Mountain Formation coal (Fig. 2.32).

High sulphur content in coal is generally attributed to incursion by marine or brackish water during peat deposition and compaction (e.g., Horne et. al. 1978). However, Phillips et. al. (1994) show that short term inundation of modern peat swamps affects the type of sulphur minerals present but does not change the total amount of sulphur in the peat. Therefore, the low sulphur content of the Mist Mountain Formation coal indicates only that they were not subjected to long term inundation by marine waters. Further investigation of sulphur types within the coal is needed to determine if they were influenced by short term marine flooding.

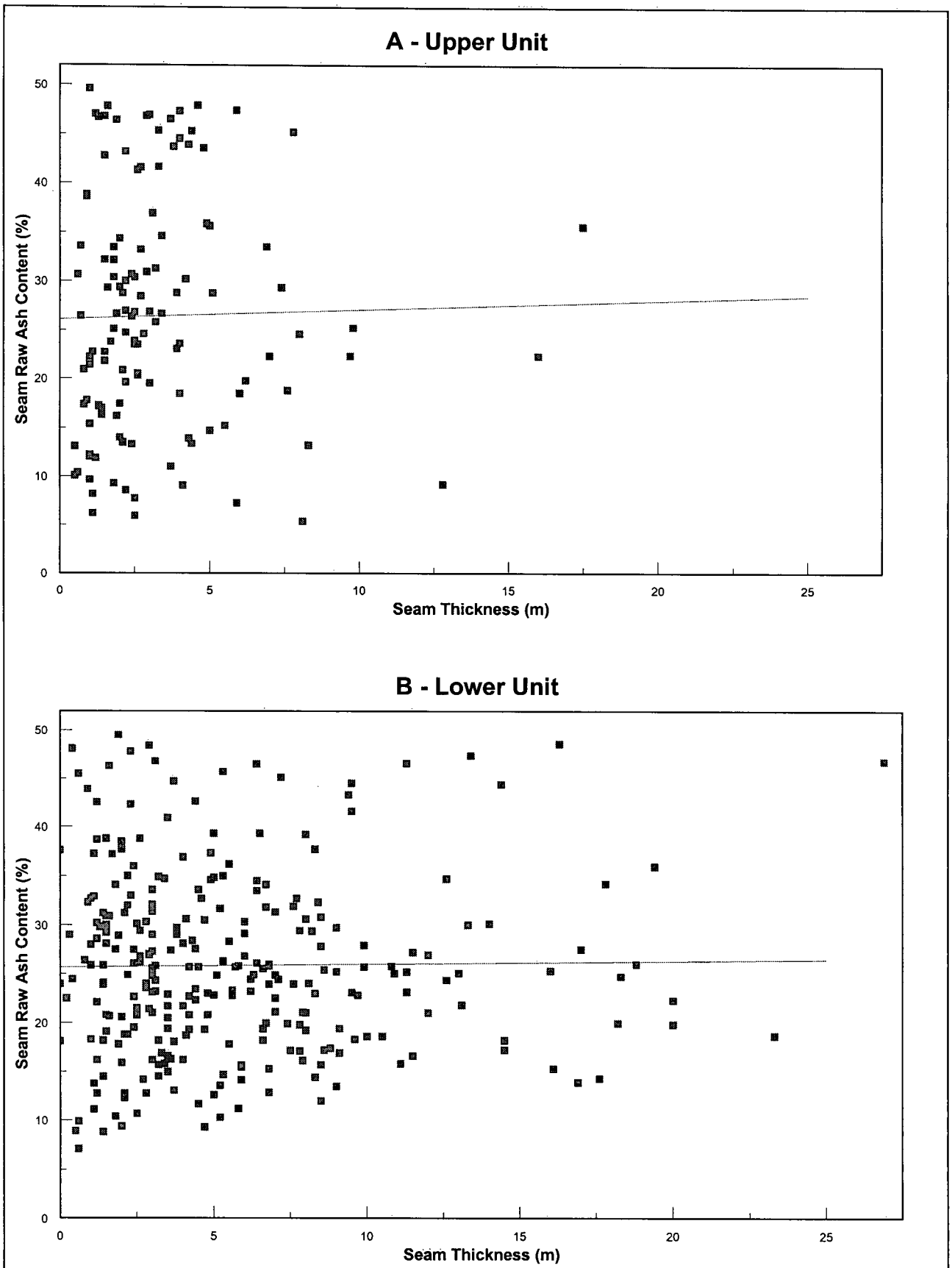

Figure 2.27 - Cross plot illustrating the lack of correlation between ash content and seam thickness of **a)** - the upper unit and **b)** - the lower unit of the Mist Mountain Formation.

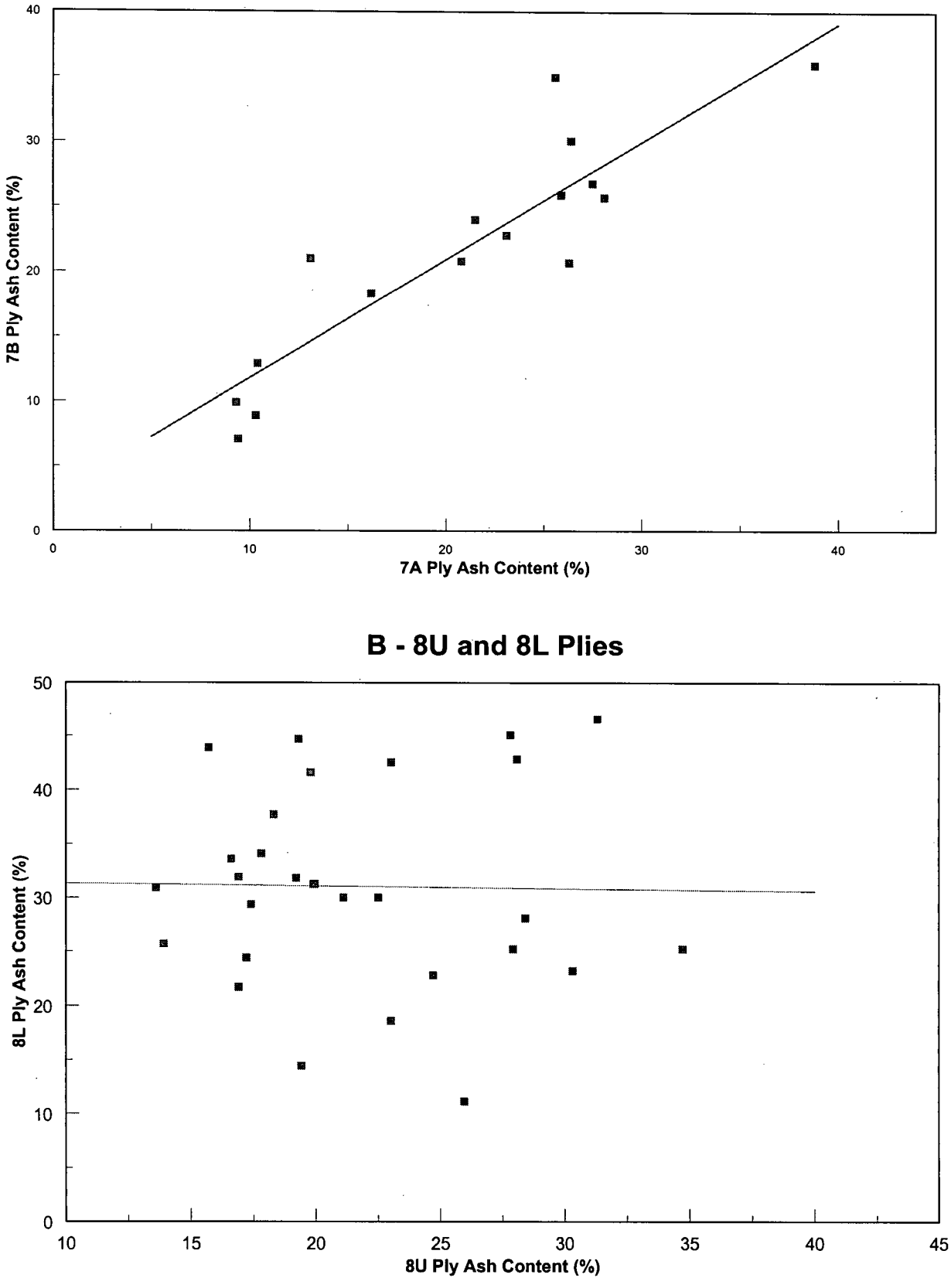

Figure 2.28 - Cross plot of the ash content of plies from **a) -** 7 seam and **b) -** 8 seam. Note the correlation between plies of 7 seam and lack of correlation in 8 seam.

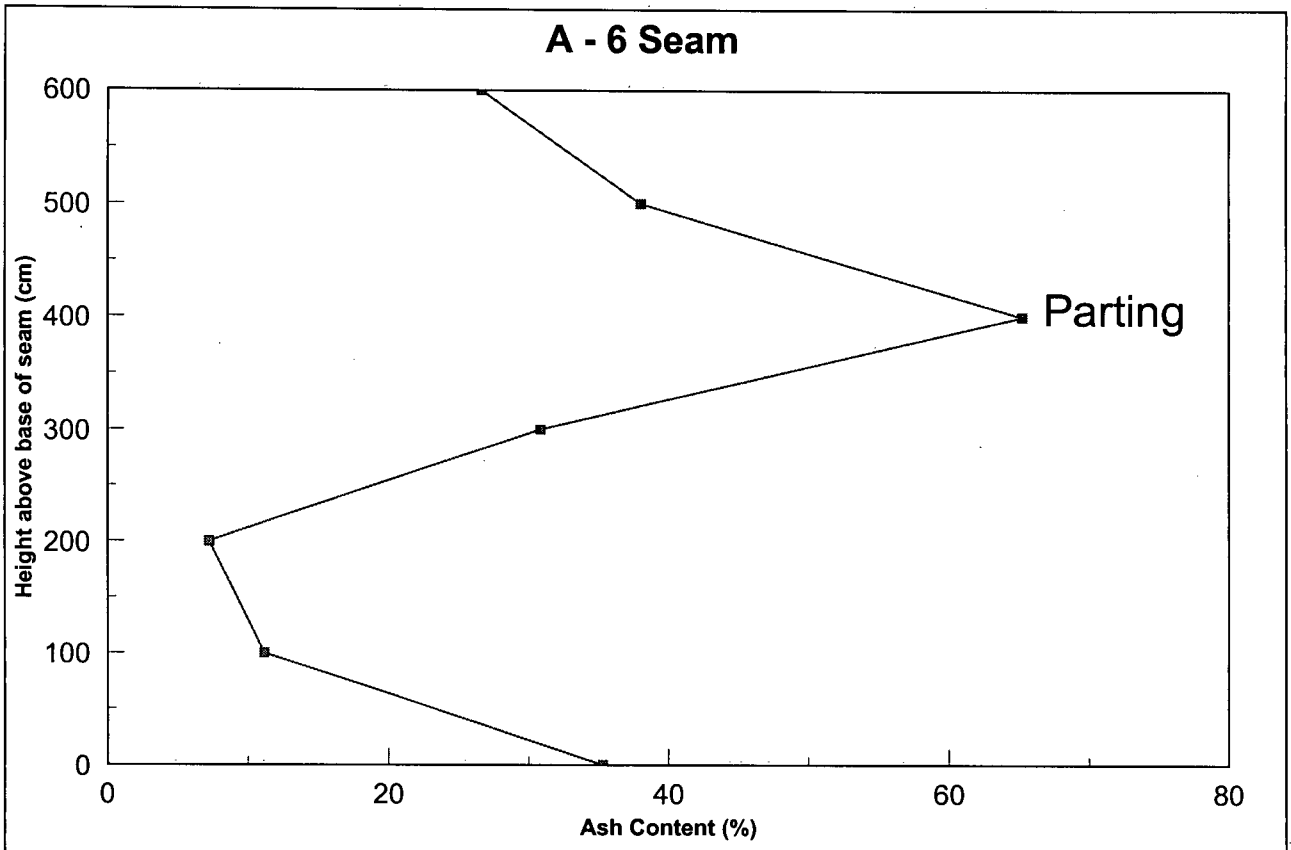

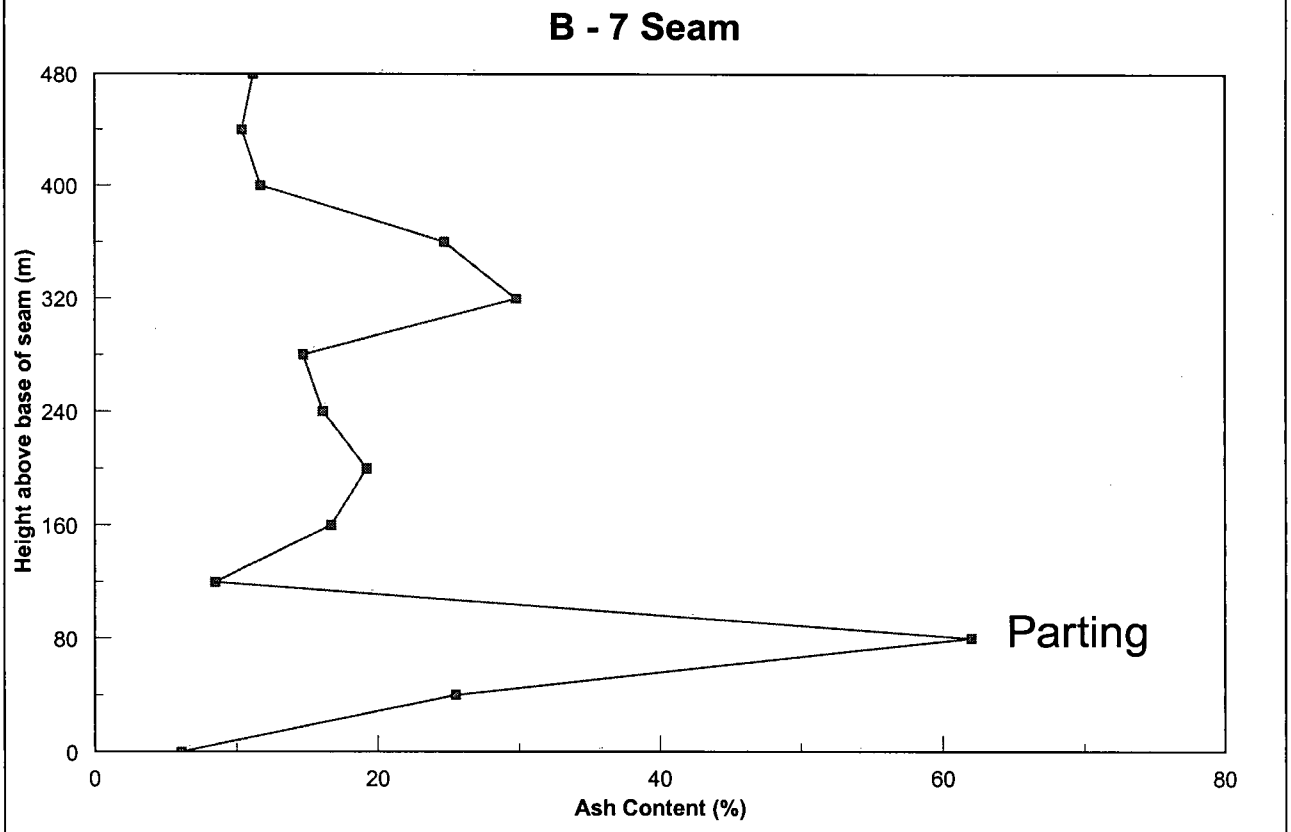

Figure 2.29 - In-seam variation in ash content of a) - 6 and b) - 7 seams.

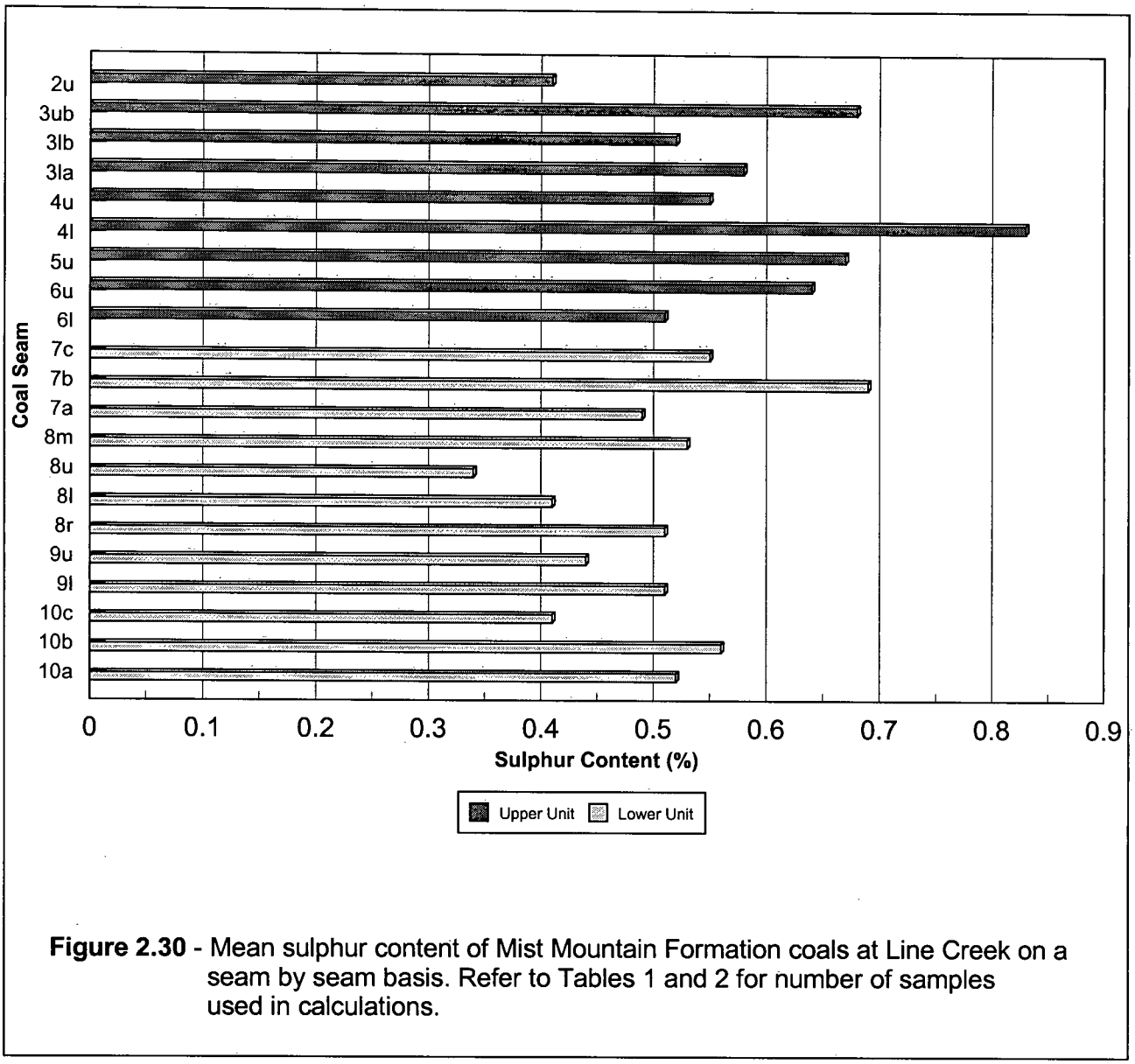

Figure 2.30 - Mean sulphur content of Mist Mountain Formation coals at Line Creek on a seam by seam basis. Refer to Tables 1 and 2 for number of samples used in calculations.

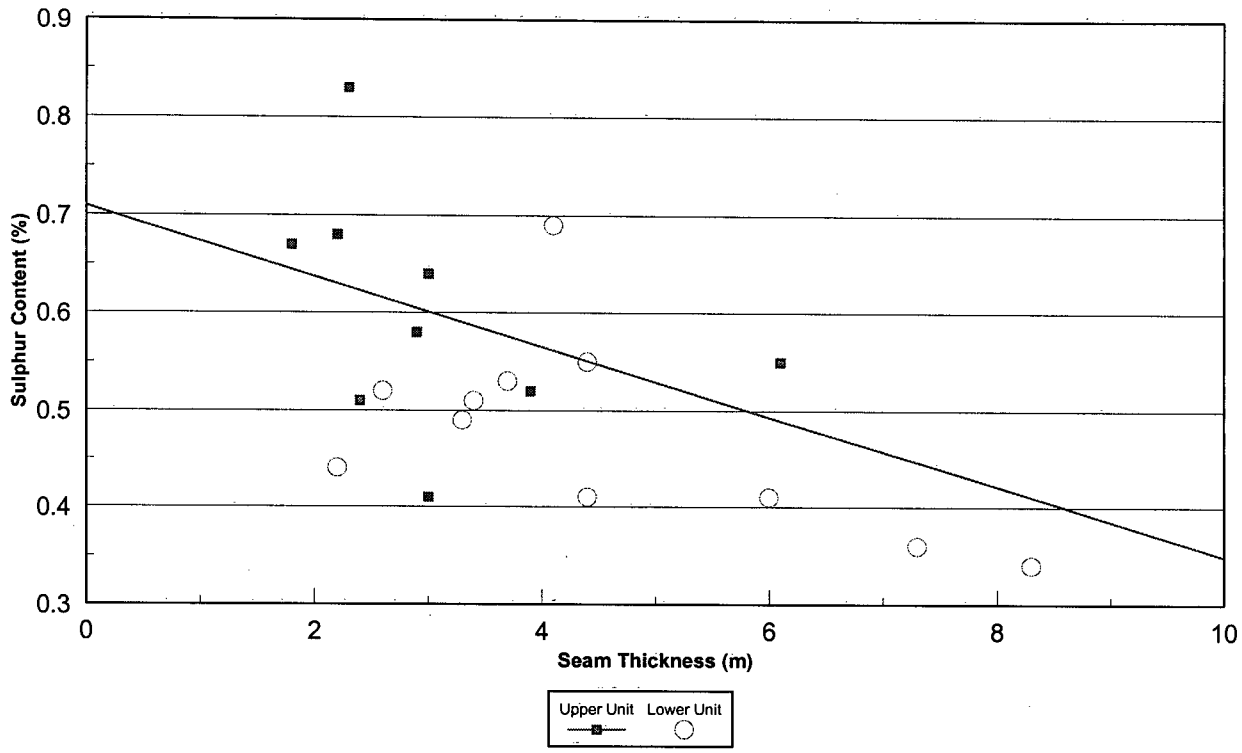

Figure 2.31 - Weak negative correlation between coal seam thickness and sulphur content of the Mist Mountain Formation coals at Line Creek (R2= 0.145).

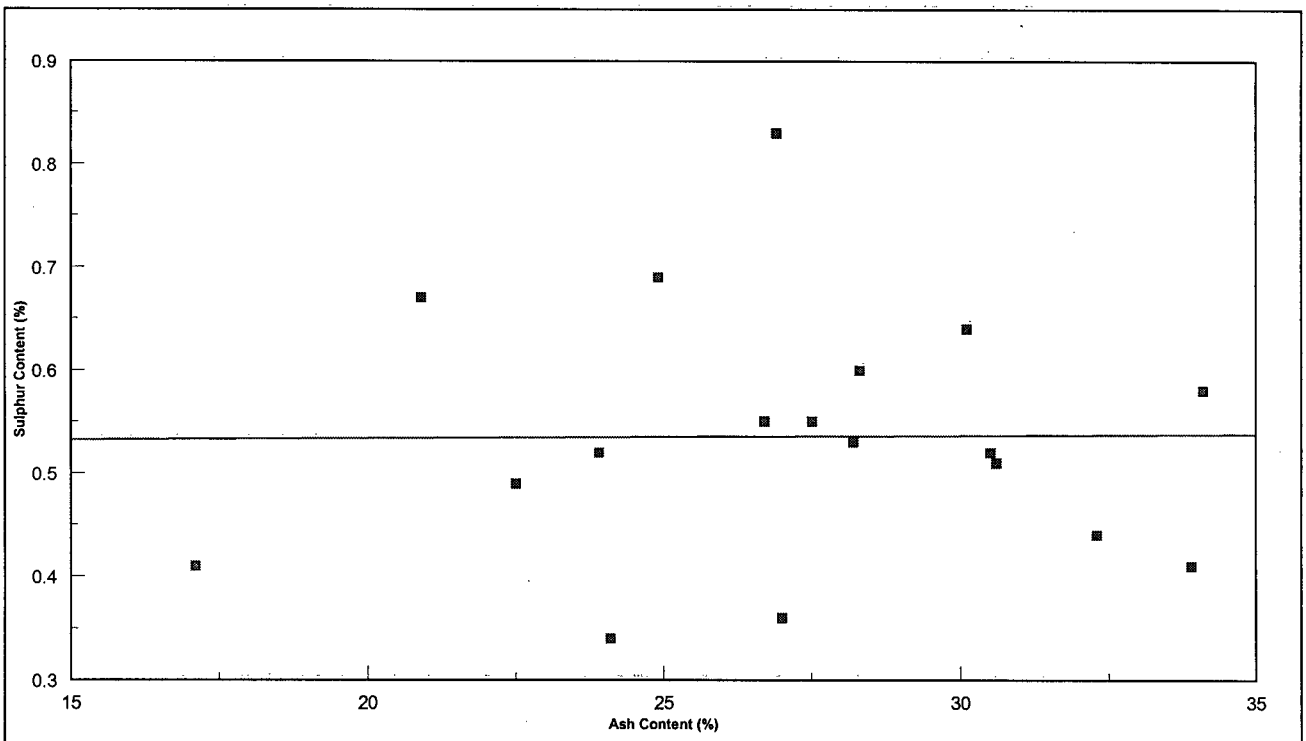

Figure 2.32 - Lack of correlation between ash and sulphur contents of the Mist Mountain Formation coal.

2.9.4. - MACERAL CONTENT OF MIST MOUNTAIN FORMATION COAL

Variation in the maceral composition of coal is a function of vegetation type, water table level, degree of decomposition and rate of peat accumulation (Ting, 1989). The three maceral groups, vitrinite, inertinite and liptinite, may be differentiated by origin and morphology. Liptinite is derived from hydrogen rich plant parts such as resins, cuticles, spores and pollens. Vitrinite is derived from lignin and cellulose from plant cell walls, which are humified before burial. Inertinite is also derived from lignin and cellulose but has undergone dehydration and oxidation or
charing before burial (Stach, 1982). Inertinite and vitrinite occur in structured (telo-), unstructured (detro-) and gelified (gelo-) forms.

2.9.4.1. - Measuring Coal Facies Variation

Petrographic indices such as the tissue preservation (TPI) and gelification indices (GI) can be used to examine the effects of vegetation type, water table level, decomposition and rate of accumulation on coal facies (Diessel, 1992). Although not originally designed for the Mist Mountain Formation, the TPI and GI do provide a means of interpreting the maceral content of the coal.

The TPI measures the preservation of cellular structure in plant tissue within coal. The TPI as defined by Diessel (1992) is:

$$TPI = \frac{\text{telo-vitrinite + telo-inertinite}}{\text{detro-vitrinite + gelo-vitrinite + detro-inertinite + gelo-inertinite}}$$

The GI is considered to measure the level of the water table within a peat mire. Diessel (1992) defines the GI as:

$$GI = \frac{\text{vitrinite + gelo-inertinite}}{\text{telo-inertinite + detro-inertinite}}$$

High TPI values correspond to increasing levels of tissue preservation in coal and is interpreted to reflect increasing percentage of arboreal vegetation in the peat mire (Lamberson et. al., 1991). The TPI will also be high if coal contains large proportions of telo-inertinite (fusinite and semifusinite). High GI values correspond to a high vitrinite content in coal. Formation of vitrinite is favoured by persistently wet peat with low oxygen levels, suggesting a high water table. Low vitrinite content and hence low GI indicates increased oxidation of the coal (Lamberson et. al., 1991).

The interaction of vegetation types and water table level of a peat can be analysed by plotting TPI and GI on a coal facies diagram (Fig. 2.33). Diessel (1986) developed the coal facies diagram for Permian Australian coal. Kalkreuth and Leckie (1989); Lamberson et. al. (1991); Kalkreuth et. al. (1991) and others have adapted the coal facies diagram for Canadian Cretaceous coal. The coal facies diagram is divided into four parts based on vegetation types and water table level. Table 2.3 gives a full description of the types of coal and environments found in each section of the coal facies diagram.

The use of coal facies diagrams and maceral ratios as indicators of depositional environment has been controversial. Crosdale (1993) found that the use of maceral ratios led to misinterpretation of the depositional environment of high bituminite coal from New Zealand. He also investigated modern analogues and suggests the theoretical basis for discrimination of mire type by maceral ratios is not well founded because the ratios tend to simplify natural processes. If a coal lacks significant quantities of telo-vitrinite and detro-inertinite, (possibly due to high rank) such as Mist Mountain Formation coal (Cameron, 1972), TPI = inertinite over vitrinite and GI = vitrinite over inertinite. The trend from a cross-plot of these parameters on a coal facies diagram may mask true depositional environments of the coal. Despite these problems, maceral ratios remain one of the only means available to interpret and compare maceral content of coal, but should be used with caution.

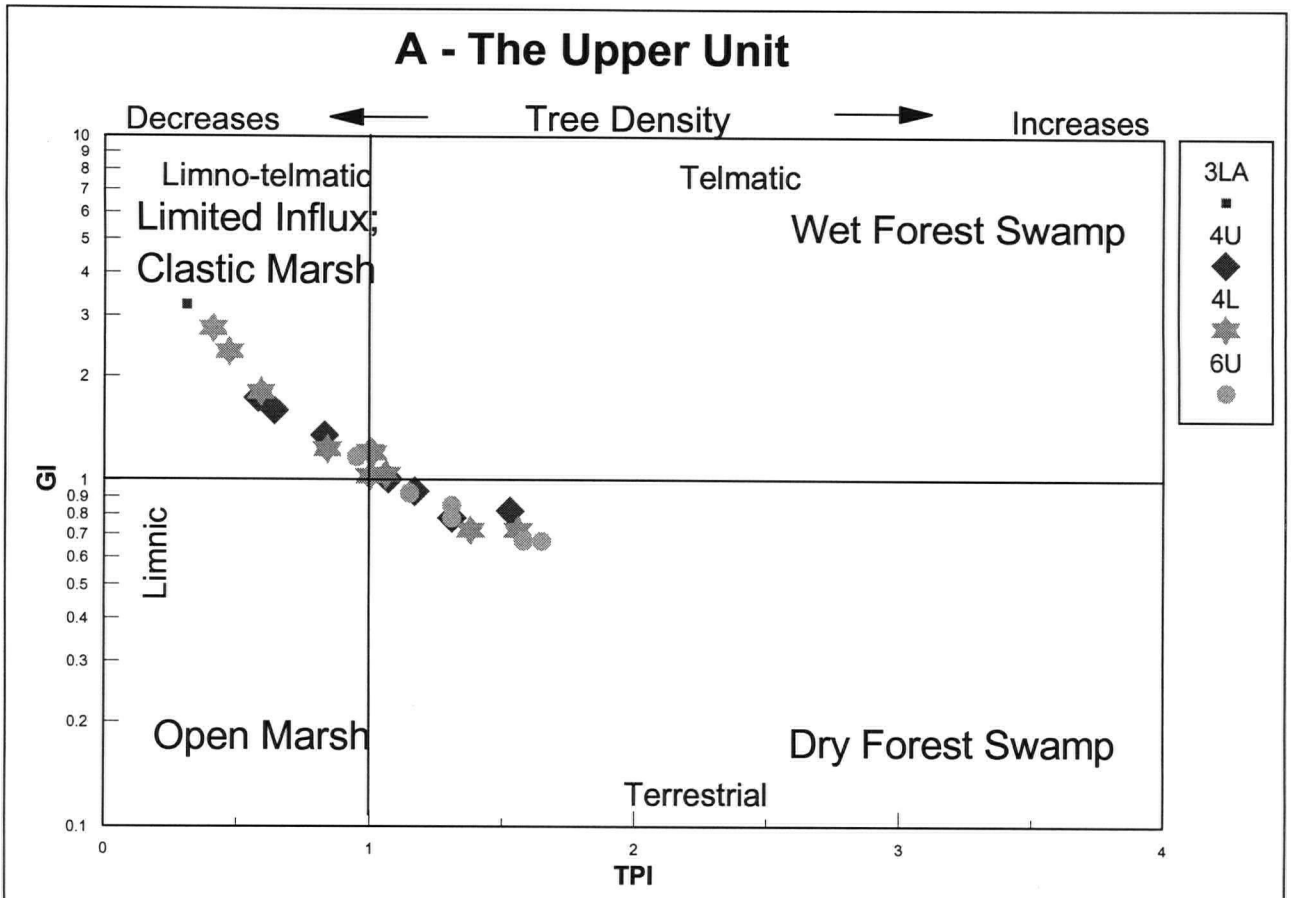

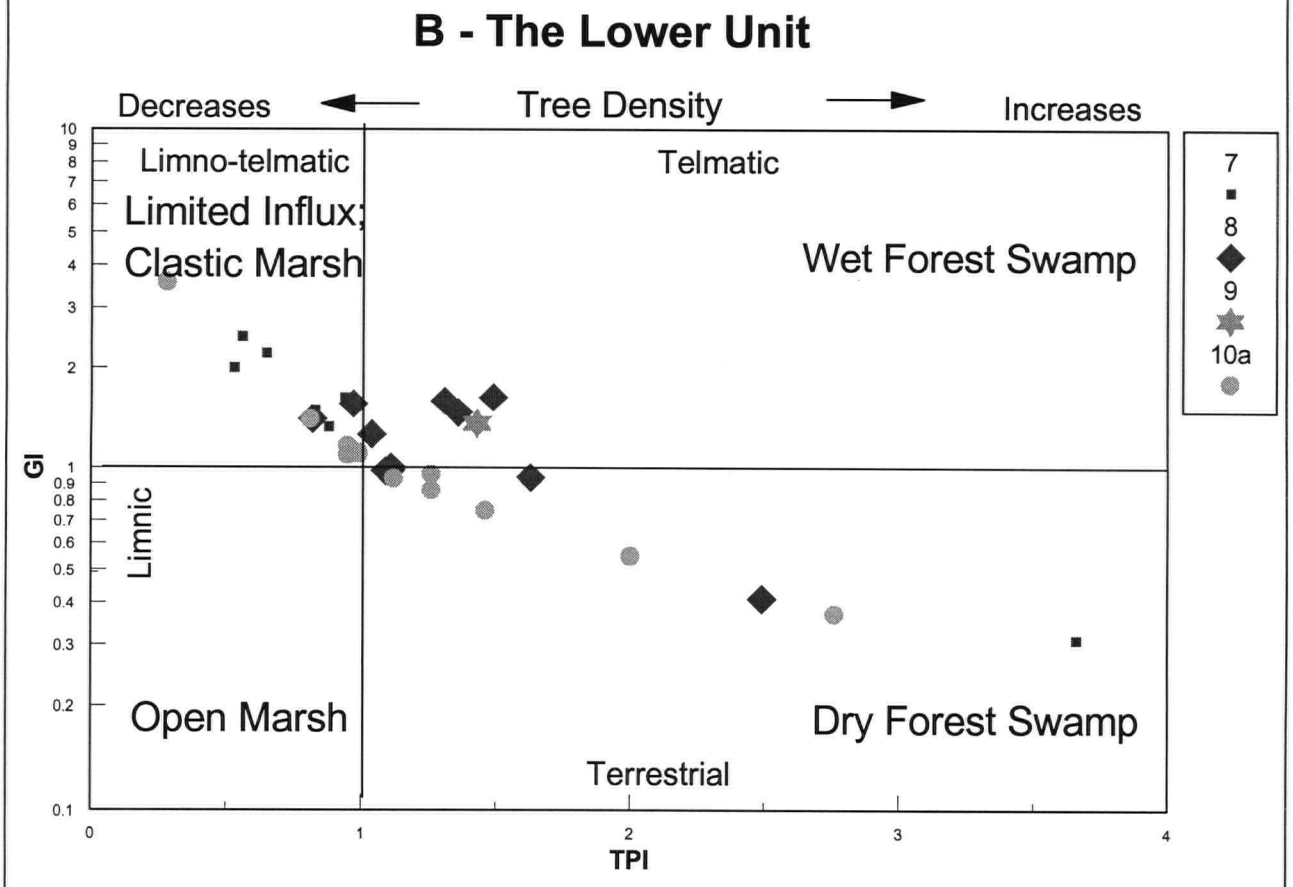

Figure 2.33 - Coal facies diagram of a) - the upper unit and b) - the lower unit of the Mist Mountain Formation.

	Low TPI	High TPI
High GI	**Origin:** - Forested peatlands from strongly decomposed wood in telmatic or limnotelmatic setting when high ash and epiclastic bands - Herbaceous plants in marshes when high ash and epiclastic bands - Herbaceous plants in continuously wet raised bogs in telmatic or limnotelmatic conditions when low ash and no epiclastic bands **Preservation**: - Advanced humification and strong gelification of plant tissue.	**Origin:** - Forested peatlands (telmatic swamps) when high in ash and/or interbedded with epiclastic stone bands. - Forested, continuously wet raised bogs when low in ash. **Preservation:** - Mild humification and strong gelification of plant tissue due to high subsidence rate.
Low GI	**Origin:** - Slowly subsidising, intermittently dry swamps from aerobically decomposed plants. - Redistributed subaqueous sediment. - Slowly subsiding relatively dry raised bogs. **Preservation:** - Advanced humification and mild gelification of plant tissue.	**Origin:** - Intermittently dry forested swamps when high in ash. - Forested raised bogs when ash is low to moderate. **Preservation:** - Mild humification and mild gelification of plant tissue.

Table 2.3 – Summary of the relationships between coal facies indices and conditions of coal formation (Modified from Deissel, 1992).

2.9.4.2. - Trends in Maceral Content at Line Creek

Vitrinite and semifusinite are the dominant macerals in the Mist Mountain Formation coal at Line Creek. The average vitrinite content of the seams ranges from 35 to 76% and is primarily in the form of unstructured detrovitrinite (Table 2.4). The coal contains between 21 and 50% semifusinite and fusinite accounts for up to 20% of the total maceral content. The Mist Mountain Formation coal lacks significant quantities of liptinite, macrinite, inertodetrinite and telovitrinite.

Seam	Samples	Vitrinite (%)			Inertinite (%)					Liptinite (%)	TPI	GI
		Telovit.	Detrovit.	Total	Semifus.	Fusinite	Macrinite	Other	Total			
3LA	1	0.3	76.0	76.3	21.0	2.6	0.0	0.1	23.7	0.0	0.31	3.23
4U	7	0.4	50.7	51.1	40.5	6.4	1.5	0.0	48.4	0.5	0.80	1.05
4L	10	1.6	53.5	55.3	36.4	7.8	0.7	0.6	45.5	0.1	0.93	1.41
6U	6	1.7	43.3	45.1	49.2	5.6	0.3	0.0	55.1	0.1	1.32	0.84
Upper	24										1.06	1.35
7	18	4.9	51.4	56.3	38.4	4.8	0.3	0.1	43.6	0.1	1.12	1.51
8M	1	-	-	53.0	26.2	19.6	0.7	0.5	47.0	0.0	-	-
8U	12	8.5	43.8	52.3	40.6	7.8	0.6	0.0	49	0.1	1.20	1.10
9	4	15.9	28.2	44.1	39.4	14.1	1.8	0.4	55.7	0.2	1.43	1.36
10B	3	-	-	34.7	49.7	14.3	1.2	0.1	65.3	0.0	-	-
10A	21	1.7	47.6	45.3	40.9	8.3	0.7	0.2	53.9	0.1	1.31	1.06
Lower	59										1.27	1.21

Table 2.4 – Summary of Point Counting results – Seam by Seam Basis.

Previous authors (Cameron, 1972; Pearson and Grieve, 1985; Dunlop and Bustin, 1987; Grieve, 1993) have noted a trend of increasing vitrinite at the expense of semifusinite up-section in the Mist Mountain Formation. Cameron (1972) related increasing vitrinite to a decreasing proportion of herbaceous vegetation up-section, but Grieve (1993) considers an increasing water table level up-section resulting in better tissue preservation a more likely explanation. Point counting results (Table 2.4) from this investigation indicate a similar trend of increasing vitrinite up-section (Fig. 2.34). The trend is a general one, the lowest seam is not the most semifusinite rich, nor is there a systematic increase in vitrinite between seams up-section, features also noted by Cameron (1972) and Grieve (1993).

Variation in maceral content within a single seam of the Line Creek coal is of the same order of magnitude as that between seams. Inter-seam variation in vitrinite content is up to 40%. However, all seams except 10B and 3LA contain between 45 and 60% vitrinite. The vitrinite content within each seam varies by up to 50%. The greatest in-seam variation generally occurs at the floor and roof of each seam (Fig. 2.35) due to marginal conditions for peat accumulation associated with the start and demise of the mire, which also suggests the contacts, are gradational. If samples from the floor and roof of the seams are discounted, compositional variation is still up to 30% within an individual seam. Such variation reflects fluctuations in mire conditions with time.

TPI values of the Mist Mountain Formation coal ranges from 0.3 to 1.5 (averaging 1.13) and are relatively constant throughout the succession. Kalkreuth and Leckie (1989) interpreted similar TPI values for the Early Cretaceous Gates Formation of northeastern British Columbia as a forest swamp paleoenvironment with periods of low water table during which oxidised and partially oxidised material was formed. The predominance of detrovitrinite over telovitrinite indicates decomposition of woody material occurred prior to burial (Kalkreuth and Leckie, 1989). GI values range from 0.8 to 3.2 (averaging 1.27), and increase up-section, mainly due to the relatively high proportion of fusinite and semifusinite (not gelified) to vitrinite (gelified) within the coal, especially in the lower unit.

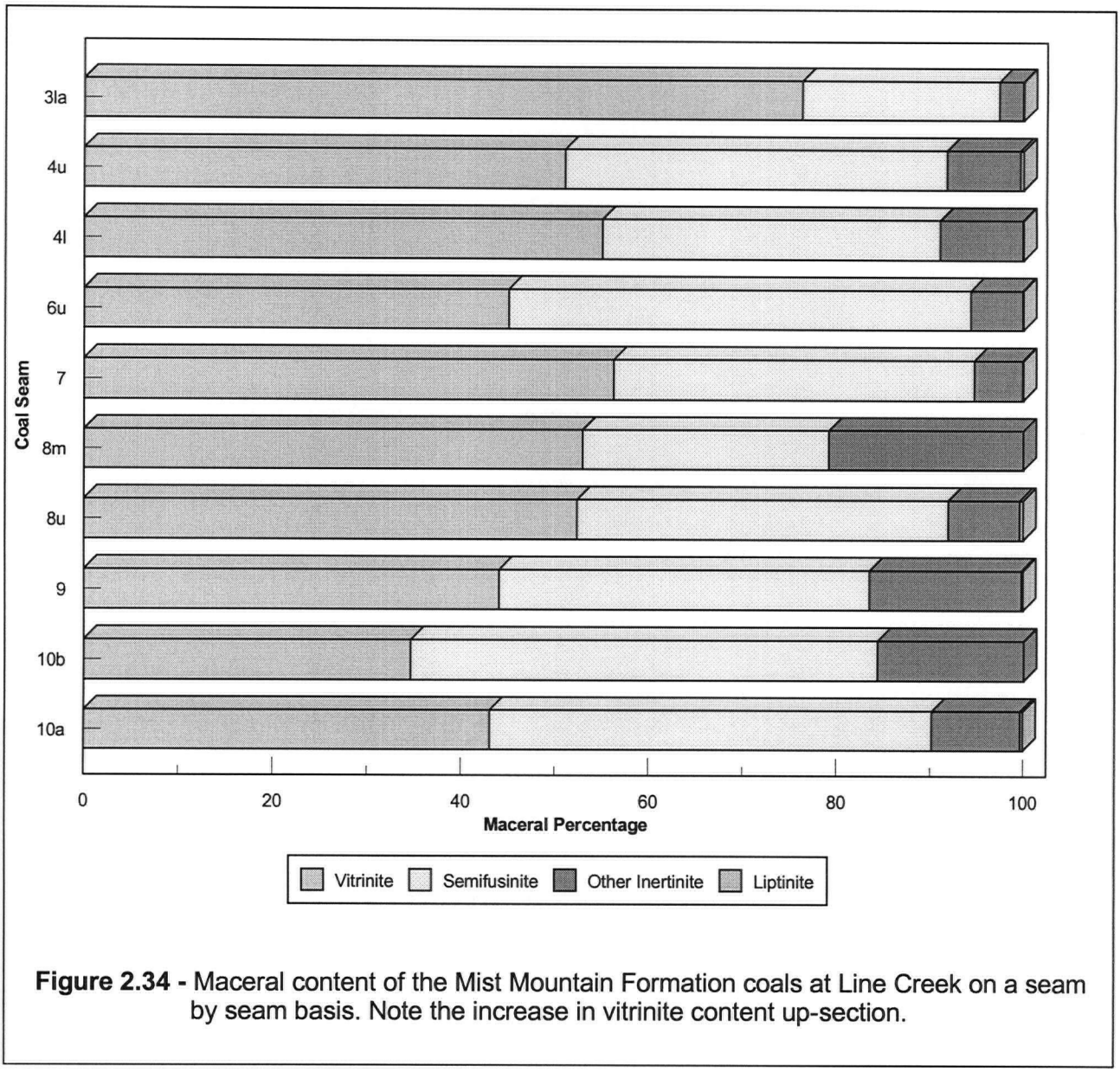

Figure 2.34 - Maceral content of the Mist Mountain Formation coals at Line Creek on a seam by seam basis. Note the increase in vitrinite content up-section.

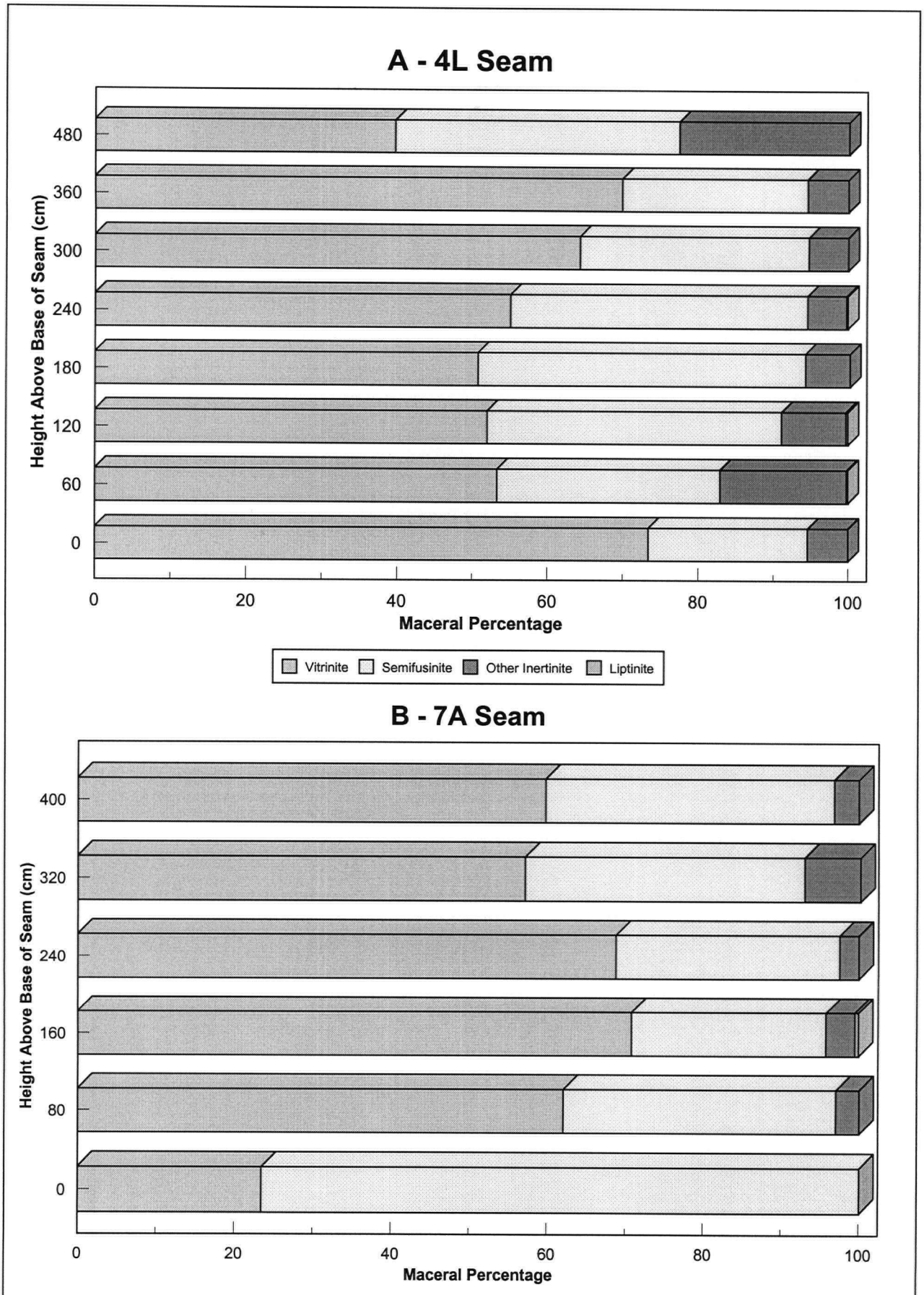

Figure 2.35 - Maceral content variation within a) - 4L and b) - 7A seams

The Mist Mountain Formation coal shows a continuous spectrum of depositional environments from herbaceous marshes to wet and dry forest swamps (Fig. 2.33) which probably represents evolution of the mires with time. Both the upper and lower units (Fig. 2.33) show similar facies trends, although there is more variation in the lower unit, possibly reflecting the larger amount of data available for the lower unit. The trends seen in figure 2.33 must be assessed with caution. The apparent lack of significant quantities of macrinite, inertodetrinite and telovitrinite may in part be due to the relatively high rank of the coal. The trend may be artificial only in that the high rank of the coal may be obscuring compositional variation.

2.10. - DISCUSSION

2.10.1. - DEPOSITIONAL ENVIRONMENTS

The Mist Mountain Formation is a regressive sequence that prograded to the north and northeast in response to uplift during the Columbian Orogeny (Jansa, 1972; Hughes and Cameron, 1985; Gibson, 1985; Dunlop and Bustin, 1987). Exposure of the underlying Morrissey Formation in the study area is limited, but where present, the thick sandstones appear consistent with a beach-ridge dune complex as proposed by Gibson (1985) and Dunlop and Bustin (1987).

Dunlop and Bustin (1987) interpreted the lower Mist Mountain Formation as a nonmarine lower coastal plain succession. A lack of lagoonal sediments suggests deposition on the coastal plain directly behind the beach-ridge dune complex of the Morrissey Formation (Dunlop and Bustin, 1987). Within the study area, the low sulphur content (<1%) and lateral continuity of facies within the lower unit supports a coastal plain depositional environment with little or no marine influence. There is no evidence that the channel sandstones of the lower unit are part of a deltaic distributory system (also see Gibson, 1985), however, the study area is too small to rule this out. Dunlop and Bustin (1987) also noted a lack of distributory channels. The absence of documented distributory channels suggests distributory sands were

reworked into the beach-ridge complexes of the Morrissey Formation by a wave-dominated delta (Bhattacharya and Walker, 1992). The upper Mist Mountain Formation has been interpreted as a fluvial-alluvial plain deposit (Gibson, 1985; Dunlop and Bustin, 1987) and results from the study area confirm this interpretation. Coal seams are numerous, laterally discontinuous and thicken locally as expected in a fluvial-alluvial depositional environment (Horne et. al, 1978).

Facies relationships within the units of the Mist Mountain Formation reflect the shift in depositional environment from coastal plain in the lower unit to fluvial-alluvial plain in the upper unit. This shift in depositional environment resulted in a change from alternating thick channel sandstones and coal seams with interspersed crevasse splay and floodplain sediments in the lower unit to floodplain dominated sediments with interbedded coal seams, crevasse splay and small channel sandstones in the upper unit. Coal seams increase in abundance but decrease in thickness and lateral continuity and channel sandstones decrease in abundance up-section. The ash and sulphur content and the ash mineralogy of the coal remain similar despite varying depositional environments. The geometry of the facies and the coal's maceral content are the only parameters that change significantly with the shift in depositional environment.

The Mist Mountain Formation coal at Line Creek shows a trend of increasing vitrinite up-section. Detrovitrinite (non-structured) is dominant over telovitrinite (structured) which indicates the increase in vitrinite is due to increasing arborescent vegetation, not greater tissue preservation. Variation within seams is greatest at the roof and base, reflecting changing conditions in the peat mire with time.

2.10.2. - DEPOSITIONAL MODELS

To understand relationships between sedimentology and coal characteristics, associations between peat mires and clastic sedimentation at the time of deposition must be examined. There are three main possible associations between modern peat mires and fluvial sediments, 1) simultaneous deposition of peat and clastics; 2) peat accumulation protected from clastic sedimentation by deposition in domed mires; and 3) peat accumulation during a hiatus in clastic deposition (McCabe, 1984).

2.10.2.1. - Simultaneous Peat and Clastic Deposition

Depositional models for fluvially deposited coal-bearing sequences have evolved from Fisk's (1960) examination of peat in overbank regions of the Mississippi River (Fig. 2.36). In this model, peat accumulates in mires close to meandering rivers and crevasse splay and levee deposits from the river form partings within the coal (for example: Horne et. al., 1978; Gersib and McCabe, 1981). In such a depositional model, coal and fluvial sediments accumulate simultaneously. Therefore the proximity of active river channels to peat accumulation, the presence of clastic partings within seams and the lateral distribution of peat accumulation influences the quality of the coal. Coal seams formed in close proximity to an active river system tend to have high ash contents, are laterally discontinuous, and form pod shaped bodies adjacent to channel sandstones (Horne et. al., 1978).

McCabe (1984) suggests that most coal formed in close proximity to active river systems as in Fisk's (1960) model, would be sub-economic due to inundation by aerated waters and clastic sediments. Low-lying peat mires in close proximity to active river channels are also unlikely to remain free of flooding for the thousands of years required for thick peat accumulation.

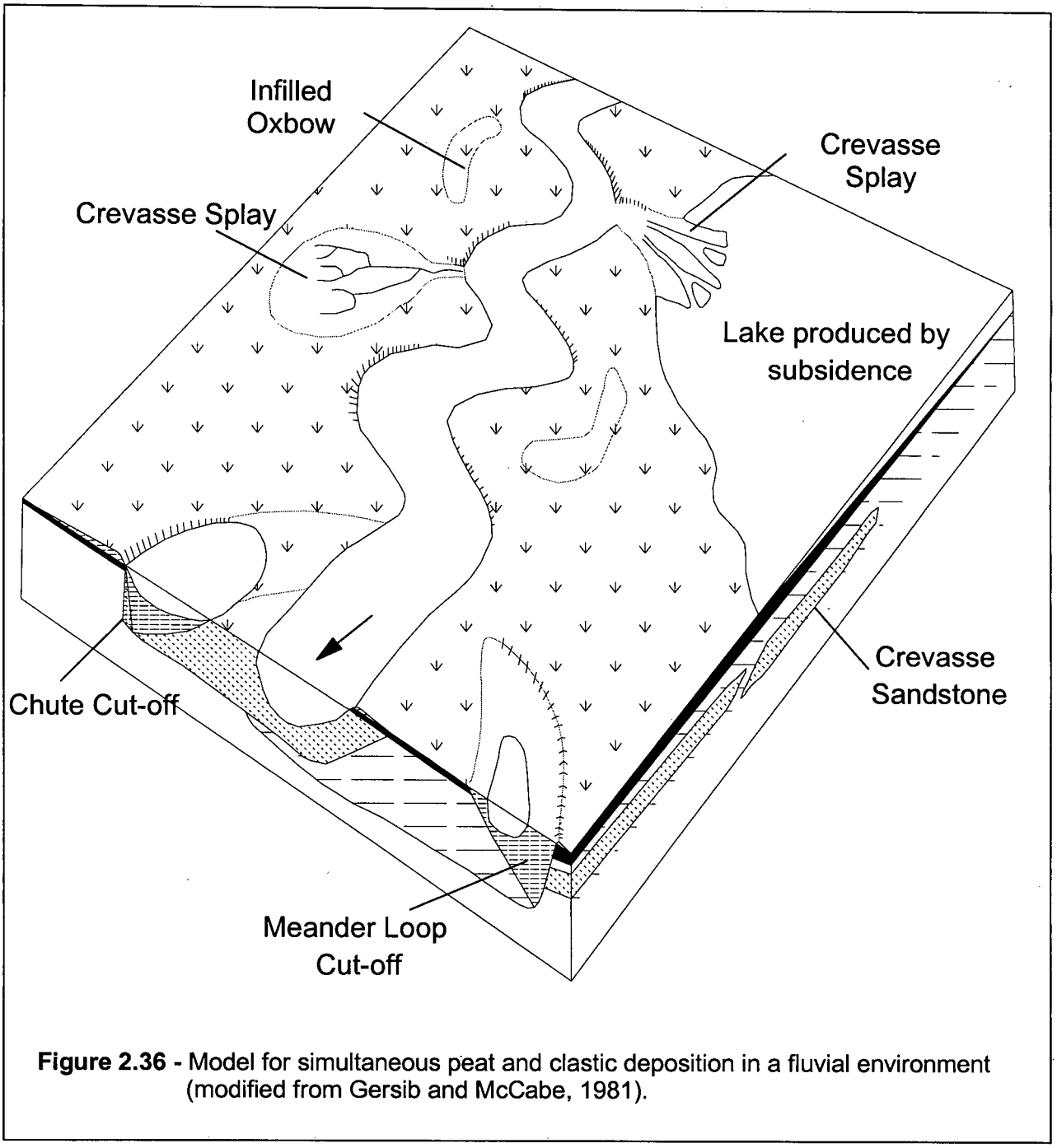

Figure 2.36 - Model for simultaneous peat and clastic deposition in a fluvial environment (modified from Gersib and McCabe, 1981).

2.10.2.2. - Peat Deposition in Domed Mires

Domed mires have convex sides and central flat areas (Fig. 2.37a) up to 10 metres above the basin floor and develop where annual precipitation is greater than annual evaporation and there is no extended dry season (Anderson, 1964). Because domed mires rise above the water table, peat is protected from clastic influx (McCabe, 1984), hence the proximity of river channels to the peat mires is not a major factor controlling coal quality. Modern domed peat mires are concentrically zoned (Anderson, 1964) and have a steep sided outer zone of poor quality peat (which coalifies to carbonaceous shale) and protects the rest of the mire from inundation. Peats formed in such an environment are generally separated from underlying sediment by sharp contacts representing a hiatus (Haszeldine, 1989). Modern domed mires are common in tropical regions such as Indonesia, Malaysia and Central America, but are also well documented in temperate regions of Europe and North America. Modern tropical domed mires are up to hundreds of square kilometres in area (Esterle and Ferm, 1994), while temperate domed mires generally do not exceed a few square kilometres (Haszeldine, 1989). Domed mires were not incorporated into depositional models until the 1980's (Ethridge et. al, 1981; Flores, 1981; 1983), despite their recognition in the rock record and documentation in modern settings in the 1960's (Anderson, 1964; Smith, 1968).

2.10.2.3. - Peat Deposition During a Hiatus in Clastic Sedimentation

Where annual precipitation does not exceed evaporation, peat can only accumulate in low lying areas below the water table, leaving mires susceptible to flooding. Therefore thick, low ash coal can only develop if peat accumulation occurs at a hiatus in clastic deposition or at sites removed from active clastic deposition, beyond the reach of most flood events (Fig.2.37b; McCabe, 1984). In this situation, contacts between coal and surrounding clastics generally represent a hiatus and the quality of coal is unlikely to reflect surrounding clastic sedimentology. Although these mires are limited to regions that lie below the water table, they are likely to be widespread when there is no clastic sedimentation to interrupt deposition. Documentation of low-lying mires that were removed from clastic influence is limited in the literature. Examples include the Paleogene Wilcox Group of Texas (Breyer and McCabe, 1986) and the

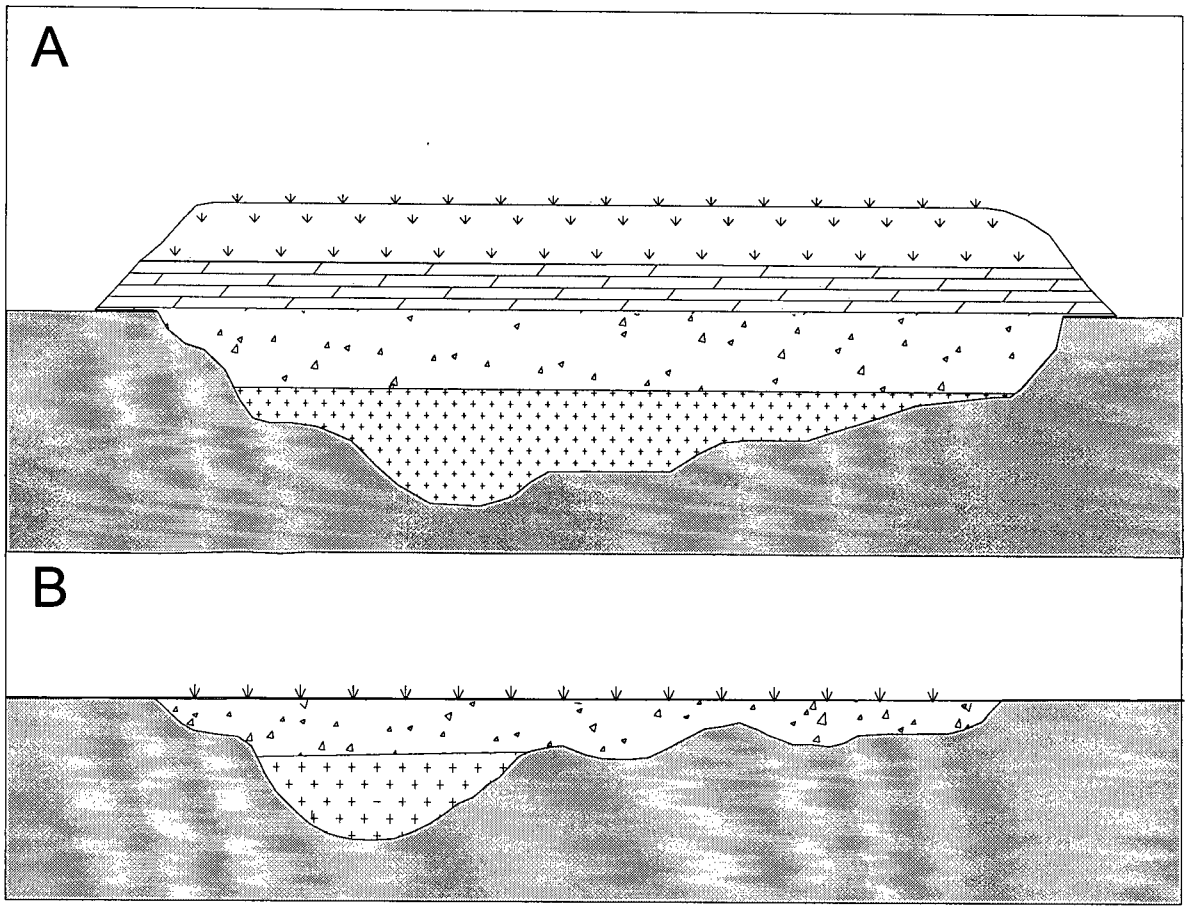

Figure 2.37 - a) - Doming of mires above the basin floor protects peat from clastic incursion.
- b) - Low-lying mires are susceptible to flooding unless they occur away from active clastic deposition (modified from McCabe, 1984).

modern Okefenokee (Cohen, 1984) and Snuggedy Swamps (Staub and Cohen, 1979) of the southeastern USA.

2.10.2.4. - Deposition of Mist Mountain Formation Coal

The sedimentology of the lower coastal plain unit of the Mist Mountain Formation suggest peat was deposited during hiatus' in clastic sedimentation. Both channel sandstones and coal seams are laterally extensive and occur one on top of the other, but are not interbedded. This suggests the region changed from almost exclusive peat deposition to almost exclusive clastic, fluvial activity through time. Small channel sandstone deposits in coal seam partings are rare, and coal generally does not pass laterally into clastic sediments, suggesting river channels were not present in areas of active peat accumulation. The ash content of the lower unit coal bears no apparent relationship to the unit's sedimentology, which also suggests peat did not accumulate in areas of active clastic sedimentation. The peat and clastic depositional environments appear to have been mutually exclusive and erosion suggests hiatus' occurred between the two regimes. It remains unclear from the sedimentology if peat mires of the lower unit were domed or not, and doming was probably a function of precipitation and climate.

The sedimentology of the upper alluvial–fluvial plain unit of the Mist Mountain Formation suggests peat accumulated in domed mires, raised above clastic sedimentation. Coal seams and channel sandstones are smaller and less laterally extensive than their counterparts in the lower unit. The laterally discontinuous and interbedded nature of these facies suggests they were not deposited in a chronologically distinctive fashion as in the lower unit but rather, peat deposition occurred coeval with clastic sedimentation. The ash content of the upper unit coal shows no relationships to the sedimentology of the unit, which suggests the mires were domed rather than exposed to clastic deposition.

The seam geometry and ash content data from the Line Creek area shows that clastic sedimentation had only limited influence on peat accumulation in the Mist Mountain Formation. The ash mineralogy is predominantly not authigenic, therefore mineral matter within the coal is derived from surrounding

clastic sediments. The geometry of the seams reflects the proximity of under- and overlying channel sandstones but rarely are the channel sandstone and organic facies laterally juxtaposed. The ash abundance and mineralogy of the coal does not reflect changes in surrounding clastic sediments.

2.11. - CONCLUSIONS

The Jurassic-Cretaceous Mist Mountain Formation at the Line Creek mine site is divisible into two units based on abundance and lateral continuity of facies. The lower unit of the Mist Mountain Formation consists of alternating laterally extensive coal seams and thick, widespread channel sandstones interspersed with crevasse splay and floodplain facies sediments. It was deposited in an interdeltaic coastal plain environment protected from marine incursion by the beach ridge-dune sandstones of the underlying Morrissey Formation. The upper unit of the Mist Mountain Formation consists of the same facies as the lower unit, however they are less laterally continuous and thinner than their counterparts in the lower unit. Channel sandstones decrease in number and thickness up-section, and are replaced by an increasing abundance of thin coal seams, floodplain and crevasse splay facies sediments. The upper unit was deposited in a distal alluvial-fluvial floodplain environment.

The coal seam geometry and ash content data from the Line Creek area shows that clastic sedimentation only had limited influence on peat accumulation during deposition of the Mist Mountain Formation. The geometry of the coal seams reflect the proximity of under- and overlying channel sandstones, however the ash content and mineralogy of the coal does not reflect changes in thickness, proximity or composition of surrounding clastic sediments. Mist Mountain Formation coals exhibits increasing vitrinite content up-section, which reflects a decreasing proportion of herbaceous vegetation. The lack of relationships between sedimentology and coal quality indicate accumulation in mires which were not directly influenced by fluvial activity, and support McCabe's (1984) suggestion that economic coal generally does not form in low-lying overbank mires beside active river systems. Characteristics of the

lower unit suggest peat mires developed only during breaks in clastic deposition, while upper unit peats appear to have been deposited in domed mires, raised above active clastic deposition.

At a regional scale, geometry, distribution and quality of Mist Mountain Formation coal can be predicted by stratigraphic stacking The effects of seam splitting, erosion, differential compaction and overall depositional environment of the coal allow the broad scale geometry of seams to be predicted. For example, coal seams generally thin where overlain by channel sandstones and the number of plies tends to increase toward the east. The sulphur content of the coal can be predicted based on seam thickness, and the ash mineralogy is constant throughout the formation. However, localised changes in seam geometry such as minor splitting and the extent of erosion by river channels and crevasse splays are unpredictable. Trends in ash content of the Mist Mountain Formation coal is also unpredictable because ash cannot be related to changes in seam thickness or proximity of channel sandstones. The lack of relationships mean that on a mine site scale the sedimentology of the formation is only of limited use in prediction of coal quality parameters.

2.12. – REFERENCES CITED

Anderson, J.A.R. 1964, The structure and development of the peat swamps of Sarawak and Brunei: Journal of Tropical Geography, v. 18.

Beach, H.H. 1943, Moose Mountain and Morley map areas, Alberta, Geological Society of Canada.

Bhattacharya, J.P. and Walker, R.G. 1992, Facies *in* Walker, R.G. and James, N.P. Facies models: response to sea level change, Geological Association of Canada, p. 157-178.

Breyer, J.A. and McCabe, P.J. 1986, Coals associated with tidal sediments in the Wilcox Group (Paleogene), south Texas: Journal of Sedimentary Petrology, v.56, p. 510-519.

Bustin, R.M., Cameron, A.R., Grieve, D.A. and Kalkreuth, W.D. 1985, Coal petrology, its principals, methods, and applications, 230 p.

Bustin, R.M. and Dunlop, R.L. 1992, Sedimentological factors affecting mining, quality, and geometry of coal seams of the Late Jurassic-Early Cretaceous Mist mountain Formation, southern Canadian Rocky Mountains, *in* McCabe, P.J. and Parrish, J.T. eds. Controls on the distribution and quality of Cretaceous coals, Volume 267: Boulder, Colorado, Geological Society of America Special Paper, p. 117-138.

Bustin, R.M. and Smith, G.G. 1993, Coal deposits in the Front Ranges and Foothills of the Canadian Rocky Mountains, southern Canadian Cordillera: International Journal of coal geology, v. 23, p. 1-27.

Cameron, A.R. 1972, Petrography of Kootenay coals in the upper Elk River and Crowsnest areas, British Columbia, Canada, *in* Mellon, G.B., Kramers, J.W. and Seagal, E.J. eds. First Geological Conference on Stern Canadian Coal, Volume 60, Research Council of Alberta Information Series, p. 31-46.

Cohen, A.D. 1984, The Okefenokee Swamp: a low sulfur end-member of a shoreline-related depositional model for coastal plain coals, *in* Rahmani, R.A. and Flores, R.M. eds. Sedimentology of coal and coal-bearing sequences, Volume 7, International Association of Sedimentologists Special Publication.

Crosdale, P.J. 1993, Coal maceral ratios as indicators of environment of deposition: do they work for ombrogenous mires? An example from the Miocene of New Zealand: Organic Geochemistry, v.20, p. 797-809.

Dawson, J.W. 1886, On the Mesozoic floras of the Rocky Mountain region of Canada: Transactions of the Royal Society of Canada, v. 3.

Diessel, C.F.K. 1986, On the correlation between coal facies and depositional environments: Advances in the study of the Sydney Basin, Proc. of the twentieth Symposium, University of Newcastle, p. 19-22.

Diessel, C.F.K. 1992, Coal-bearing depositional systems: Berlin, Springer-Verlag, 721 p.

Donald, R.L. 1984, Sedimentology of the Mist Mountain Formation in the Fording River area, southeastern Canadian Rocky Mountains [Masters of Science thesis]: Vancouver, The University of British Columbia.

Dunlop, R.L. and Bustin, R.M. 1987, Depositional environments of the coal-bearing Mist Mountain Formation, Eagle Mountain, southeastern Canadian Rocky Mountains: Bulletin of Canadian Petroleum Geology, v. 35, p. 389-415.

Esterle, J.S. and Ferm, J.C. 1994, Spatial variability in modern tropical peat deposits from Sarawak, Malaysia and Sumatra, Indonesia: analogues for coal: International Journal of Coal Geology, v. 26, p. 1-41.

Ethridge, F.G., Jackson, T.J. and Youngberg, A.D. 1981, Floodbasin sequence of a fine-grained meander belt sub-system: the coal-bearing Lower Wasatch and Upper Fort Union Formations, southern Powder River Basin, Wyoming, *in* Ethridge, F.G. and Flores, R.M. eds. Recent and ancient nonmarine

depositional environments: Models for exploration, Volume 31: Special Publication of the SEPM: Tulsa, p. 191-219.

Fielding, C.R. 1987, Coal depositional models for deltaic and alluvial plain sequences: Geology, v. 15, p. 661-664.

Fisk, H.N. 1960, Recent Mississippi River sedimentation and peat accumulation, C.r.4 Congre l'avancement des etudes de stratigraphie et de geologie du Carbonifere, Volume 1: Heerlen, p. 187-199.

Flores, R.M. 1981, Coal deposition in fluvial paleoenvironments of the Paleocene Tongue River Member of the Fort Union Formation, Powder River area, Powder River Basin, Wyoming and Montana: SEPM Special Publication, v. 31, p. 169-190.

Flores, R.M. 1983, Basin facies analysis of coal-rich Tertiary fluvial deposits, northern Powder River Basin, Montana and Wyoming, *in* Collinson, J.D. and Lewin, J. eds. Modern and ancient fluvial systems, Volume 6: International Association of Sedimentologists Special Publication: Oxford, Blackwell Scientific Publications, p. 501-515.

Gersib, G.A. and McCabe, P.J. 1981, Continental coal-bearing sediments of the Port Hood Formation (Carboniferous), Cape Linzee, Nova Scotia, Canada, *in* Ethridge, F.G. and Flores, R.M. eds. Recent and ancient nonmarine depositional environments: Models for exploration, Volume 31: Special Publication of the SEPM: Tulsa, p. 95-108.

Gibson, D.W. 1977, The Kootenay Formation of Alberta and British Columbia - a stratigraphic summary, Geological Survey of Canada.

Gibson, D.W. 1979, The Morrissey and Mist Mountain Formations - newly defined lithostratigraphic units of Jura-Cretaceous Kootenay Group, Alberta and British Columbia: Bulletin of Canadian Petroleum Geology, v. 27, p. 183-208.

Gibson, D.W. 1985, Stratigraphy, sedimentology and depositional environments of the coal-bearing Jurassic - Cretaceous Kootenay Group, Alberta and British Columbia: Geological Society Canada Bulletin, v. 357, p. 108.

Gibson, D.W. and Hughes, J.D. 1981, Structure, stratigraphy, sedimentary environments and coal deposits of the Jurassic-Cretaceous Kootenay Group, Crowsnest Pass area, Alberta and British Columbia, The Mesozoic of Middle North America C.S.P.G. Conference, Volume Field trip guidebook no. 4: Calgary, C.S.P.G.

Grieve, D.A. 1989, Stratigraphy of the Mist Mountain Formation (Jurassic-Cretaceous Kootenay Group) in the Elk Valley Coalfield, southeastern British Columbia, *in* Langenberg, W. ed. Advances in Western Canadian Coal Geoscience - Forum Proceedings, Volume Information Series 103, Alberta Research Council, p. 24-41.

Grieve, D.A. 1993, Geology and rank distribution of the Elk Valley Coalfield, southeastern British Columbia, British Columbia Geological Survey Branch.

Grieve, D.A. and Fraser, J.A. Line Creek and Crown Mountain areas, Elk Valley Coalfield.

Haszeldine, R.S. 1989, Coal reviewed: depositional controls, modern analogues and ancient climates, *in* Whateley, M.K.G. and Pickering, K.T. eds. Deltas: sites and traps for fossil fuels, Volume 41: Geological Society Special Publication: Oxford, Blackwell Scientific Publications, p. 289-308.

Horne, J.C., Ferm, J.C., Caruccio, F.T. and Baganz, B.P. 1978, Depositional models in coal exploration and mine planning in Appalachian region: AAPG Bulletin, v. 62, p. 2379-2411.

Hughes, J.D. and Cameron, A.R. 1985, Lithology, depositional setting and coal rank - depth relationships in the Jurassic-Cretaceous Kootenay Group at Mount Allan, Cascade Coal Basin, Alberta, Geological Society of Canada, p. 41.

Jansa, L.F. 1972, Depositional history of the coal bearing Upper Jurassic-Lower Cretaceous Kootenay Formation, southern Rocky Mountains, Canada: Geological society of America bulletin, v. 83, p. 3199-3222.

Kalkreuth, W.D. and Leckie, D.A. 1989, Sedimentological and petrographical characteristics of Cretaceous strandplain coals: a model for coal accumulation from the North American Western Interior Seaway: International Journal of Coal Geology, v. 12, p. 381-424

Kalkreuth, W.D., Marchioni, D.L., Calder, J.H., Lamberson, M.N., Naylor, R.D. and Paul J. 1991, The relationship between coal petrology and depositional environments from selected coal basins in Canada: International Journal of Coal Geology, v. 19, p. 21-76

Lamberson, M.N., Bustin, R.M. and Kalkreuth, W. 1991, Lithotype (maceral) composition and variation as correlated with paleo-wetland environments, Gates Formation, northeastern British Columbia, Canada: International Journal of Coal Geology, v. 18, p. 87-124.

Leach, W.W. 1912, Geology of Blairmore map area, Alberta, Geological Survey of Canada.

Levey, R.A. 1985, Depositional model for understanding geometry of Cretaceous coals: major coal seams, Rock Springs Formation, Green River Basin, Wyoming: AAPG Bulletin, v. 69, p. 1359-1380.

McCabe, P.J. 1984, Depositional environments of coal and coal-bearing strata, *in* Rahmani, R.A. and Flores, R.M. eds. Sedimentology of coal and coal-bearing sequences, Volume 7, International Association of Sedimentologists Special Publication.

Mastalerz, M. and Bustin, R.M. 1997, Variation in the chemistry of macerals in coals of the Mist Mountain Formation. Elk Valley Coalfield, British Columbia, Canada: International Journal of Coal Geology, v. 33, p. 43-59.

Miall, A.D. 1996, The geology of fluvial deposits: sedimentary facies, basin analysis and petroleum geology: Berlin: Springer-Verlag, 582 p.

Newmarch, C.B. 1953, Geology of the Crowsnest coal basin, with special reference to the Fernie area: British Columbia Department of Mines Bulletin, v. 33.

Norris, D.K. 1959, Type section of the Kootenay Formation, Grassy Mountain, Alberta: Journal of the Alberta Society of Petroleum Geologists, v. 7, p. 223-233.

Pearson, D.E. and Grieve, D.A. 1980, Elk Valley Coalfield, Volume 1980-1, British Columbia Geological Survey Paper, p. 91-96.

Phillips, S., Bustin, R.M. and Lowe, L.E. 1994, Earthquake-induced flooding of a tropical coastal peat swamp: A modern analogue for high-sulfur coals? Geology, v. 22, p. 929-932.

Smith, A.H.V. 1968, Seam profiles and seam characters, *in* Murchison, D.G., and Westoll, T.S., eds, Modern and ancient fluvial systems: Edinburgh, Oliver and Boyd, p. 31-40.

Stach, E., Mackowsky, M-TH, Teichmuller, M., Taylor, G.H., Chandra, D. and Teichmuller, R. 1982, Stach's textbook of coal petrology, third ed., Berlin, Gebruder Borntraeger, 535 p.

Staub, J.R. and Cohen, A.D. 1979, The Snuggedy Swamp of South Carolina: a back barrier estuarine coal forming environment, Journal of Sedimentary Petrology, v. 48. p. 203-210.

Stott, D.F. 1984, Cretaceous sequences of the Foothills of the Canadian Rocky Mountains, *in* Stott, D.F., and Glass, D.J., eds, The Mesozoic of Middle North America, Volume 9: Canadian Society of Petroleum Geologists Memoir, p. 85-107.

Ting, F.T.C. 1989, Facies in the Lower Kittaning coal bed, Appalachian Basin (USA) *in* Lyons, P.C. and Alpern, B., Peat and Coal: Facies and depositional models: International Journal of Coal Geology, v. 12, p. 425-442.

Williams, E.G. and Keith, M.L. 1963, Relationships between sulfur in coals and the occurrences of marine roof beds, Economic Geology, v. 58, p. 720-729.

Chapter 3

Coalbed Methane Characteristics of the Mist Mountain Formation, Southern Canadian Cordillera: Effect of Shearing and Oxidation.

Chapter 3

Coalbed Methane Characteristics of the Mist Mountain Formation, Southern Canadian Cordillera: Effect of Shearing and Oxidation.

3.1. – ABSTRACT

The coalbed methane potential of the Jurassic-Cretaceous Mist Mountain Formation was investigated to determine if shearing and oxidation of coal could account for low volumes of methane encountered in the formation. The coal is of suitable rank and composition to host significant coalbed methane reserves, yet tests to date indicate lower than the expected volumes of methane are present.

Adsorption isotherms indicate that Mist Mountain Formation has good to excellent reservoir capacity (Langmuir volumes 13 to 30 cc/g daf bases). Shearing does not significantly affect the methane adsorption capacity of coal; any effect shearing may have on adsorption capacity is overshadowed by the effect of variation in maceral content and oxidation. Adsorption tends to increase with increasing vitrinite content, irrespective of whether or not the coal is sheared. Oxidation results in decreased methane adsorption capacity in the Mist Mountain Formation coals. However, the decreased volume of methane adsorbed due to oxidation alone is unlikely to result in the sub-economic volumes of methane that desorb from some samples.

It appears that shearing and oxidation have enhanced leakage of methane resulting in under saturation: both shearing and oxidation enhance the permeability of coal and therefore have facilitated the diffusion and pressure dependent flow of methane from the coal to groundwater.

3.2. - INTRODUCTION

During coalification, large volumes of natural gas are produced by the thermal alteration of plant material. As well as acting as a source for methane, coal is also able to act as a reservoir, because it has a large internal pore volume (Rightmire, 1984). The ability of coal to produce and retain methane is dependent on several factors, including seam thickness and continuity, rank, pressure, mineral matter content, water table depth, hydrological conditions and fracture permeability.

The Jurassic-Cretaceous Mist Mountain Formation of the southern Canadian Cordillera (Fig. 3. 1) contains up to 1975 megatonnes of measured coal reserves (Smith, 1989). The coal is of suitable rank and composition to host significant quantities of coalbed methane (CBM). The Mist Mountain Formation contains up to 17 major coal seams that are often thick (up to 20 metres) and laterally continuous, particularly in the lower part of the formation. The rank of the coal ranges from high volatile bituminous to semi-anthracite, the coal is rich in vitrinite and although the ash content is variable (4-45%), it is commonly low to moderate.

Despite its apparent suitability as a CBM reservoir, preliminary investigations indicate that the Mist Mountain Formation coal contains only limited CBM resources (Feng et. al., 1984; Johnson and Smith, 1991; Dawson and Clow, 1992). The reason for the low methane content of the coal is unclear. Possibilities include escape of methane along shear zones that are common in Mist Mountain Formation coal (Feng et. al., 1984) and an apparent under-saturation of the coal due to changes in temperature and pressure because of uplift and erosion since the gas was generated.

The aims of this study are to:

a) present new CBM adsorption data from the Mist Mountain Formation in the Line Creek area of southeastern British Columbia and;

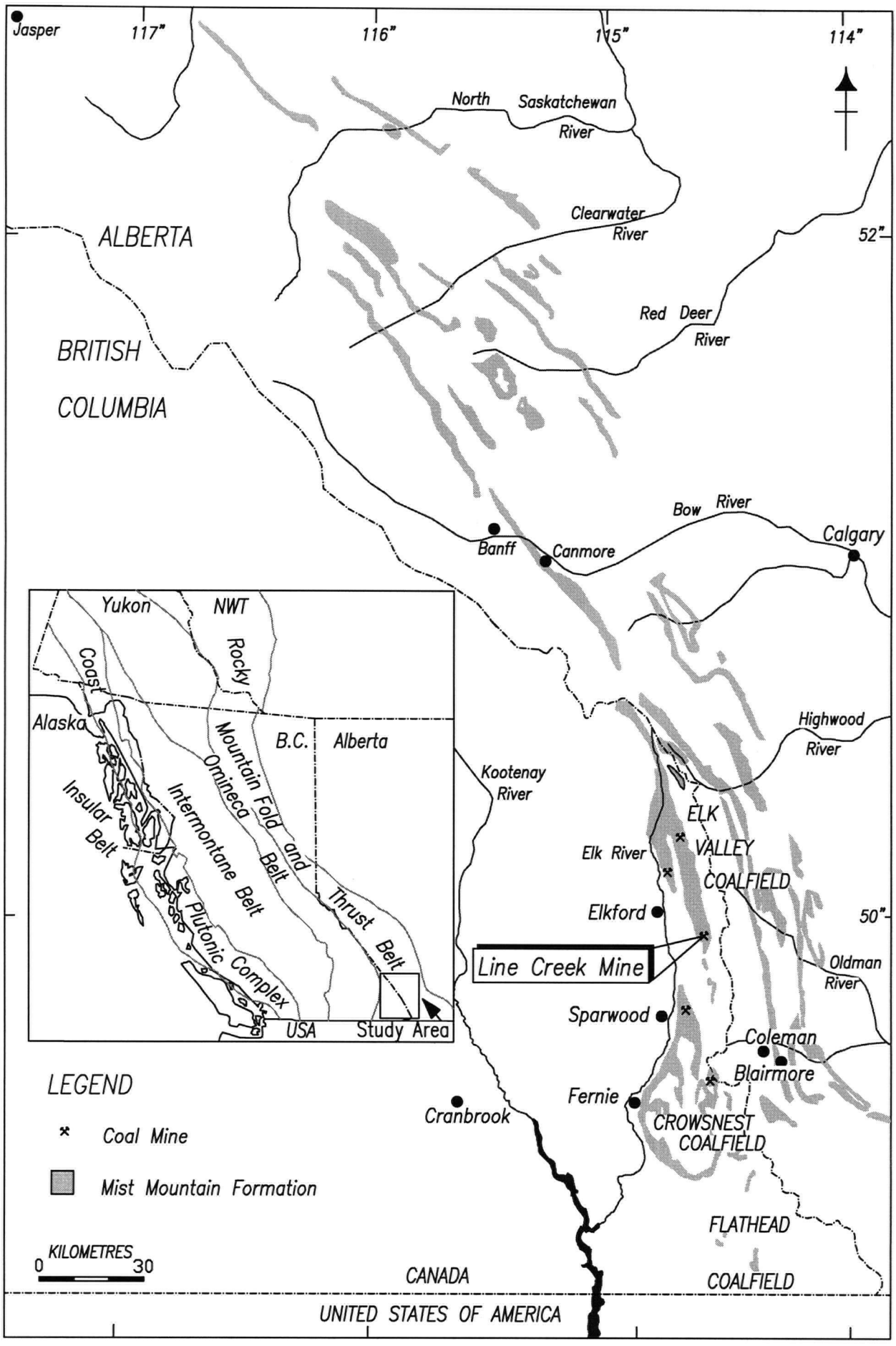

Figure 3.1 – Location map of the study area showing outcrop of the Mist Mountain Formation (modifed from Gibson, 1985).

b) determine if shearing and oxidation could be responsible for the low volumes of methane encountered in Mist Mountain Formation coal by examination and comparison of the effect of these parameters on methane adsorption.

3.3. - FACTORS AFFECTING THE GAS STORAGE CAPACITY OF COAL

Methane can be retained in coal in one of three states: as adsorbed molecules on the internal surfaces of coal; as free gas within pores and fractures; and as a solute in pore fluids. Adsorption is the primary mechanism of methane retention in coal; excess methane exists as free gas which may then be dissolved into solution (Rightmire, 1984). The amount of gas that coal can adsorb is dependant on the internal surface area of the coal, which in turn, is dependant on pore size distribution and porosity (Gan et. al., 1972). Three standard pore size classes are recognised by current 1994 IUPAC classification; macro- (> 50 nm), meso- (2 - 50 nm), and micropores (< 2 nm). Macro- and mesopores fill with gas by multilayer absorption on to internal pore surfaces so the total internal surface area of the coal is the main factor controlling the volume of gas adsorbed (Gan et. al., 1972). Gas adsorption in micropores is thought to occur by volume filling rather than multilayer adsorption, therefore gas storage in microporous coal is dependent on pore space volume, which enables greater gas adsorption than in meso- or macroporous coal (Gan et. al., 1972).

Previous studies have attributed variable gas contents primarily to coal rank and composition (Kim, 1977; Meissner, 1984; Ayers and Kelso, 1989; Levine, 1992, 1993; Schraufnagel and Schafer, 1996). Coal rank plays an important role in determining the gas storage capacity of coal because it directly influences porosity and pore size distribution (Lamberson and Bustin, 1993). Coal porosity decreases to a minimum at high volatile bituminous rank, then increases rapidly between the ranks of low volatile bituminous and anthracite (Gan et al., 1972). The predominant pore size in coal also changes with rank; low rank coal is mainly macroporous, while coal above high volatile bituminous rank is typically

microporous (Mahajan and Walker, 1978). The method of pore filling therefore changes with rank and high rank coal is capable of storing more gas than low rank coal.

Maceral composition of coal also directly influences gas storage capacity through porosity and pore size distribution (i.e. Lamberson and Bustin, 1993; Clarkson and Bustin, 1996; 1997). Porosity is greatest in inertinite, intermediate in vitrinite and least in liptinite (Harris and Yust, 1976). Pore size distribution also varies between macerals; inertinite is mesoporous, liptinite is macroporous, and vitrinite contains both meso- and micropores. Although vitrinite is less porous than inertinite, it adsorbs a greater volume of gas because it contains a high proportion of micropores (Clarkson and Bustin, 1996). Lamberson and Bustin (1993) demonstrate that maceral content is at least as important as rank in determining the gas storage capacity of some Canadian coals.

Other factors that play a role in gas storage capacity include percentage mineral matter, reservoir pressure, permeability, and hydrological conditions within the reservoir. Mineral matter adsorbs very little methane, therefore a high ash content reduces the quantity of gas a coal sample is able to store (Meissner, 1984). Reservoir conditions such as pressure, permeability, hydrology and surrounding rock types affect the amount of methane stored by controlling gas flow within and away from the reservoir. Pressure and temperature due to current depth of burial dictates how much gas is adsorbed and retained by the coal.

The effect of shearing and oxidation on the gas storage capacity of coal is not well understood. Shearing increases the number of microfissures and reduces the grain size of coal (Bustin, 1982), features which might be expected to increase the gas storage capacity of coal. However, research at The University of British Columbia has shown that subjecting coal to up to 30% strain does not significantly affect the micropore capacity or distribution, but does increase the coals permeability (Bustin, 1998, pers. comm.) Feng et al. (1984) noted that sheared coal desorbs more methane at a faster rate than unsheared coal. Oxidation results in oxidation rims, microfissures and a change in surface chemistry of coal (Chandra,

1982). The effect of these oxidation features on gas storage capacity is not well documented. Clarkson (1992) found that laboratory oxidation resulted in a slight reduction in the gas storage capacity of coal.

3.4. - MEASUREMENT OF GAS STORAGE CAPACITY

Adsorption is used to measure the methane capacity of coal. Adsorption tests involve saturating a sample with methane and measuring the volume adsorbed at a series of known pressures. Plotting pressure versus volume adsorbed generates an adsorption isotherm. The relationship between pressure and gas storage capacity for coal is commonly described by the Langmuir equation (Mavor et al. 1990).

$$P / V = P / Vm + 1 / a\ Vm$$

Where P = pressure, V = volume of methane adsorbed, Vm = monolayer volume, and a = constant related to the heat of adsorption. Langmuir adsorption theory predicts a straight line on P vs. P/V plots and the reciprocal of the slope of the line corresponds to the methane monolayer capacity of the coal (Gregg and Sing, 1982). Adsorption tests indicate the maximum gas storage capacity but not the actual volume of gas stored within a reservoir because the coal maybe undersaturated.

The volume of gas present in a coal can only be determined directly from freshly drilled core. The amount of gas that desorbs from the coal is measured and an extrapolation is made for gas that escapes before the sample is sealed. The results from adsorption and desorption testing are not directly comparable, but it may be useful to equate the amount of methane a coal contains with what it is capable of storing.

3.5. - STRATIGRAPHY AND STRUCTURE OF THE MIST MOUNTAIN FORMATION

The Late Jurassic-Early Cretaceous Mist Mountain Formation is the major coal-bearing sequence of the southern Canadian Cordillera. At the Line Creek Coal Mine (Fig. 3. 1), the Mist Mountain Formation is in excess of 650 metres thick and contains up to 17 major and numerous minor coal seams (Fig. 3. 2) of high to low volatile bituminous rank.

In the Line Creek vicinity, the Mist Mountain Formation can be divided into two units based on the abundance and lateral continuity of sedimentary facies. The lower unit extends from the base of the formation to the top of 7 seam (Fig. 3. 2) and consists of alternating thick, laterally continuous coal seams and channel sandstones interspersed with crevasse splay and floodplain facies sediments. Coal seams in this coastal plain deposited unit average 4.5 metres thick and 26% raw ash content. Above 7 seam, both coal seams and channel sandstone decrease in thickness and lateral continuity and sandstones are replaced by a greater proportion of crevasse splay and floodplain facies sediments. Upper unit coal seams average 2.5 metres thick, 28% raw ash content, and were deposited in a fluvial-alluvial floodplain environment.

The Mist Mountain Formation strata are faulted and folded into a series of northwest trending synclinal structures bounded by high angle reverse and normal faults (Pearson and Grieve, 1980). Coal seams are cut by numerous high to low angle reverse faults and are commonly sheared and thickened (Bustin, 1982).

3.6. - COALBED METHANE IN THE MIST MOUNTAIN FORMATION

The rank and thickness of Mist Mountain Formation coals, particularly in the lower unit, suggest that they should contain large CBM resources (Johnson and Smith, 1991). Gas has been noted in the Mist Mountain Formation coal since mining began in the late 1800's. Early underground mines experienced gas blowouts and consequently drilling to control gas pressure was common (Johnson and Smith, 1991). All mines currently in operation are open pit, hence gas build-up does not affect mining. Interest in the CBM potential of the Mist Mountain Formation coal developed with increased CBM production in the USA in the 1980's. At least ten CBM exploration wells have been drilled into the Mist Mountain Formation but none have intersected economically viable CBM reserves (Dawson, 1995).

Feng et. al. (1984) noted a change in stored methane related to depth of burial of the Mist Mountain Formation while testing methane desorption from three drillholes in the Elk Valley Coalfield (Fig. 3.1). Coal seams less than 200 metres deep appear to have degassed naturally and contain less than one quarter the amount of methane of seams at a depth of 300 metres. Feng et. al. (1984) also noted that sheared coal seams released more methane than unsheared seams during desorption, and that less methane was retained in sheared coal once desorption ceased.

Dawson and Clow (1992) found that the adsorption capacity of Mist Mountain Formation coal was at least an order of magnitude more than the gas content of the coal, indicating the coal is markedly undersaturated. They suggest that the low volumes of methane encountered during desorption is due to natural degassing of the coal because drilling occurred close to outcrop of the seams tested. Dawson and Clow (1992) also suggest that differences in adsorption between seams may be due to the extent of shearing of the coal.

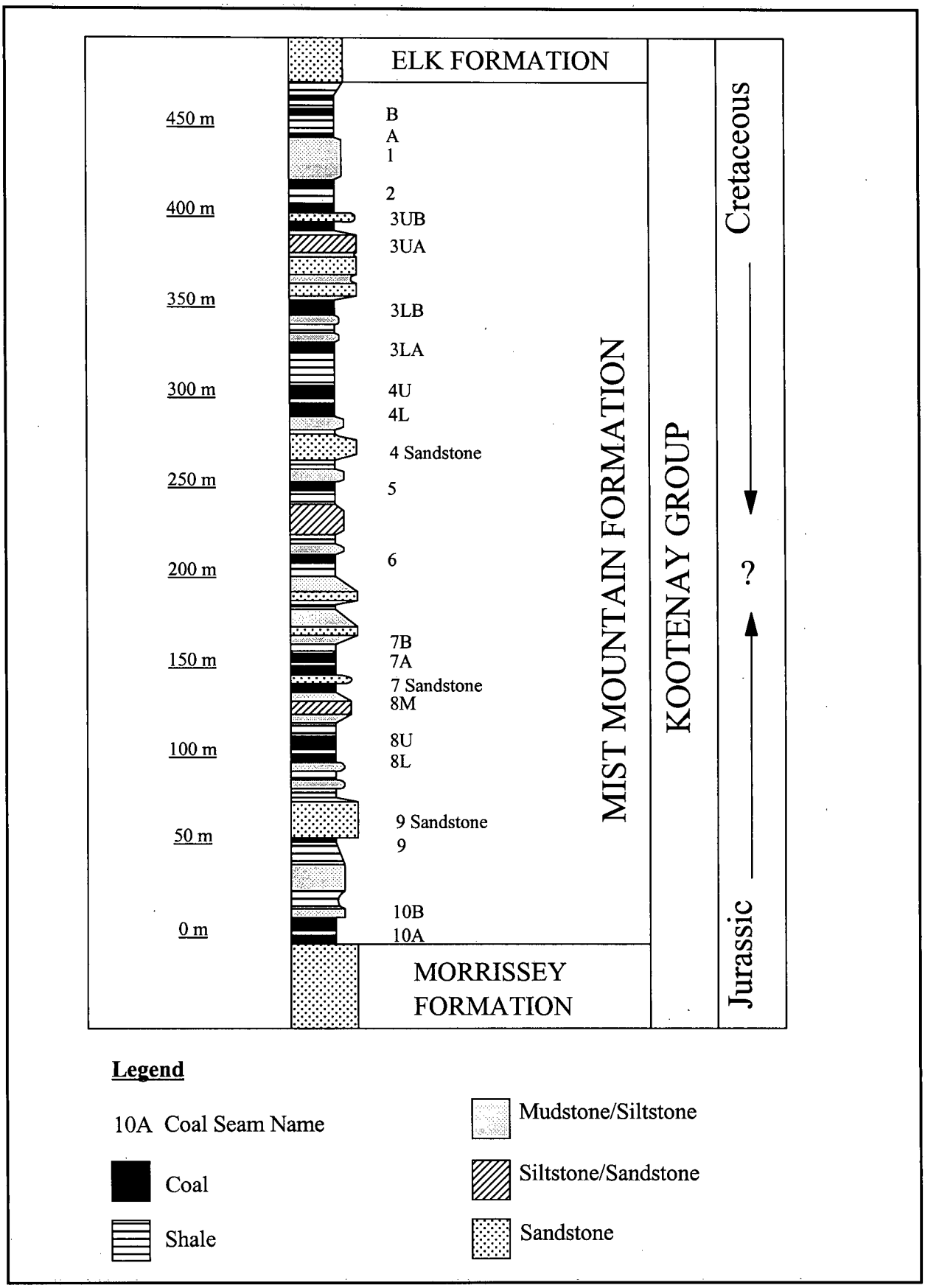

Figure 3.2 - Generalised Stratigraphic Section of the Mist Mountian Formation at Line Creek Showing Coal Seam Nomenclature

3.7. - METHODS

Fourteen samples were obtained from the Line Creek Coal Mine, southeastern British Columbia and were supplemented by an additional sample of higher rank Mist Mountain Formation coal from Canmore, Alberta for comparative purposes. Three pairs of samples were collected to test the effect of shearing on methane adsorption. In each pair, a sheared and unsheared sample of similar ash content was selected. Two sets of samples were collected to test the effect of oxidation on methane adsorption. The first set was collected at intervals away from the oxidised face of a road cut. The second set was divided in two, half of which was left to oxidise under laboratory conditions at room temperature for a period of one year. The last sample was separated into lithotypes for comparison of the CBM potential of durain, vitrain and clarain. The sample did not contain sufficient fusain to test for methane adsorption.

Samples were ground to pass through a 250-micrometre mesh and the moisture, ash content and free swelling index (FSI) were established using standard ASTM procedures. Maceral composition of the coal was established, based on a 300-point count (mineral matter free) of a polished, crushed particle pellet according to standard procedures (Bustin et. al., 1985). Mean random vitrinite reflectance (R_o) was also determined for each sample using standard techniques (Bustin et. al., 1985), based on a minimum of 30 reflectance measurements per pellet. High-pressure methane adsorption was performed on approximately 100 grams of each of the samples at 30°C, at equilibrium moisture and in a high-pressure volumetric adsorption analyser similar to that described in Mavor et. al. (1990). The volume of methane adsorbed by each sample at nine successively higher pressures (0.4 to 11 MPa) was measured over a period of up to five days. Results were fitted to the Langmuir equation and recalculated to an ash free basis.

3.8. - RESULTS

3.8.1. - COAL COMPOSITION AND RANK

Ash, moisture, FSI and random reflectance data for all samples are presented in table 3. 1. The ash content of the samples ranges from 4% to 44% and FSI values range from 0 to 4. Random reflectance values for the Line Creek samples range from 0.7% to 1.27% which correspond to high to medium-volatile bituminous ranks. The Canmore sample has a low volatile bituminous rank and random reflectance of 1.73%.

The relative percentage of each maceral was calculated on an ash free basis (table 3. 2 and figure 3.3). Vitrinite content of the samples ranges from 27.6% to 84.5% and is primarily in the form of unstructured detrovitrinite. The coal contains between 13% and 57% semifusinite and other inertinite accounts for up to 16% of the total maceral content. The coals studied contain less than 1% liptinite.

Sample	Seam	Ash Content (%)	EQ Moisture (%)	FSI	Reflectance (Ro%)
Sheared suite					
96-28-346	6 – unsheared	43.04	3.02	1.5	1.09
96-28-347	6 – sheared	36.84	2.50	0	1.26
97-06-038	10A – sheared	18.05	2.02	1	1.20
97-06-039	10A – unsheared	15.72	2.16	3	1.07
97-07-074	10A – sheared	44.34	2.71	1	1.27
97-07-075	10A - unsheared	38.66	2.08	1	1.17
Oxidised Suite					
96-23-268	4L – unoxidised	13.84	8.09	0	0.70
96-23-268a	4L – lab oxidised	13.84	6.27	0	0.90
97-03-026	8U – oxidised	35.05	2.30	0	1.12
97-03-027	8U – partly oxidised	6.81	3.37	0	1.06
97-03-028	8U - unoxidised	5.69	4.35	0	1.13
Lithotype Suite					
98-01-002	8U – durain	5.10	2.16	4	1.07
98-01-003	8U – clarain	20.68	1.17	1.5	1.13
98-01-004	8U – vitrain	7.52	1.06	3.5	1.11
Rank Suite					
98-01-001	Canmore anthracite	4.32	1.46	0	1.73

Table 3.1 – Ash, Moisture, Free Swelling Index and Rank Data for all Samples.

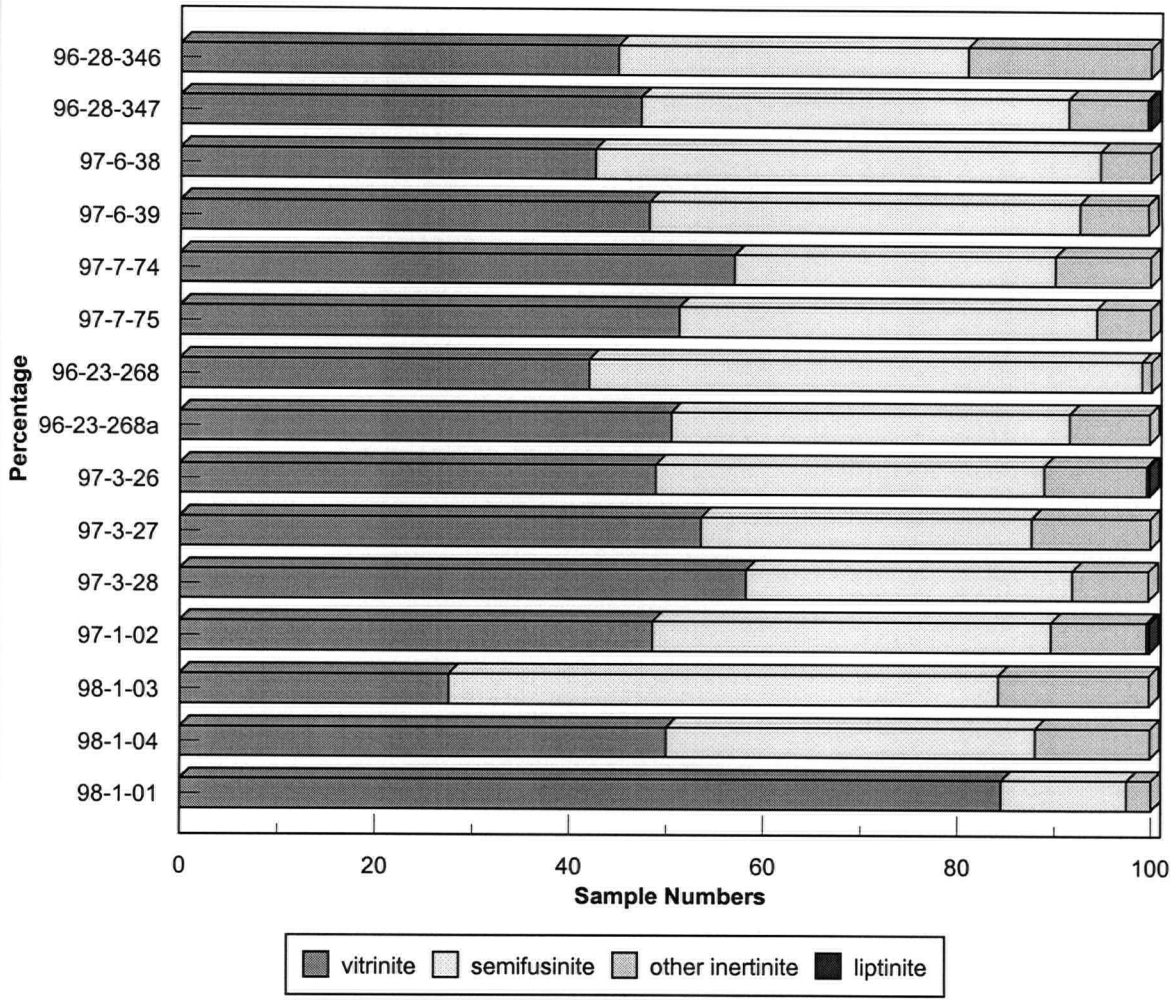

Figure 3.3 - Maceral Composition of all Samples on a Mineral Matter Free Basis, as Determined by Point Counting.

Sample	Vitrinite (%)		Inertinite (%)				Liptinite (%)
	Telo.	Detro.	Fusinite	Macrinite	Inertodet.	Semifus.	
Sheared Suite							
96-28-346	2.6	42.3	18.0	1.0	0.0	36.0	0.0
96-28-347	1.3	46.0	8.0	0.3	0.0	44.0	0.3
97-06-038	2.3	40.3	5.0	0.3	0.0	52.0	0.0
97-06-039	4.6	43.6	6.6	0.6	0.0	44.3	0.0
97-07-074	3.0	54.0	8.6	1.3	0.0	33.0	0.0
97-07-075	2.3	49.0	4.3	1.3	0.0	43.0	0.0
Oxidised Suite							
96-23-268	0.0	42.0	1.0	0.0	0.0	57.0	0.0
96-23-268a	2.3	48.3	8.0	0.3	0.0	41.0	0.0
97-03-026	2.3	46.6	10.0	0.6	0.0	40.0	0.3
97-03-027	6.6	47.0	10.3	2.0	0.0	34.0	0.0
97-03-028	3.6	54.6	7.6	0.0	0.3	33.6	0.0
Lithotype Suite							
98-01-002	1.6	47.0	9.3	0.6	0.0	41.0	0.3
98-01-003	0.6	27.0	14.0	1.6	0.0	56.6	0.0
98-01-004	3.0	47.0	11.6	0.3	0.0	38.0	0.0
Rank Suite							
98-01-001	22.0	62.5	2.5	0.0	0.0	13.0	0.0

Table 3.2 – Maceral Composition Data for all Samples.

3.8.2. - METHANE ADSORPTION

Methane adsorption isotherms for all 14 samples are illustrated on an ash and moisture free basis in figure 3.4. The methane monolayer capacities range from 11.5 to 27 cc/g for the Line Creek samples and 30.3 cc/g for the Canmore sample (Table 3. 3). The volume of methane adsorbed by the Mist Mountain Formation coal increases with rank (Fig. 3. 5).

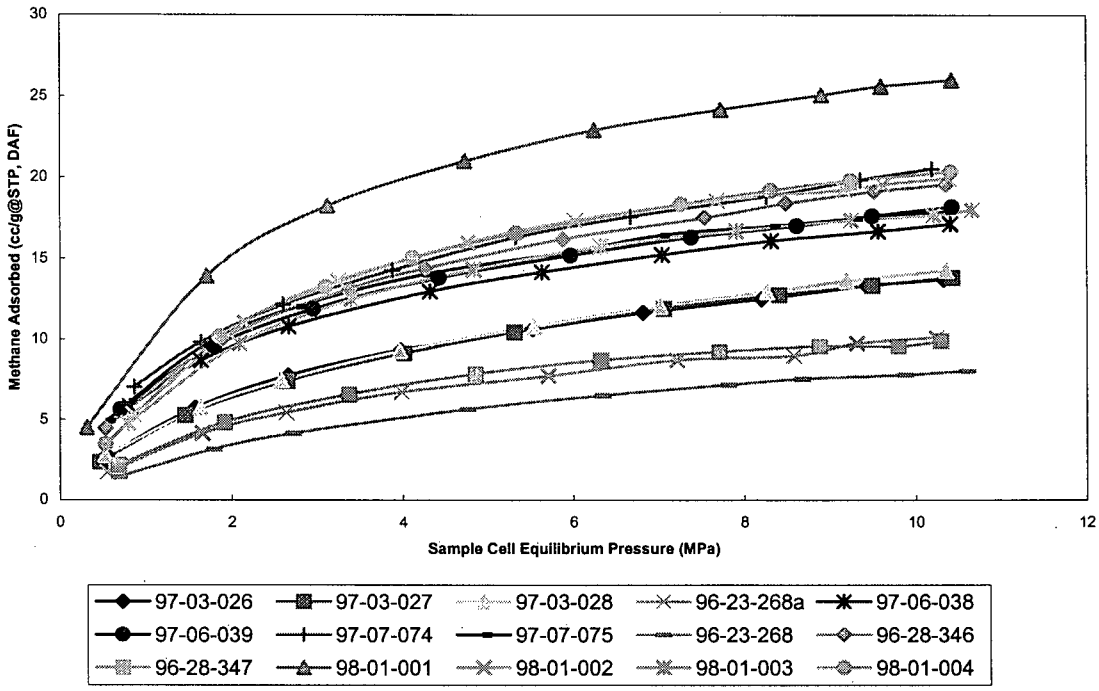

Figure 3.4 - Methane Adsorption Isotherms for all Samples

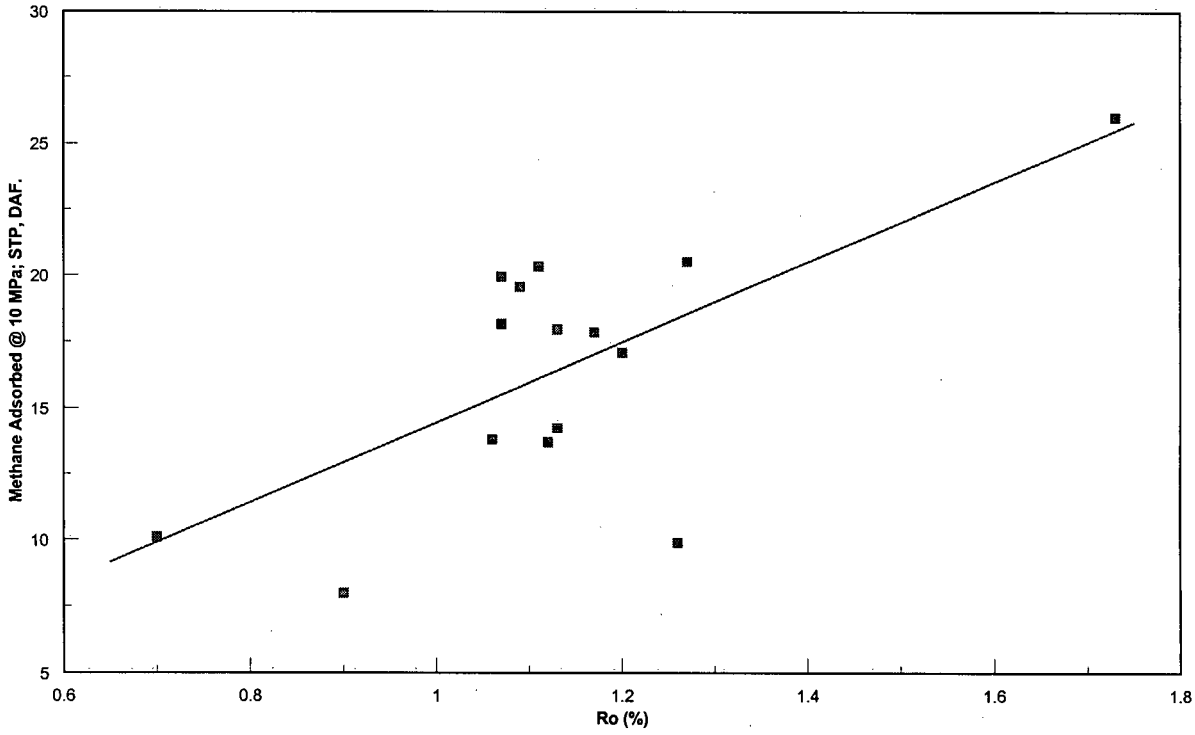

Figure 3.5 - Cross-plot of Volume of Methane Adsorbed and Sample Rank.

Sample	Methane Monolayer Capacity (cc/g @ STP, DAF)
Sheared Suite	
96-28-346	24.2
96-28-347	13.0
97-06-038	20.6
97-06-039	21.8
97-07-074	25.2
97-07-075	21.1
Oxidised Suite	
96-23-268	11.5
96-23-268a	13.5
97-03-026	17.8
97-03-027	18.3
97-03-028	18.8
Lithotype Suite	
98-01-002	25.7
98-01-003	23.0
98-01-004	27.0
Rank Suite	
98-01-001	30.3

Table 3.3 – Methane Monolayer Volumes for all Samples.

3.8.2.1. - The Effect of Maceral Content on Methane Adsorption

Small changes in the adsorption capacity of the Mist Mountain Formation coal can be related to changes in maceral content. Within the lithotype suite of samples, adsorption increases with increasing brightness (vitrinite content; Figs. 3.6 and 3.7). Vitrain contains the highest proportion of vitrinite (50%) and therefore adsorbs the most methane. The clarain sample has a high inertinite content (72%), and it adsorbed the least methane. Fusain was not present in sufficient quantities to test its methane adsorption capacity

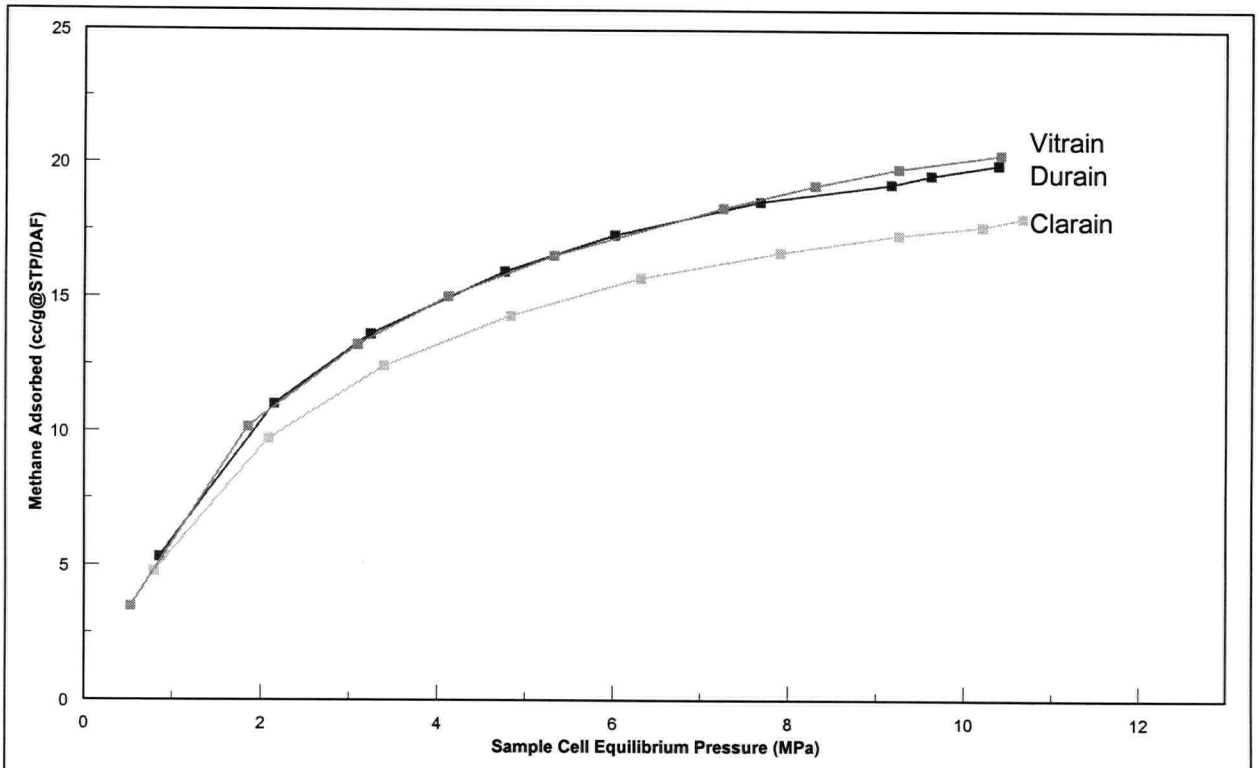

Figure 3.6 - Methane Adsorption Isotherms of the Lithotype Suite of Samples

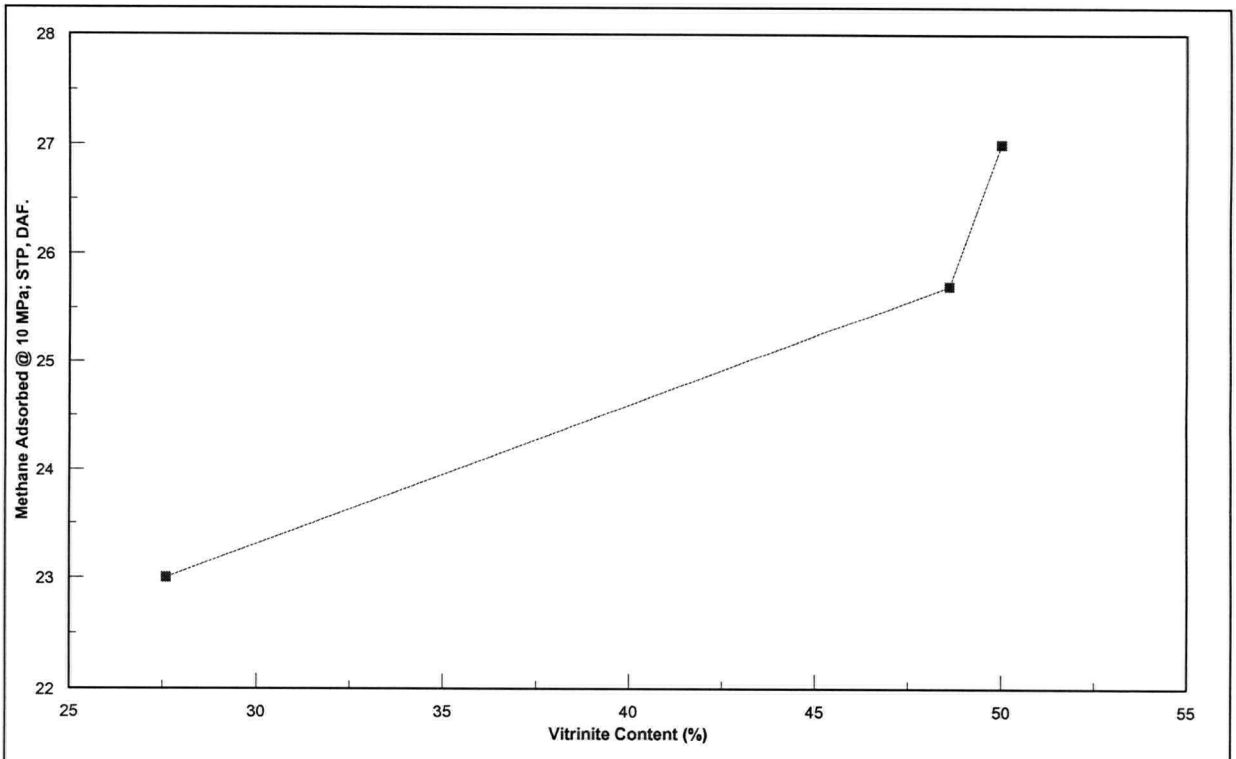

Figure 3.7 - Cross-plot of Volume of Methane Adsorbed and Vitrinite Content of the Lithotype Suite of Samples.

3.8.2.2. - The Effect of Oxidation on Methane Adsorption

Natural and laboratory oxidation affects the methane adsorption of coal in different ways. Natural oxidation led to a small decrease in adsorption with increased oxidation (Fig. 3. 8). Monolayer capacities of the three samples increase from 17.8 to 18.8 cc/g with decreasing oxidation. In contrast, laboratory oxidation increased the monolayer capacity of the coal from 11.5 to 13.5 cc/g (Fig. 3. 8). Bustin (1998, pers. comm.) has also noted increased methane adsorption from laboratory oxidised coal. These results confirm that laboratory oxidation is not equivalent to the natural oxidation process (Huggins et. al., 1983; Huggins and Huffman, 1989). It is possible that without the influence of water, the changes in surface chemistry that occur in natural oxidation cannot be reproduced in the laboratory.

3.8.2.3. - The Effect of Shearing on Methane Adsorption

Interpretation of the effect of shearing on methane adsorption is complicated by compositional variation between sheared and unsheared samples. The sheared suite of samples collectively do not show a consistent trend in methane adsorption (Fig. 3. 9). In two sets of samples, (10A and 6U seams) the sheared coal adsorbed less methane than the unsheared coal, but the third sample set (also from 10A seam) had increased methane adsorption capacity in the sheared sample (Fig. 3. 8). The adsorption capacity of the two sets of samples from 10A seam can be related to composition of the coal. Samples with the highest vitrinite content adsorb the most methane, irrespective of whether or not the coal is sheared (Fig. 3.10).

The adsorption capacity of the samples from 6U seam is not related to the maceral content of the coal. The vitrinite content of the samples are similar, at 47% in the sheared and 45% in the unsheared sample. However the unsheared coal, adsorbed a much greater volume of methane than the sheared sample (Fig. 3. 10); monolayer volumes are 24.2 cc/g and 13 cc/g respectively (Fig. 3. 9). Therefore maceral content does not account for the large difference in methane adsorption of 6U seam coal. Given the results from 10A seam, the large difference in adsorption of 6U samples is unlikely to be the result of shearing. The only notable difference in quality between 6U seam samples is the free swelling index. The unsheared

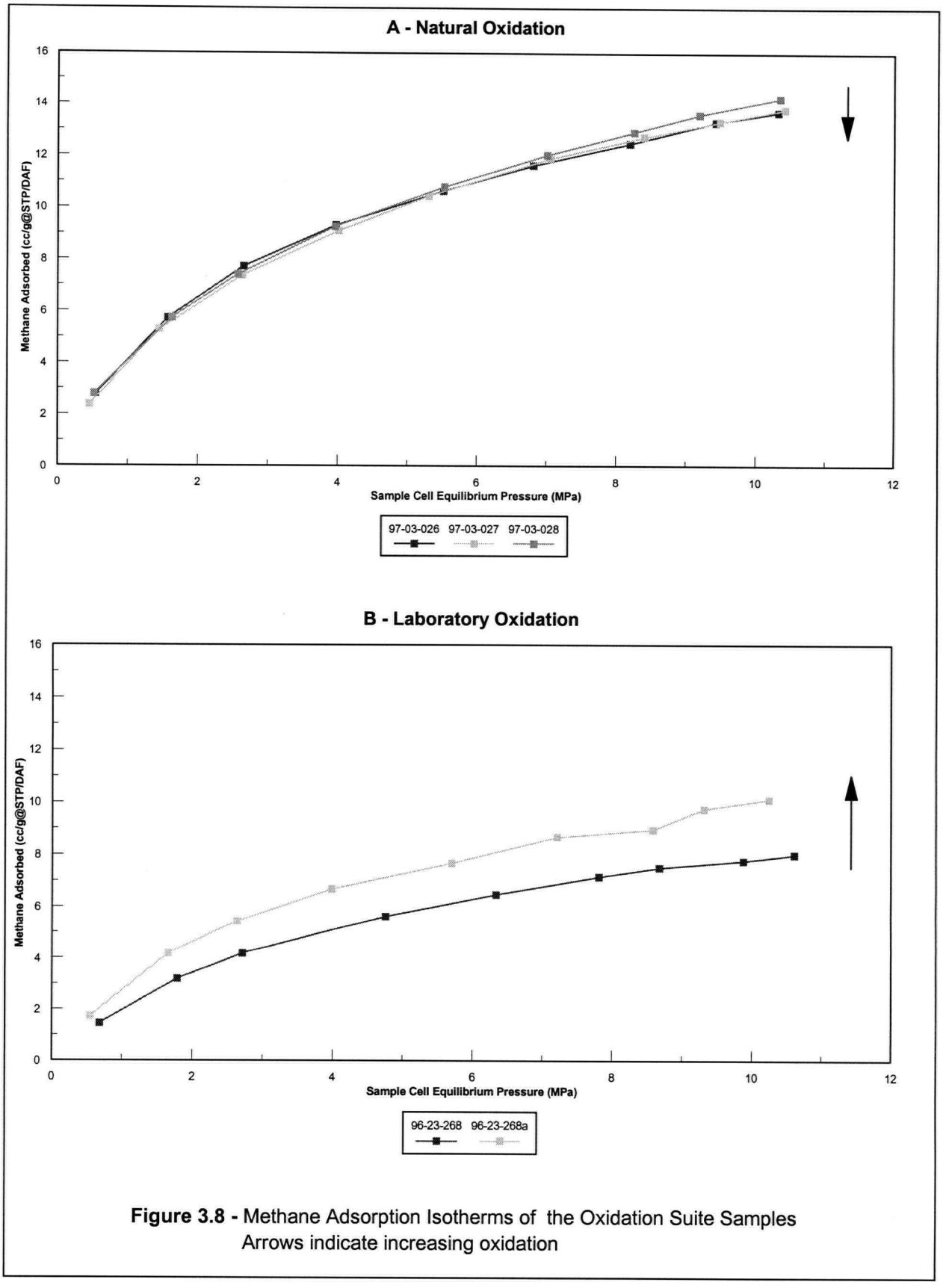

Figure 3.8 - Methane Adsorption Isotherms of the Oxidation Suite Samples
Arrows indicate increasing oxidation

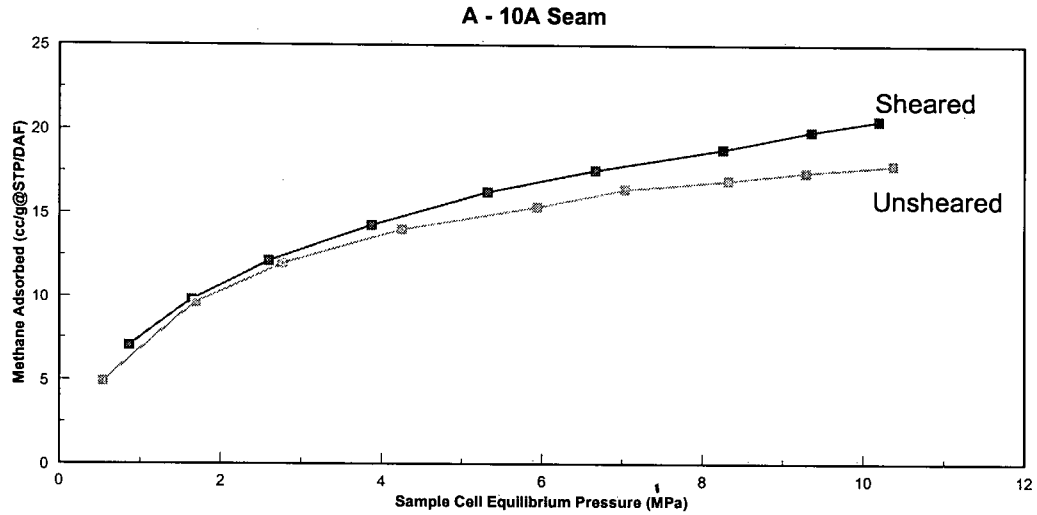

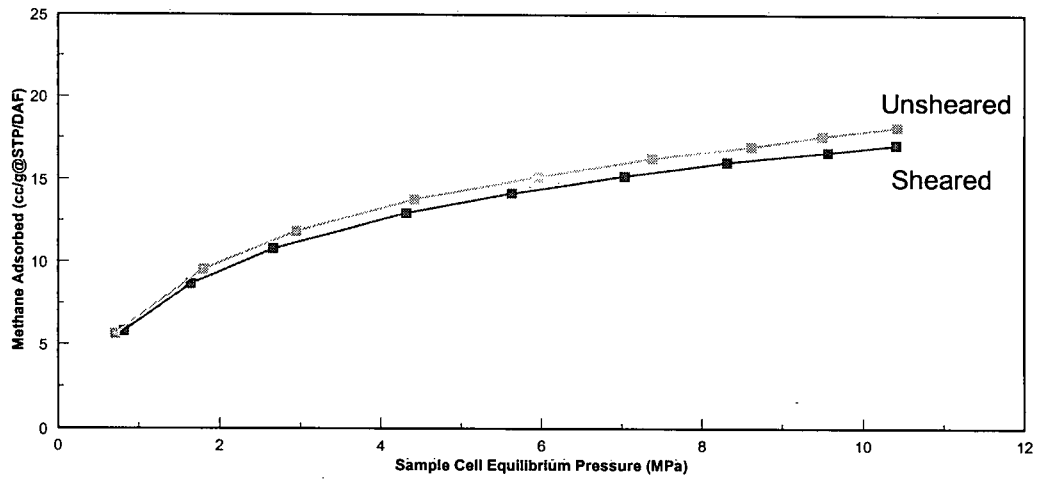

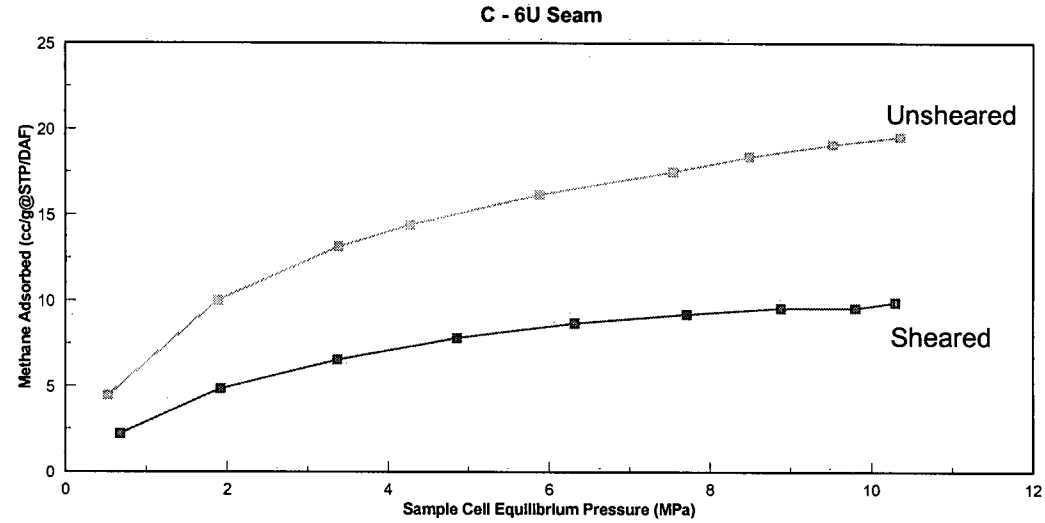

Figure 3.9 - Methane Adsorption Isotherms for the Sheared Suite of Samples

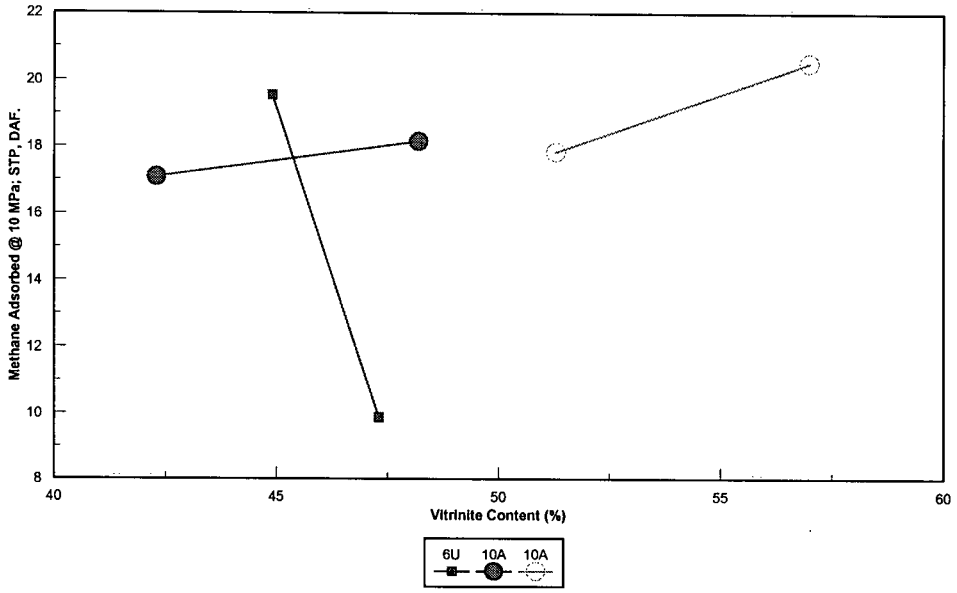

Figure 3.10 - Cross-plot of Volume of Methane Adsorbed and Vitrinite Content of the Sheared Suite of Samples.

sample has a FSI of 1.5 while the sheared sample did not fuse at all (FSI = 0). The decreased FSI is undoubtedly reflects oxidation, which suggests that oxidation maybe the factor that controls the methane adsorption in this case.

3.9. - DISCUSSION

Adsorption isotherm analyses demonstrates that coals of the Mist Mountain Formation have moderate to high reservoir capacities. Shearing does not influence the methane adsorption capacity of the Mist Mountain Formation coal enough to account for the low volume of methane retained. Maceral content is a more important control on methane adsorption capacity than shearing. Vitrinite contains a large proportion of micropores, and accordingly, is capable of storing greater volumes of methane than inertinite or liptinite (Lamberson and Bustin, 1993). Small changes in vitrinite content in the Mist Mountain Formation coals appear to mask any influence of shearing on methane adsorption capacity. Natural oxidation decreases the gas storage capacity of coal, but it is unlikely that the decrease due to oxidation alone is enough to result in the sub-economic volumes of methane that desorb from the Mist Mountain Formation. Results from this study do not indicate whether oxidation or maceral content has a greater influence on methane adsorption capacity.

The rank and composition of the Mist Mountain Formation coal suggests large volumes of methane were produced during coalification which, when combined with the moderate to high measured reservoir capacity indicates gas leakage must account for the low measured gas contents. A decrease in formation temperature due to erosion and uplift may have increased the methane adsorption capacity of the coal subsequent to gas generation, as suggested by Mavor et. al. (1990). The coal will therefore appear undersaturated because it is capable of storing more methane than is actually adsorbed to the coal. However, Levy et. al. (1997) found that each 1°C increase in temperature results in only a 0.12 mLg^{-1} decrease in methane adsorption capacity in Bowen Basin coals of Australia. Such small decreases in methane adsorption capacity with increased temperature are unlikely to result in the low volumes of gas found in Mist Mountain Formation coal.

Coal acts as a groundwater aquifer. Shearing increases the permeability of coal so water will preferentially travel through sheared zones. As water passes through sheared zones, methane will diffuse from the coal to the water, which then passes from the coal, leaving it understaturated with respect to methane. Oxidation also decreases the methane adsorption capacity of coal, forcing methane to desorb. It is likely that a combination of decreased adsorption capacity and increased diffusion of methane from the coal accounts for the order of magnitude difference Dawson and Clow (1992) noted between adsorption and desorption values from the Mist Mountain Formation.

3.10. - CONCLUSIONS

The thickness, rank and depth of burial of coal seams within the Mist Mountain Formation suggest they may be a favourable reservoir for significant CBM reserves. Data presented herein confirms that the coal is theoretically capable of storing economic quantities of methane. However, desorption data indicate that lower volumes of methane than expected are present in the coal (Dawson, 1995).

Shearing and oxidation enhance the permeability of coal (Bustin, 1982) and therefore may facilitate the escape of methane from coal reservoirs. Shearing does not significantly affect the methane adsorption capacity of the coal. Any effect shearing may have on adsorption capacity appears to be overshadowed by the effect of variation in maceral content and oxidation. Adsorption tends to increase with increasing vitrinite content, irrespective of whether or not the coal is sheared. Natural oxidation results in decreased methane adsorption capacity in the Mist Mountain Formation coals. However, the decreased volume of methane adsorbed due to oxidation alone is unlikely to result in the sub-economic volumes of methane that desorb from the coal. It is probable that a combination of decreased adsorption due to oxidation and reduced retention of the methane in the coal due to shearing and oxidation account for the low volumes of methane in the Mist Mountain Formation.

A number of avenues are open for future investigation of the CBM potential of the Mist Mountain Formation. Measurement of pore volume and pore size distribution of sheared and oxidised coal would confirm the effect these factors have on methane adsorption, and allow comparison of the effects of oxidation and maceral content. Further desorption testing, specifically targeting sheared and oxidised coal would confirm if these factors aid desorption of methane from the coal.

3.11. – REFERENCES CITED

Ayers, W.B., and Kelso, B.S., 1989. Knowledge of methane potential for coalbed resources grows, but needs more study. Oil and Gas Journal, 87: 64-67.

Bustin, R.M. 1982, The effect of shearing on the quality of some coals in the Southeastern Canadian Cordillera: CIM Bulletin, v. 75, p. 76-83.

Bustin, R.M., Cameron, A.R., Grieve, D.A. and Kalkreuth, W.D. 1985, Coal petrology, its principals, methods, and applications, 230 p.

Chandra, D. 1982, Oxidised coals, *in* Stach, E., Mackowsky, M.-T., Teichmuller, M., Taylor, G.H., Chandra, D. and Teichmuller, R. Stach's textbook of coal petrology: Berlin, Gebruder Borntraeger, p. 198-205.

Clarkson, C.R. 1992, Effect of low temperature oxidation on micropore surface area, pore distribution and physical and chemical properties of coal, UBC Department of Geological Sciences.

Clarkson, C.R. and Bustin, R.M. 1996, Variation in micropore capacity and size distribution with composition in bituminous coal of the Western Canadian Sedimentary Basin: Fuel, v. 75, p. 1483-1498.

Clarkson, C.R. and Bustin, R.M. 1997, Variation in permeability with lithotype and maceral composition of Cretaceous coals of the Canadian Cordillera: International Journal of Coal Geology, v. 33, p. 135-151.

Dawson, F.M. and Clow, J.T. 1992, Coalbed methane research: Elk Valley Coalfield, In the Canadian Coal and Coalbed methane geoscience forum: Parksville, BC., p. 57-71.

Dawson, F.M. 1995, Coalbed methane: a comparison between Canada and the United States: Geological Survey of Canada Bulletin, v. 489, p. 60.

Feng, K.K., Cheng, K.C. and Augsten, R. 1984, Preliminary evaluation of the methane production potential of coal seams at Greenhills Mine, Elkford, British Columbia: CIM Bulletin, v. 77, p. 56-61.

Gan, H., Nandi, S.P. and Walker, P.L. Jr. 1972, Nature of the porosity in American coals: Fuel, v. 51, p. 272-277.

Gibson, D.W. 1985, Stratigraphy, sedimentology and depositional environments of the coal-bearing Jurassic - Cretaceous Kootenay Group, Alberta and British Columbia: Geological Society Canada Bulletin, v. 357, p. 108.

Gregg, S.J. and Sing, K.S.W. 1982, Adsorption surface area and porosity: New York, Academic Press.

Harris, L.A. and Yust, C.S. 1976, Transmission electron microscope observations of porosity in coal: Fuel, v. 55, p. 233-236.

Huggins, F.E., Huffman, G.P. and Lin, M.C. 1983, Observations on low-temperature oxidation of minerals in bituminous coals: International Journal of Coal Geology, v. 3, p. 157-182.

Huggins, F.E. and Huffman, G.P. 1989, Coal weathering and oxidation the early stages *in* Nelson. C.R., ed, Chemistry of coal weathering, Elsevier, Amsterdam, 230 p.

Johnson, D.G.S. and Smith, L.A. 1991, Coalbed methane in Southeast British Columbia, British Columbia Geological Survey, p. 19.

Kim, A.G., 1977. Estimating methane content of bituminous coalbeds from adsorption data. U.S. Bureau of Mines Report of Investigations 8245: 22 pp.

Lamberson, M.N. and Bustin, R.M. 1993, Coalbed methane characteristics of Gates Formation coals, northeastern British Columbia: effect of maceral composition: AAPG Bulletin, v. 77, p. 2062-2076.

Levine, J.R., 1992. Influence of coal composition on coal seam reservoir quality: a review. Coalbed Methane Symposium, Townsville Australia, 1992: I to XXVIII.

Levine, J.R., 1993. Coalification: the evolution of coal as source rock and reservoir. In Law, B.E. and Rice, D.D. (Editors), Hydrocarbons From Coal. American Association of Petroleum Geologists, AAPG Studies in Geology. 38: 39-77.

Levy, J.H., Day, S.J. and Killingly, J.S. 1997. Methane capacities of Bowen Basin coals related to coal properties: Fuel, v. 74, p. 1-7.

Mahajan, O.P. and Walker, P.L. Jr. 1978, Porosity of coal and coal products, *in* Karr, C. Jr. ed. Analytical methods for coal and coal products, Volume 1: New York, Academic Press, p. 125-162.

Mavor, M.J., Owen, L.B. and Pratt, T.J. 1990, Measurement and evaluation of isotherm data, Proceedings of 65th annual technical conference and exhibition, Society of Petroleum Engineers, Volume SPE 20728, p. 157-170.

Meissener, F.F. 1984, Cretaceous and lower Tertiary coals as sources for gas accumulations in the Rocky Mountains area, *in* Woodward, J., Meissener, F.F. and Clayton, J.L. eds. Source rocks of the Rocky Mountain region, Volume 1984 Guidebook, Rocky Mountain Association of Geologists, p. 401-431.

Pearson, D.E. and Grieve, D.A. 1980, Elk Valley Coalfield, Volume 1980-1, British Columbia Geological Survey Paper, p. 91-96.

Rightmire, C.T. 1984, Coalbed methane resources, *in* Rightmire, C.T., Eddy, G.E. and Kirr, J.N. eds. Coalbed methane resources of the United States, Volume 17, AAPG studies in geology series, p. 1-13.

Schraufnagel, R.A. and P.S. Schafer, 1996. The success of coalbed methane. In: Saulsberry, J.L., Scahfer, P.S., Schraufnagel, R.A. (Editors) A Guide to Methane Reservoir Engineering Gas Research Institute (GRI Reference Number GRI-94/0397), Chicago, Illinois. P. 1.1- 1.10.

Smith, G.G. 1989, Coal resources of Canada, Geological Survey of Canada, Paper 89-4, 146 p.

Chapter 4

Conclusions.

Chapter 4

Conclusions.

4.1. – SEDIMENTOLOGY AND DEPOSITIONAL ENVIRONMENTS OF THE MIST MOUNTAIN FORMATION

At the Line Creek mine site, coals of the Jurassic-Cretaceous Mist Mountain Formation vary in thickness, lateral continuity and ash content. Thus the Line Creek area is an ideal location to investigate relationships between coal quality and other features of the coal measures such as sedimentology, stratigraphic stacking, depositional environment and coalbed methane potential.

The Mist Mountain Formation is made up of four lithofacies; channel, crevasse splay, floodplain and organic rich facies. Variation in abundance and lateral continuity of the facies allows the formation to be divided into two units. The lower unit consists of thick, laterally extensive coal seams and channel sandstones interspersed with crevasse splay and floodplain facies sediments. Coal seams in the lower unit have an average thickness of 4.5 metres, 26% raw ash and 0.5% sulphur content. Deposition of the lower unit occurred in an interdeltaic coastal plain environment, protected from marine incursion by the beach-ridge sandstones of the underlying Morrissey Formation. Lithofacies in the upper unit are thinner and less laterally continuous than their counterparts in the lower unit. Channel sandstones decrease in number and thickness up section, and are replaced by an increasing number of coal seams, floodplain and crevasse splay facies sediments. Coal seams in the upper unit have an average thickness of 2.5 metres, 28% raw ash and 0.6% sulphur content. The upper unit of the Mist Mountain Formation was deposited in a distal alluvial-fluvial floodplain environment.

4.2. – RELATIONSHIPS BETWEEN COAL QUALITY, SEDIMENTOLOGY AND DEPOSITIONAL ENVIRONMENT

Coal seam geometry and quality data from the Line Creek area indicates that clastic sedimentation had only limited influence on peat accumulation during deposition of the Mist Mountain Formation. Differential compaction and erosion influence the geometry of coal seams, however the ash content and detrital mineralogy of the coal does not reflect surrounding sedimentology. The lack of relationships between sedimentology, ash content and mineralogy indicate peat accumulated in mires that were not directly influenced by clastic activity. This supports McCabe's (1984) suggestion that economic coal generally does not form in low-lying mires beside active fluvial or deltaic systems. Characteristics of lower unit coals suggest peat mires developed only during hiatus' in clastic deposition, whereas upper unit peats appear to have accumulated in domed mires raised above clastic activity.

At a regional scale, geometry and distribution of Mist Mountain Formation coals can be predicted in part by the sedimentology and may be of use in coal exploration. The effects of seam splitting, erosion, differential compaction and overall depositional environment on the coal determine the broad scale geometry of seams. However, localised changes in seam geometry and relationships between sedimentology and ash abundance and mineralogy of the coals are unpredictable. The lack of relationships mean that on a mine site scale the sedimentology of the Mist Mountain Formation cannot be used in the prediction of coal quality parameters.

4.3. – INFLUENCE OF SHEARING AND OXIDATION ON COALBED METHANE POTENTIAL

The thickness, rank and depth of burial of coal seams within the Mist Mountain Formation suggest they should be a favourable reservoir for significant coalbed methane reserves. Data presented in this thesis confirms that the coal is theoretically capable of storing economic quantities of methane. However, desorption data indicate that lower than the expected volumes of methane are present in the coal (Feng et. al., 1984; Dawson and Clow, 1992; Dawson, 1995).

Shearing does not significantly alter the methane adsorption capacity of the Mist Mountain Formation coal. The effect of shearing is overshadowed by the effect of variation in maceral content and oxidation on methane adsorption. Adsorption tends to increase with increasing vitrinite content, irrespective of whether or not the coal is sheared. Sheared coal is more susceptible to oxidation than unsheared coal, which complicates measurement of the effect of shearing on methane adsorption capacity. Natural oxidation decreases the methane adsorption capacity of Mist Mountain Formation coal. The decreased volume of methane adsorbed due to oxidation alone is unlikely to result in the sub-economic volumes of methane in the coal, although it is unclear whether the effect of oxidation is greater than that of maceral content.

Shearing and oxidation enhance the permeability of coal (Bustin, 1982) and therefore may facilitate escape of methane from coal reservoirs. It is probable that a combination of decreased adsorption due to oxidation and enhanced leakage of methane due to shearing and oxidation of the coal account for the low volumes of methane encountered in the Mist Mountain Formation.

4.4. – FUTURE RESEARCH POSSIBILITIES

Geologists have often assumed that peat accumulates close to active clastic sedimentation and therefore expect the quality of coal to change with surrounding sedimentology. However, results from this study agree with McCabe's (1984) suggestion that economic coal deposits generally do not accumulate in association with active clastic sedimentation. Coal measures that have been interpreted as forming in close proximity to active clastic sedimentation in the past require re-interpretation in light of the results presented herein. Studies of modern peat mire sedimentology have become common in the literature (Staub and Cohen, 1979; Staub and Esterle, 1994; Phillips and Bustin, 1996). Results from these investigations should be better incorporated into the study of ancient coal forming environments so more realistic models of coal measure deposition can be developed.

Preliminary results from this investigation into the coalbed methane potential of the Mist Mountain Formation suggest shearing does not significantly affect the ability of coal to adsorb methane, whereas oxidation decreases methane adsorption. Further adsorption testing from both Mist Mountain Formation and other coal deposits is required to confirm the results of this study. Analysis of pore volume and pore size distribution in sheared and oxidised coals will allow more detailed interpretation of the effect these parameters have on methane adsorption. Additional desorption testing that focuses specifically on sheared and oxidised coals is also required to confirm the hypothesis that these factors aid the escape of methane from coal reservoirs.

4.5. – REFERENCES CITED

Bustin, R.M. 1982, The effect of shearing on the quality of some coals in the Southeastern Canadian Cordillera: CIM Bulletin, v. 75, p. 76-83.

Dawson, F.M. and Clow, J.T. 1992, Coalbed methane research: Elk Valley Coalfield, In the Canadian Coal and Coalbed methane geoscience forum: Parksville, BC., p. 57-71.

Dawson, F.M. 1995, Coalbed methane: a comparison between Canada and the United States: Geological Survey of Canada Bulletin, v. 489, p. 60.

Feng, K.K., Cheng, K.C. and Augsten, R. 1984, Preliminary evaluation of the methane production potential of coal seams at Greenhills Mine, Elkford, British Columbia: CIM Bulletin, v. 77, p. 56-61.

Haszeldine, R.S. 1989, Coal reviewed: depositional controls, modern analogues and ancient climates, *in* Whateley, M.K.G. and Pickering, K.T. eds., Deltas: sites and traps for fossil fuels, Volume 41: Geological Society Special Publication: Oxford, Blackwell Scientific Publications, p. 289-308.

McCabe, P.J. 1984, Depositional environments of coal and coal-bearing strata, *in* Rahmani, R.A. and Flores, R.M. eds. Sedimentology of coal and coal-bearing sequences, Volume 7, International Association of Sedimentologists Special Publication.

Phillips, S. and Bustin, R.M. 1996b, Sedimentology of the Changuinola peat deposit: organic and clastic sedimentary response to punctuated coastal subsidence: GSA Bulletin, v. 108, p. 794-814.

Staub, J.R. and Cohen, A.D. 1979, The Snuggedy Swamp of South Carolina: a back barrier estuarine coal forming environment, Journal of Sedimentary Petrology, v. 48. p. 203-210.

Staub, J.R. and Esterle, J.S. 1994, Peat-accumulating depositional systems of Sarawak, East Malaysia: Sedimentology Geology, v. 89, p. 91-106.

Appendix A

Drill Hole Locations And

Coal Seam Data

Appendix A

DRILLHOLE LOCATIONS AND COAL SEAM DATA

well name	palinspastic x	palinspastic y	Coal Seam	Seam Thickness	Ash (%)	Sulphur (%)
HC205	659841.0	5534221.6	7A	5.8	11.20	
HC205A	659905.0	5534216.0	7B	9.1	7.10	
HC205A	659905.0	5534216.0	7A	2.4	9.40	
HC205A	659905.0	5534216.0	8U	9.1	16.90	
HC205A	659905.0	5534216.0	8L	7.6	31.90	
HC205A	659905.0	5534216.0	8R	2.4	55.30	
HC205A	659905.0	5534216.0	10C	1.2	12.80	
HC205A	659905.0	5534216.0	10B	1.0		
HC205A	659905.0	5534216.0	10A	2.8		
HC401	660232.0	5533522.6	4L	2.2		
HC401	660232.0	5533522.6	5U	9.8	25.24	
HC401	660232.0	5533522.6	5L	1.5	32.18	
HC401	660232.0	5533522.6	6U	5.9		
HC401	660232.0	5533522.6	7C	9.3		
HC401	660232.0	5533522.6	7B	2.1		
HC401	660232.0	5533522.6	7A	1.6		
HC401A	660525.0	5533493.5	8U	8.3	23.00	
HC401A	660525.0	5533493.5	8L	10.5	18.60	
HC401A	660525.0	5533493.5	8R	2.2	24.90	
HC402	659388.0	5533854.7	4U	0.6	30.65	
HC402	659388.0	5533854.7	5U	1.1	6.19	
HC402	659388.0	5533854.7	6U	1.2	47.02	
HC402	659388.0	5533854.7	7C	3.1	23.20	
HC402	659388.0	5533854.7	7B	1.4	23.90	
HC402	659388.0	5533854.7	7A	0.4		
HC402A	660557.0	5533853.1	8L	6.2	24.43	
HC402A	660557.0	5533853.1	8R	1.8		
HC403	659858.0	5534637.8	6U	1.9	46.40	
HC403	659858.0	5534637.8	6L	1.1		
HC403	659858.0	5534637.8	7C	3.0	16.20	
HC403	659858.0	5534637.8	7B	0.5	8.90	
HC403	659858.0	5534637.8	7A	5.2	10.30	
HC403A	660937.0	5534773.9	8U	8.8	17.40	
HC403A	660937.0	5534773.9	8L	8.2	29.37	
HC403A	660937.0	5534773.9	8R	3.1	24.30	
HC405	660546.0	5534949.9	8U	5.5	17.80	
HC405	660546.0	5534949.9	8L	1.8	34.10	
HC405	660546.0	5534949.9	8R	6.7	34.10	
HC405	660546.0	5534949.9	10C	3.5	15.00	
HC405	660546.0	5534949.9	10B	7.3	18.20	
HC405	660546.0	5534949.9	10A	1.1		
HC406	658878.0	5533556.5	5L	1.2		
HC406	658878.0	5533556.5	6U	1.5	22.70	
HC406	658878.0	5533556.5	6L	1.4	17.00	
HC406	658878.0	5533556.5	7C	6.4	34.50	

well name	palinspastic x	palinspastic y	Coal Seam	Seam Thickness	Ash (%)	Sulphur (%)
HC406	658878.0	5533556.5	8U	0.4	48.10	
HC406	658878.0	5533556.5	8L	0.4	64.80	
HC407	659235.0	5533605.0	4L	6.0		
HC407	659235.0	5533605.0	5U	1.8	9.29	
HC407	659235.0	5533605.0	5L	1.0		
HC407	659235.0	5533605.0	6U	3.8		
HC407	659235.0	5533605.0	7C	3.1	46.80	
HC407	659235.0	5533605.0	7B	1.4	25.90	
HC407	659235.0	5533605.0	7A	1.0	25.90	
HC407	659235.0	5533605.0	8U	4.0	38.00	
HC407	659235.0	5533605.0	8L	5.0	23.90	
HC407	659235.0	5533605.0	8R	2.4	27.48	
HC408	658919.0	5534069.9	2U	1.0		
HC408	658919.0	5534069.9	3UB	1.6		
HC408	658919.0	5534069.9	3UA	1.4		
HC408	658919.0	5534069.9	3LB	1.6		
HC408A	659921.3	5534087.5	6U	2.5		
HC408A	659921.3	5534087.5	6L	1.7		
HC408A	659921.3	5534087.5	7C	3.6	16.30	
HC408A	659921.3	5534087.5	7B	1.0	18.30	
HC408A	659921.3	5534087.5	7A	1.2	16.20	
HC408A	659921.3	5534087.5	8U	5.2	13.60	
HC408A	659921.3	5534087.5	8L	1.5	30.90	
HC409	660260.0	5533177.3	7C	6.4	46.50	
HC409	660260.0	5533177.3	7B	2.3	42.30	
HC409	660260.0	5533177.3	7A	2.8	12.80	
HC409	660260.0	5533177.3	8U	9.9	27.90	
HC409	660260.0	5533177.3	8L	11.3	25.20	
HC409	660260.0	5533177.3	8R	1.5		
HC9203	660999.0	5532176.8	9	1.0		
HC9203	660999.0	5532176.8	10B	17.9		
HC9203	660999.0	5532176.8	10A	3.7		
HC9301	660998.0	5532537.2	8U	6.0	30.30	
HC9301	660998.0	5532537.2	8L	6.2	23.20	
HC9301	660998.0	5532537.2	8R	1.4	14.50	
HC9302	661367.0	5532859.6	10C	2.2		
HC9302	661367.0	5532859.6	10B	12.1	32.30	
HC9302	661367.0	5532859.6	10A	1.0	32.30	
HC9303	659983.0	5533800.0	7C	6.8		0.52
HC9303	659983.0	5533800.0	7B	1.8	12.90	0.76
HC9303	659983.0	5533800.0	7A	1.3	10.40	0.84
HC9303	659983.0	5533800.0	8U	9.6	18.30	0.30
HC9303	659983.0	5533800.0	8L	8.3	8.30	0.33
HC9303	659983.0	5533800.0	8R	2.1	18.80	0.58
HC9304	659576.0	5533159.4	10C	2.2	22.30	
HC9304	659576.0	5533159.4	10B	13.4	47.40	
HC9304	659576.0	5533159.4	10A	5.9	15.70	
HC9305	659864.0	5534386.5	5U	5.0	67.90	0.29
HC9305	659864.0	5534386.5	6U	4.9	35.90	0.38
HC9305	659864.0	5534386.5	7C	4.2	19.30	0.59
HC9305	659864.0	5534386.5	7B	1.4	8.80	0.76

well name	palinspastic x	palinspastic y	Coal Seam	Seam Thickness	Ash (%)	Sulphur (%)
HC9305	659864.0	5534386.5	8L	7.1	24.40	0.34
HC9305	659864.0	5534386.5	8R	3.2	34.90	0.45
HC9306	660788.0	5533596.5	7C	1.2	22.10	0.57
HC9306	660788.0	5533596.5	7B	0.6	9.90	1.00
HC9306	660788.0	5533596.5	7A	4.7	9.30	0.59
HC9306	660788.0	5533596.5	8U	8.5	15.70	0.37
HC9306	660788.0	5533596.5	8L	0.9	43.90	0.33
HC9306	660788.0	5533596.5	8R	2.7		
HC9307	660524.0	5535428.2	8U	16.9	13.90	0.32
HC9307	660524.0	5535428.2	8L	9.9	25.70	0.33
HC9307	660524.0	5535428.2	8R	4.1	18.70	0.51
HC9307	660524.0	5535428.2	10C	2.1	12.30	0.37
HC9307	660524.0	5535428.2	10B	8.0	39.20	0.23
HC9307	660524.0	5535428.2	10A	1.1	13.80	0.77
HC9308	661003.0	5534575.4	8U	4.7	19.30	
HC9308	661003.0	5534575.4	8L	3.7	44.70	
HC9308	661003.0	5534575.4	10C	2.0	15.90	
HC9308	661003.0	5534575.4	10B	7.8		
HC9308	661003.0	5534575.4	10A	1.5		
HC9309	661598.0	5535159.2	8U	3.3	16.90	0.50
HC9309	661598.0	5535159.2	8L	4.0	21.70	0.46
HC9309	661598.0	5535159.2	10C	3.4	15.80	0.44
HC9309	661598.0	5535159.2	10B	11.5	27.20	0.32
HC9309	661598.0	5535159.2	10A	2.1	12.80	0.60
HC9310	661529.0	5535538.6	10C	4.8		
HC9310	661529.0	5535538.6	10B	9.8		
HC9310	661529.0	5535538.6	10A	0.6		
HC9310A	661565.0	5535544.9	10C	3.2		
HC9310A	661565.0	5535544.9	10B	18.0		
HC9310B	661695.0	5535567.9	10C	4.0		
HC9310B	661695.0	5535567.9	10B	12.4		
HC9310B	661695.0	5535567.9	10A	0.9		
HR9302	660988.0	5532496.5	8U	12.6	34.70	
HR9302	660988.0	5532496.5	8L	9.0	25.20	
HR9302	660988.0	5532496.5	8R	1.9	28.90	
HR9305	660054.0	5534767.1	7C	4.0	16.20	
HR9305	660054.0	5534767.1	7B	0.5		
HR9305	660054.0	5534767.1	7A	0.4		
HR9305	660054.0	5534767.1	8M	0.5	62.60	
HR9305	660054.0	5534767.1	8U	7.8	19.76	
HR9305	660054.0	5534767.1	8L	9.5	41.59	
HR9305	660054.0	5534767.1	8R	3.6	27.40	
HR9313	659974.0	5535386.7	8U	1.9	49.50	
HR9313	659974.0	5535386.7	8L	16.3	48.60	
HR9313	659974.0	5535386.7	8R	2.9	48.40	
HR9313	659974.0	5535386.7	9	1.2	28.60	
HR9313	659974.0	5535386.7	9	1.2		
HR9315	659970.0	5535565.1	10C	4.7		
HR9315	659970.0	5535565.1	10B	12.4		
HR9315	659970.0	5535565.1	10A	1.1		
HR9316	660188.0	5534731.4	7A	1.6		

well name	palinspastic x	palinspastic y	Coal Seam	Seam Thickness	Ash (%)	Sulphur (%)
HR9316	660188.0	5534731.4	8R	3.4	34.70	
HR9401	661422.0	5535309.0	10C	4.5	11.70	
HR9401	661422.0	5535309.0	10B	10.0	18.60	
HR9401	661422.0	5535309.0	10A	1.1	30.20	
HR9401A	661429.0	5535310.6	8L	5.5	28.30	
HR9401A	661429.0	5535310.6	8R	4.0	36.90	
HR9402	661580.0	5535342.8	10A	0.8	60.30	
HR9402A	661616.0	5535349.1				
HR9402B	661746.0	5535347.1	8L	1.9		
HR9402B	661746.0	5535347.1	8R	5.3	45.70	
HR9403	660971.0	5534789.6	8U	11.5	16.60	
HR9403	660971.0	5534789.6	8L	4.5	33.60	
HR9403	660971.0	5534789.6	8R	3.5	40.90	
HR9404	661711.0	5535591.2	10C	3.5	19.40	
HR9404	661711.0	5535591.2	10B	9.0	29.70	
HR9404	661711.0	5535591.2	10A	2.1	49.20	
HR9404A	661484.0	5535591.2	9	1.3		
HR9404A	661484.0	5535591.2	10C	2.8		
HR9404A	661484.0	5535591.2	10B	9.5		
HR9404A	661484.0	5535591.2	10A	0.7		
HR9405	660563.0	5534611.7	7C	2.0	20.60	
HR9405	660563.0	5534611.7	7B	3.0	21.00	
HR9405	660563.0	5534611.7	7A	3.7	13.10	
HR9405	660563.0	5534611.7	8U	8.5	27.80	
HR9405	660563.0	5534611.7	8L	7.2	45.10	
HR9405A	661103.0	5534707.0	8L	3.4		
HR9405A	661103.0	5534707.0	8R	2.6		
HR9406	661675.0	5535738.1	10C	3.5	16.60	
HR9406	661675.0	5535738.1	10B	8.0	21.00	
HR9406	661675.0	5535738.1	10A	0.8		
HR9407	661582.0	5535645.8	10C	6.0	29.10	
HR9407	661582.0	5535645.8	10B	17.8	34.20	
HR9407A	661748.0	5535675.0	8L	2.7	42.00	
HR9407A	661748.0	5535675.0	8R	2.0	23.60	
HR9407A	661748.0	5535675.0	10C	2.4		
HR9407A	661748.0	5535675.0	10B	13.6		
HR9407A	661748.0	5535675.0	10A	3.6		
HR9408	661319.0	5535430.9	8U	8.0	19.20	
HR9408	661319.0	5535430.9	8L	6.7	31.80	
HR9408	661319.0	5535430.9	8R	2.0	37.30	
HR9408	661319.0	5535430.9	9	0.9		
HR9408	661319.0	5535430.9	10C	3.5		
HR9408	661319.0	5535430.9	10B	6.8		
HR9408	661319.0	5535430.9	10A	1.0		
HR9409	661277.0	5535768.6	10C	8.5	12.00	
HR9409	661277.0	5535768.6	10B	15.0		
HR9409	661277.0	5535768.6	10A	1.2		
HR9410	661258.0	5535557.9	8U	3.0	33.60	
HR9410A	661188.0	5535539.1	8U	7.0	31.30	
HR9410A	661188.0	5535539.1	8L	11.3	46.60	
HR9410A	661188.0	5535539.1	8R	3.5		

well name	palinspastic x	palinspastic y	Coal Seam	Seam Thickness	Ash (%)	Sulphur (%)
HR9410A	661188.0	5535539.1	10B	7.3		
HR9410A	661188.0	5535539.1	10A	2.2		
HR9411	661597.0	5535845.4	10C	2.2		
HR9411	661597.0	5535845.4	10B	6.8	25.80	
HR9411	661597.0	5535845.4	10A	0.7		
HR9412	660024.0	5535189.8	6U	1.9	16.20	
HR9412	660024.0	5535189.8	6L	1.5		
HR9412	660024.0	5535189.8	7A	2.5	26.40	
HR9412A	660036.0	5535190.5	7B	1.9	17.80	
HR9412A	660036.0	5535190.5	7A	0.8	50.70	
HR9412A	660036.0	5535190.5	8U	3.9		
HR9412A	660036.0	5535190.5	8L	1.3		
HR9412A	660036.0	5535190.5	8R	1.7		
HR9413	661399.0	5535404.7	8U	7.0	21.10	
HR9413	661399.0	5535404.7	8L	1.5	30.00	
HR9413	661399.0	5535404.7	8R	3.0	32.10	
HR9414	659843.0	5535578.7	8U	11.0	57.32	
HR9414	659843.0	5535578.7	8L	26.9	46.80	
HR9414	659843.0	5535578.7	8R	7.7		
HR9415	659555.0	5535532.7	7C	3.5	20.50	
HR9415A	659567.0	5535534.8	7C	2.9	21.40	
HR9415A	659567.0	5535534.8	7B	1.4	29.80	
HR9415A	659567.0	5535534.8	7A	1.5		
HR9415A	659567.0	5535534.8	8U	8.0	30.60	
HR9416	659702.0	5535615.0	8U	9.5	44.50	
HR9416	659702.0	5535615.0	8L	10.3		
HR9416	659702.0	5535615.0	8R	4.1		
HR9416	659702.0	5535615.0	9	0.6		
HR9416	659702.0	5535615.0	10C	9.0	13.50	
HR9416	659702.0	5535615.0	10B	9.4	43.30	
HR9416	659702.0	5535615.0	10A	0.9		
HR9417	659814.0	5535861.6	8R	5.5	36.20	
HR9417	659814.0	5535861.6	9	1.0		
HR9417	659814.0	5535861.6	10C	7.0	22.50	
HR9417	659814.0	5535861.6	10B	13.0	42.30	
HR9417A	659825.0	5535863.7	10B	17.0	27.50	
HR9417A	659825.0	5535863.7	10A	2.9		
HR9418	659872.0	5535875.2	9	1.0		
HR9418	659872.0	5535875.2	10C	3.5	22.90	
HR9418	659872.0	5535875.2	10B	14.0	30.10	
HR9418	659872.0	5535875.2	10A	0.3		
HR9419	659711.0	5535756.3	8U	0.2	22.50	
HR9419	659711.0	5535756.3	8L	13.3	30.00	
HR9419	659711.0	5535756.3	8R	6.0	26.80	
LC004	654512.0	5533297.6	4L	3.6		
LC004	654512.0	5533297.6	5U	1.4		
LC004	654512.0	5533297.6	5L	2.5		
LC004	654512.0	5533297.6	6U	2.4		
LC004	654512.0	5533297.6	6L	2.2		
LC004	654512.0	5533297.6	7B	1.6		
LC004	654512.0	5533297.6	7A	1.8		

well name	palinspastic x	palinspastic y	Coal Seam	Seam Thickness	Ash (%)	Sulphur (%)
LC006A	654774.0	5532694.0	8L	7.0		
LC006A	654774.0	5532694.0	9	3.0		
LC006A	654774.0	5532694.0	10B	5.0		
LC006A	654774.0	5532694.0	10A	2.5		
LC007	654561.0	5533132.8	7A	2.1		
LC007	654561.0	5533132.8	8U	14.0		
LC007	654561.0	5533132.8	8L	20.0		
LC007	654561.0	5533132.8	9U	6.0		
LC007	654561.0	5533132.8	9L	3.0		
LC016	653555.2	5534043.0				
LC016A	653649.1	5534077.1	4U	2.2		
LC016A	653649.1	5534077.1	4L	1.6		
LC016A	653649.1	5534077.1	6U	2.4		
LC016A	653649.1	5534077.1	6L	1.8		
LC016A	653649.1	5534077.1	7B	2.0		
LC016A	653649.1	5534077.1	7A	4.0		
LC017	656442.0	5535692.0	1L	1.1		
LC017	656442.0	5535692.0	2U	7.4		
LC017	656442.0	5535692.0	3UB	2.2		
LC017	656442.0	5535692.0	3UA	0.9		
LC017	656442.0	5535692.0	3UA	0.4		
LC017	656442.0	5535692.0	3LB	1.9		
LC017	656442.0	5535692.0	3LA	1.5		
LC017	656442.0	5535692.0	4U	1.6		
LC017	656442.0	5535692.0	4L	0.5		
LC017	656442.0	5535692.0	5U	0.6		
LC017	656442.0	5535692.0	6U	8.0		
LC017	656442.0	5535692.0	6L	5.0		
LC017	656442.0	5535692.0	7B	6.2		
LC017	656442.0	5535692.0	8U	8.3		
LC073	652935.0	5534168.5	4U	8.0		
LC073A	653029.0	5534202.7	4U	5.3		
LC073A	653029.0	5534202.7	5U	1.9		
LC073A	653029.0	5534202.7	6U	8.0		
LC073A	653029.0	5534202.7	7B	3.5		
LC073A	653029.0	5534202.7	7A	11.2		
LC301	654338.8	5534407.0	5U	0.9		
LC301	654338.8	5534407.0	6U	1.0		
LC301	654338.8	5534407.0	7B	20.1		
LC301	654338.8	5534407.0	7A	3.0		
LC301	654338.8	5534407.0	8M	2.0		
LC301	654338.8	5534407.0	8U	19.4	35.96	
LC303	655898.0	5535066.0	A	3.7		
LC303	655898.0	5535066.0	1U	2.2		
LC303	655898.0	5535066.0	2U	2.5		
LC303	655898.0	5535066.0	3UB	4.0		
LC303	655898.0	5535066.0	3UA	9.2	28.80	
LC303	655898.0	5535066.0	3UB	5.1		
LC303	655898.0	5535066.0	3UA	9.0		
LC303	655898.0	5535066.0	3LB	4.2		
LC303	655898.0	5535066.0	3LA	1.1		

well name	palinspastic x	palinspastic y	Coal Seam	Seam Thickness	Ash (%)	Sulphur (%)
LC413	655682.0	5535064.0	3UB	5.8		
LC413	655682.0	5535064.0	3UA	0.6		
LC413	655682.0	5535064.0	3LB	0.7		
LC413	655682.0	5535064.0	3LA	9.1		
LC413	655682.0	5535064.0	4U	16.9		
LC413	655682.0	5535064.0	4L	0.8		
LC413A	655777.0	5535097.0	4U	17.5	35.60	
LC413A	655777.0	5535097.0	5U	4.0		
LC413A	655777.0	5535097.0	6U	2.7	64.99	
LC413A	655777.0	5535097.0	6L	4.9	28.45	
LC413A	655777.0	5535097.0	7A	2.9	27.00	
LC413A	655777.0	5535097.0	8U	7.6	23.96	
LC413A	655777.0	5535097.0	8L	5.4		
LC413A	655777.0	5535097.0	8R	2.2		
LC413A	655777.0	5535097.0	9	10.7		
LC413A	655777.0	5535097.0	10B	5.0	12.60	
LC413A	655777.0	5535097.0	10A	3.0	23.10	
LC414	656043.0	5534964.0	2U	2.0		
LC414	656043.0	5534964.0	3UB	4.2		
LC414	656043.0	5534964.0	3UA	0.9		
LC414	656043.0	5534964.0	3LB	5.6		
LC414	656043.0	5534964.0	3LA	2.9		
LC414	656043.0	5534964.0	4U	3.8	43.72	
LC414	656043.0	5534964.0	4L	2.6	20.49	
LC414A	656135.0	5534999.0	4U	1.5	21.75	
LC414A	656135.0	5534999.0	4L	5.0		
LC414A	656135.0	5534999.0	5U	2.3	60.21	
LC414A	656135.0	5534999.0	6U	2.5		
LC414A	656135.0	5534999.0	7A	2.3	47.80	
LC414A	656135.0	5534999.0	8U	9.0		
LC414A	656135.0	5534999.0	8L	2.0		
LC414B	656278.0	5535051.0	8U	5.2	31.65	
LC414B	656278.0	5535051.0	10B	6.4	26.10	
LC414B	656278.0	5535051.0	10A	7.9	16.10	
LC416	655565.0	5535285.0	5U	1.0	56.39	
LC416	655565.0	5535285.0	6U	1.0	9.67	
LC416	655565.0	5535285.0	7B	7.8	29.40	
LC416	655565.0	5535285.0	7A	4.9		
LC416	655565.0	5535285.0	8M	8.3		
LC416	655565.0	5535285.0	8U	12.6	24.35	
LC416	655565.0	5535285.0	9	1.5	29.61	
LC416	655565.0	5535285.0	10B	6.8	57.50	
LC416	655565.0	5535285.0	10A	0.8		
LC416A	655659.0	5535322.0	10B	5.9		
LC416A	655659.0	5535322.0	10A	4.4		
LC416B	655707.0	5535341.0	10B	5.9	14.20	
LC416B	655707.0	5535341.0	10A	4.4	22.30	
LC416B	655707.0	5535341.0	3UB	1.6		
LC416B	655707.0	5535341.0	3UA	2.8		
LC416B	655707.0	5535341.0	3LB	1.3		0.48
LC416B	655707.0	5535341.0	3LA	2.6		0.85

well name	palinspastic x	palinspastic y	Coal Seam	Seam Thickness	Ash (%)	Sulphur (%)
LC417A	653476.7	5534025.1	5U	2.2		0.86
LC417A	653476.7	5534025.1	6U	3.2		0.51
LC417A	653476.7	5534025.1	6L	1.7		0.56
LC417A	653476.7	5534025.1	7A	6.5	39.30	0.50
LC417A	653476.7	5534025.1	8U	6.6	19.37	0.27
LC417A	653476.7	5534025.1	8L	9.4		
LC417A	653476.7	5534025.1	9U	4.6		0.51
LC417A	653476.7	5534025.1	9L	1.5		0.62
LC418	655795.0	5535641.0	4U	7.9		
LC418A	655681.0	5535596.0	5L	1.0		
LC419	653643.3	5534181.5	A	2.0		
LC419	653643.3	5534181.5	1U	0.5		
LC419	653643.3	5534181.5	1L	1.0		
LC419	653643.3	5534181.5	2U	1.4		
LC419	653643.3	5534181.5	3UB	1.0		
LC419	653643.3	5534181.5	3UA	1.4		
LC419A	653737.1	5534215.6	3UA	2.5		
LC419A	653737.1	5534215.6	3LB	1.8		
LC419A	653737.1	5534215.6	3LA	2.1		
LC419A	653737.1	5534215.6	4U	1.8	30.38	
LC419A	653737.1	5534215.6	4L	1.0		
LC419A	653737.1	5534215.6	5U	0.8		
LC419A	653737.1	5534215.6	6U	4.4		
LC419A	653737.1	5534215.6	6L	2.6		
LC419A	653737.1	5534215.6	7B	6.9	20.70	
LC419B	654518.0	5534498.0	7A	2.1	26.30	
LC419B	654518.0	5534498.0	8M	1.1		
LC419B	654518.0	5534498.0	8U	18.2	19.95	
LC419B	654518.0	5534498.0	8L	2.1	31.23	
LC419B	654518.0	5534498.0	10B	4.0	38.50	
LC419B	654518.0	5534498.0	10A	3.0	19.80	
LC419B	654518.0	5534498.0	2U	5.0		
LC419B	654518.0	5534498.0	3UB	0.9		
LC419B	654518.0	5534498.0	3UA	1.0	14.71	
LC419B	654518.0	5534498.0	3LB	5.0		
LC419B	654518.0	5534498.0	3LA	1.1		
LC420A	656495.0	5535741.0	3LA	5.8		
LC420A	656495.0	5535741.0	4U	6.0		
LC420A	656495.0	5535741.0	4L	1.2		
LC420A	656495.0	5535741.0	5U	1.4		
LC420A	656495.0	5535741.0	6U	2.8		
LC420A	656495.0	5535741.0	7B	4.8		
LC420A	656495.0	5535741.0	7A	1.2		
LC420A	656495.0	5535741.0	8M	10.7		
LC420A	656495.0	5535741.0	8U	4.5		
LC420A	656495.0	5535741.0	8L	1.1		
LC420A	656495.0	5535741.0	8R	1.1		
LC420A	656495.0	5535741.0	9	0.9		
LC420A	656495.0	5535741.0	10A	12.0		
LC422	653084.6	5533903.7	4U	7.6	18.77	
LC422A	653136.9	5533876.2	5L	1.5		

well name	palinspastic x	palinspastic y	Coal Seam	Seam Thickness	Ash (%)	Sulphur (%)
LC422A	653136.9	5533876.2	7A	8.5	30.80	
LC422A	653136.9	5533876.2	8M	1.6		
LC422A	653136.9	5533876.2	8U	13.0	25.06	
LC422A	653136.9	5533876.2	9U	3.2		
LC422A	653136.9	5533876.2	9L	1.1		
LC422A	653136.9	5533876.2	10B	5.0	39.30	
LC422A	653136.9	5533876.2	10A	2.4	23.60	
LC423	653722.0	5534335.0	2U	1.8		
LC423	653722.0	5534335.0	2L	0.7		
LC423	653722.0	5534335.0	3UB	1.5		
LC423A	653817.0	5534369.0	3UB	2.2		
LC423A	653817.0	5534369.0	3UA	2.5		
LC423A	653817.0	5534369.0	3LB	0.9		
LC423A	653817.0	5534369.0	3LA	9.4		
LC423A	653817.0	5534369.0	4U	5.0	35.63	
LC423A	653817.0	5534369.0	4L	5.9	47.40	
LC423A	653817.0	5534369.0	6U	4.7		
LC423A	653817.0	5534369.0	6L	2.2		
LC423B	654144.0	5534496.0	5L	1.9		
LC423B	654144.0	5534496.0	6U	7.4		
LC423B	654144.0	5534496.0	7B	2.4	36.00	
LC423B	654144.0	5534496.0	7A	1.5	38.80	
LC423B	654144.0	5534496.0	8U	4.3	28.40	
LC423B	654144.0	5534496.0	8L	1.5	28.09	
LC423B	654144.0	5534496.0	8R	1.5		
LC424	655914.0	5534819.0	1L	1.0		
LC424	655914.0	5534819.0	2U	1.7		
LC424	655914.0	5534819.0	2L	0.9		
LC424	655914.0	5534819.0	3UB	2.8		
LC424	655914.0	5534819.0	3UA	2.4		
LC424	655914.0	5534819.0	3LB	8.1		
LC424A	656007.0	5534846.0	3LB	4.8		
LC424A	656007.0	5534846.0	3LA	4.2		
LC424A	656007.0	5534846.0	4U	1.8	25.14	
LC424A	656007.0	5534846.0	4L	4.3	13.90	
LC424A	656007.0	5534846.0	5U	2.2		
LC424B	656149.0	5534898.0	5U	0.5		
LC424B	656149.0	5534898.0	5L	2.7		
LC424B	656149.0	5534898.0	6U	2.2		
LC424B	656149.0	5534898.0	7B	4.5	25.70	
LC424B	656149.0	5534898.0	7A	4.0	28.10	
LC424B	656149.0	5534898.0	8M	7.0	24.86	
LC424B	656149.0	5534898.0	8U	10.9	25.03	0.33
LC424C	656170.0	5534916.0	8U	5.8	25.82	
LC424C	656170.0	5534916.0	10A	3.2	14.50	
LC425	656546.0	5535054.0	4L	0.9		
LC425	656546.0	5535054.0	5U	0.8		
LC425	656546.0	5535054.0	6U	0.8		
LC425	656546.0	5535054.0	6L	7.2		
LC425	656546.0	5535054.0	7B	1.5	20.80	
LC425	656546.0	5535054.0	7A	4.2	20.80	

well name	palinspastic x	palinspastic y	Coal Seam	Seam Thickness	Ash (%)	Sulphur (%)
LC425	656546.0	5535054.0	8L	8.4		
LC425	656546.0	5535054.0	9	0.7		
LC425	656546.0	5535054.0	10A	3.9	40.00	
LC425A	656688.0	5535107.0	10A	7.9	21.10	
LC426	654427.0	5534761.0	3LB	2.5		
LC426	654427.0	5534761.0	3LA	4.0		
LC426	654427.0	5534761.0	4U	4.3	43.92	0.69
LC426	654427.0	5534761.0	4L	0.9		0.84
LC426	654427.0	5534761.0	5U	0.7		0.80
LC426	654427.0	5534761.0	6U	3.3		0.79
LC426	654427.0	5534761.0	6L	2.8		0.45
LC426	654427.0	5534761.0	7C	1.6	30.90	
LC426	654427.0	5534761.0	7B	6.0		
LC426	654427.0	5534761.0	7A	1.8		0.54
LC427	654729.0	5534697.0	6U	3.5		
LC427	654729.0	5534697.0	7B	9.2	46.30	
LC427	654729.0	5534697.0	8U	9.1	19.41	
LC427	654729.0	5534697.0	8L	8.3	14.44	
LC427	654729.0	5534697.0	10C	4.2		
LC427	654729.0	5534697.0	10B	2.9	26.90	
LC427	654729.0	5534697.0	10A	15.0	19.10	
LC428	655678.0	5534721.0	3UA	1.2		
LC428	655678.0	5534721.0	3LB	5.5		
LC428	655678.0	5534721.0	3LA	1.7		
LC428	655678.0	5534721.0	4U	3.4		
LC428	655678.0	5534721.0	4L	3.8		
LC428A	655769.0	5534755.0	5U	1.9		
LC428A	655769.0	5534755.0	6U	1.3		
LC428A	655769.0	5534755.0	6L	2.9		
LC428A	655769.0	5534755.0	7B	2.7		
LC428A	655769.0	5534755.0	7A	2.9	19.10	
LC428B	655910.0	5534817.0	7B	6.1		
LC428B	655910.0	5534817.0	7A	2.8		
LC428B	655910.0	5534817.0	8M	4.4	27.56	
LC428B	655910.0	5534817.0	8U	7.7		
LC428B	655910.0	5534817.0	8L	10.4		
LC428B	655910.0	5534817.0	10B	4.0		
LC428B	655910.0	5534817.0	10A	4.4		
LC429	656198.0	5534897.0	A	2.0		
LC429	656198.0	5534897.0	1U	2.0		
LC429	656198.0	5534897.0	2U	1.4		
LC429	656198.0	5534897.0	2L	1.0		
LC429	656198.0	5534897.0	3UB	3.0		
LC429	656198.0	5534897.0	3UA	2.2	50.08	
LC429	656198.0	5534897.0	3LB	3.7	44.53	
LC429	656198.0	5534897.0	3LA	4.0	46.51	
LC429	656198.0	5534897.0	4U	3.7	46.51	
LC429	656198.0	5534897.0	4L	4.0	18.44	
LC429A	656222.0	5534891.0	4U	1.6		
LC429A	656222.0	5534891.0	4L	3.4		
LC429A	656222.0	5534891.0	5U	0.8	62.60	

well name	palinspastic x	palinspastic y	Coal Seam	Seam Thickness	Ash (%)	Sulphur (%)
LC429A	656222.0	5534891.0	6L	5.1		
LC429A	656222.0	5534891.0	7B	1.7	37.15	
LC429A	656222.0	5534891.0	7A	4.5		
LC429A	656222.0	5534891.0	8M	3.5		
LC429A	656222.0	5534891.0	8U	4.8	23.01	
LC429A	656222.0	5534891.0	8L	1.2	42.54	
LC429A	656222.0	5534891.0	10B	2.4	26.10	
LC429A	656222.0	5534891.0	10A	6.0		
LC430	653404.8	5534398.0	2U	2.1		
LC430	653404.8	5534398.0	3UB	1.3		
LC430	653404.8	5534398.0	3UA	3.9		
LC430	653404.8	5534398.0	3LB	4.9		
LC430	653404.8	5534398.0	3LA	1.2		
LC430A	653498.6	5534432.1	3LB	5.1		
LC430B	653804.0	5534534.0	3LB	3.4		
LC430B	653804.0	5534534.0	3LA	3.0		
LC430B	653804.0	5534534.0	4U	1.1	22.72	
LC430B	653804.0	5534534.0	4L	2.1	20.82	
LC430B	653804.0	5534534.0	5U	0.4		
LC432	655486.0	5535068.0	3UB	1.2		
LC432	655486.0	5535068.0	3UA	2.3	30.20	
LC432	655486.0	5535068.0	3LB	4.2	47.82	
LC432	655486.0	5535068.0	3LA	1.6	22.39	
LC432	655486.0	5535068.0	4U	9.7	22.29	
LC432	655486.0	5535068.0	4L	2.0	17.44	
LC432A	655577.0	5535107.0	4L	2.0		
LC432A	655577.0	5535107.0	5U	1.5	42.78	
LC432A	655577.0	5535107.0	5L	2.9		
LC432B	655718.0	5535160.0	6L	0.4		
LC432B	655718.0	5535160.0	7C	6.3		
LC432B	655718.0	5535160.0	7B	2.3	24.90	
LC432C	655733.0	5535166.0	7A	6.2		
LC432C	655733.0	5535166.0	8M	8.0		
LC432C	655733.0	5535166.0	8U	18.8	25.98	
LC433	655205.0	5534764.0	4L	1.2	11.88	
LC433	655205.0	5534764.0	5U	3.9		
LC433	655205.0	5534764.0	5L	3.1		
LC433	655205.0	5534764.0	6U	1.3		
LC433	655205.0	5534764.0	7B	5.0	22.80	
LC433	655205.0	5534764.0	7A	9.5	23.10	
LC433	655205.0	5534764.0	8M	3.8	29.71	
LC433	655205.0	5534764.0	8U	23.3	18.65	
LC433A	655299.0	5534799.0	8U	8.1	24.01	
LC433A	655299.0	5534799.0	8L	10.8	25.76	
LC433A	655299.0	5534799.0	8R	10.1		
LC434	655298.0	5534582.0	4L	1.6	51.57	
LC434	655298.0	5534582.0	5U	1.0		
LC434	655298.0	5534582.0	5L	1.5		
LC434	655298.0	5534582.0	6U	1.5		
LC434	655298.0	5534582.0	7C	5.6	23.30	
LC434	655298.0	5534582.0	7B	5.3	35.00	

well name	palinspastic x	palinspastic y	Coal Seam	Seam Thickness	Ash (%)	Sulphur (%)
LC434	655298.0	5534582.0	8U	20.0	22.29	
LC434A	655392.0	5534619.0	8U	2.5	10.70	
LC434A	655392.0	5534619.0	9U	1.0		
LC434A	655392.0	5534619.0	9L	2.4		
LC434A	655392.0	5534619.0	10B	4.7	30.50	
LC434A	655392.0	5534619.0	10A	5.4	22.80	
LC435	655957.0	5535826.0	5U	1.4		0.68
LC435	655957.0	5535826.0	6U	6.2		0.70
LC435	655957.0	5535826.0	7B	2.8	24.00	0.48
LC435	655957.0	5535826.0	7A	2.5	21.50	0.35
LC435	655957.0	5535826.0	8M	2.6	26.24	0.37
LC435	655957.0	5535826.0	8U	20.0	19.83	0.32
LC435	655957.0	5535826.0	10C	8.9		
LC435	655957.0	5535826.0	10B	9.2		
LC435	655957.0	5535826.0	10A	5.0		
LC436	654625.0	5534345.0	4U	7.0	22.23	0.71
LC436	654625.0	5534345.0	4L	2.9	30.91	0.88
LC436	654625.0	5534345.0	5U	1.3		
LC436	654625.0	5534345.0	5L	3.6		
LC436A	654682.0	5534407.0	6U	4.0		
LC436A	654682.0	5534407.0	6L	3.0		
LC436A	654682.0	5534407.0	7C	2.6		
LC436A	654682.0	5534407.0	7B	1.5		
LC437	654892.0	5534324.0	7A	5.0		
LC437	654892.0	5534324.0	8U	15.1	17.16	0.36
LC437	654892.0	5534324.0	8L	1.1		
LC437	654892.0	5534324.0	8R	0.9		
LC437	654892.0	5534324.0	9	2.2		
LC437	654892.0	5534324.0	10B	0.3	29.00	
LC437	654892.0	5534324.0	10A	1.0	35.70	
LC438	655101.0	5534539.0				
LC438A	655146.0	5534552.0	10B	6.7	20.00	
LC438B	655336.0	5534626.0	10C	5.3		0.46
LC438B	655336.0	5534626.0	10B	7.1		0.38
LC438B	655336.0	5534626.0	10A	2.6	33.50	0.58
LC439	655648.0	5535624.0	5L	2.0		
LC439	655648.0	5535624.0	6U	1.1		0.79
LC439	655648.0	5535624.0	6L	0.4		
LC439A	655692.0	5535640.0	6L	1.2		
LC439A	655692.0	5535640.0	7B	2.3	33.00	0.34
LC439A	655692.0	5535640.0	7A	4.5		
LC439A	655692.0	5535640.0	8M	6.7	23.93	0.41
LC439A	655692.0	5535640.0	8U	13.1	21.80	0.30
LC439A	655692.0	5535640.0	9	0.8		
LC439B	655732.0	5535655.0	8M	5.5		
LC439B	655732.0	5535655.0	8U	18.1	23.29	
LC439B	655732.0	5535655.0	9	0.3		
LC439B	655732.0	5535655.0	10C	0.7		
LC439B	655732.0	5535655.0	10B	8.6		0.37
LC439B	655732.0	5535655.0	10A	6.2	25.80	0.43
LC441	656164.0	5535491.0	2U	1.2		

well name	palinspastic x	palinspastic y	Coal Seam	Seam Thickness	Ash (%)	Sulphur (%)
LC441	656164.0	5535491.0	3LB	3.6		0.50
LC441	656164.0	5535491.0	3LA	2.8		
LC441	656164.0	5535491.0	4U	6.0	18.45	0.53
LC441	656164.0	5535491.0	4L	1.8	33.43	
LC441A	565085.0	5535478.0	7B	1.3		
LC442	657263.0	5535415.0	7B	0.6	45.50	
LC442	657263.0	5535415.0	7A	3.2	15.70	
LC442	657263.0	5535415.0	8U	1.1	37.24	0.62
LC442	657263.0	5535415.0	8L	0.9		
LC442	657263.0	5535415.0	8R	0.3		
LC442A	657405.0	5535470.0	8U	3.0	31.35	
LC442A	657405.0	5535470.0	8L	0.8		
LC442A	657405.0	5535470.0	9	0.5		
LC442A	657405.0	5535470.0	10B	6.3	38.80	
LC442A	657405.0	5535470.0	10A	4.2	24.10	
LC443	656759.0	5535670.0	3LB	5.9		
LC443	656759.0	5535670.0	3LA	2.0		
LC443	656759.0	5535670.0	4U	7.8	45.19	
LC443A	656644.0	5535629.0	4U	5.5		
LC443A	656644.0	5535629.0	4L	1.0		
LC443B	656740.0	5535664.0	4L	1.0		
LC443C	656787.0	5535680.0	4L	2.1	28.78	
LC443C	656787.0	5535680.0	5U	1.8		
LC443C	656787.0	5535680.0	6U	2.9		
LC443C	656787.0	5535680.0	6L	0.8		
LC443C	656787.0	5535680.0	8M	3.8	48.40	
LC443C	656787.0	5535680.0	8U	8.0	28.07	
LC443C	656787.0	5535680.0	8L	14.0	42.83	
LC444	655737.4	5535924.0	5L	2.1		
LC444	655737.4	5535924.0	6U	1.6		
LC444	655737.4	5535924.0	6L	1.2		
LC444	655737.4	5535924.0	7B	4.2	25.70	
LC444	655737.4	5535924.0	7A	2.4		
LC444	655737.4	5535924.0	8M	5.7	25.70	
LC444	655737.4	5535924.0	8U	11.3	23.13	
LC444	655737.4	5535924.0	9	0.8		
LC444	655737.4	5535924.0	10B	6.4	18.00	
LC444	655737.4	5535924.0	10A	4.3	18.80	
LC445	654461.7	5534223.9	5U	0.6		
LC445	654461.7	5534223.9	5L	0.4		
LC445	654461.7	5534223.9	6U	1.0		
LC445	654461.7	5534223.9	6L	1.3		
LC445	654461.7	5534223.9	7B	6.8	15.30	
LC445	654461.7	5534223.9	8M	2.4	19.52	
LC445	654461.7	5534223.9	8U	14.5	18.20	
LC445	654461.7	5534223.9	9	4.9		
LC445	654461.7	5534223.9	10B	6.2	30.30	
LC445	654461.7	5534223.9	10A	2.7	18.20	
LC445A	654529.2	5534219.9	10A	10.0		
LC446	655415.0	5535001.0	6U	1.0		
LC446	655415.0	5535001.0	6L	4.0		

well name	palinspastic x	palinspastic y	Coal Seam	Seam Thickness	Ash (%)	Sulphur (%)
LC446	655415.0	5535001.0	7A	3.5		
LC446	655415.0	5535001.0	8U	10.8		
LC446	655415.0	5535001.0	9	2.8		
LC446	655415.0	5535001.0	10B	8.3	32.70	
LC446	655415.0	5535001.0	10A	4.0	22.70	
LC447	655665.0	5535092.0	A	2.8		
LC447	655665.0	5535092.0	1U	0.8		
LC447	655665.0	5535092.0	1L	0.6		
LC447	655665.0	5535092.0	2U	4.0		
LC447	655665.0	5535092.0	2L	3.4		
LC447	655665.0	5535092.0	3UB	1.3		
LC447	655665.0	5535092.0	3UA	0.8		
LC447	655665.0	5535092.0	3LB	5.7		
LC447	655665.0	5535092.0	3LA	4.6		
LC447	655665.0	5535092.0	4U	5.1	55.40	
LC447	655665.0	5535092.0	4L	2.0	14.00	
LC447	655665.0	5535092.0	5U	2.1		
LC447	655665.0	5535092.0	5L	0.6		
LC447A	655757.0	5535127.0	5U	1.5		
LC447A	655757.0	5535127.0	5L	0.8		
LC447A	655757.0	5535127.0	6U	2.2		
LC447A	655757.0	5535127.0	7B	2.1		
LC447A	655757.0	5535127.0	7A	4.0		
LC447A	655757.0	5535127.0	8M	6.6	25.50	
LC448	653574.0	5534417.0	2U	2.5		
LC448	653574.0	5534417.0	3UB	2.5		
LC448	653574.0	5534417.0	3UA	2.4		
LC448	653574.0	5534417.0	3LB	4.6		
LC448	653574.0	5534417.0	3LA	2.6		
LC448	653574.0	5534417.0	4U	16.0	22.30	
LC448	653574.0	5534417.0	4L	2.0		
LC448A	653667.0	5534453.0	4U	0.7	26.50	
LC448A	653667.0	5534453.0	4L	2.0	84.00	
LC448B	653996.0	5534578.0	6U	2.4		
LC449	657264.0	5535221.0	8M	1.4		
LC449	657264.0	5535221.0	8U	4.9	37.31	
LC449	657264.0	5535221.0	10A	4.9	20.80	
LC450	654446.0	5534559.0	3LA	2.8		
LC450	654446.0	5534559.0	4U	1.7		
LC450	654446.0	5534559.0	4L	4.4	45.29	
LC450	654446.0	5534559.0	5U	0.9		
LC450	654446.0	5534559.0	5L	2.2		
LC450	654446.0	5534559.0	6U	3.2		
LC450	654446.0	5534559.0	6L	2.7		
LC450	654446.0	5534559.0	7B	1.4	41.64	
LC450	654446.0	5534559.0	7A	3.5		
LC450	654446.0	5534559.0	8M	1.4		
LC450	654446.0	5534559.0	8U	6.8	25.95	
LC450	654446.0	5534559.0	8L	1.1	11.14	
LC451	654416.0	5534768.0	3LA	2.0		
LC451	654416.0	5534768.0	4U	1.2		

well name	palinspastic x	palinspastic y	Coal Seam	Seam Thickness	Ash (%)	Sulphur (%)
LC451	654416.0	5534768.0	5L	1.9		
LC451	654416.0	5534768.0	6U	3.3		
LC451	654416.0	5534768.0	7B	3.0	57.30	
LC451	654416.0	5534768.0	7A	3.5		
LC451	654416.0	5534768.0	8M	1.0	32.71	
LC451	654416.0	5534768.0	8U	5.1	19.90	
LC451	654416.0	5534768.0	8L	1.6		
LC452	654862.0	5534376.0	7B	3.8	29.00	
LC452	654862.0	5534376.0	7A	1.5		
LC452	654862.0	5534376.0	8U	7.4		
LC452	654862.0	5534376.0	8L	1.4	31.22	
LC452	654862.0	5534376.0	8R	1.4		
LC452	654862.0	5534376.0	10B	1.9		
LC452	654862.0	5534376.0	10A	12.0	26.90	
LC453	656199.0	5535476.0	3UB	1.0		
LC453	656199.0	5535476.0	3UA	1.0		
LC453	656199.0	5535476.0	3LB	9.5		
LC453	656199.0	5535476.0	3LA	1.1		
LC453	656199.0	5535476.0	4U	11.0		
LC453A	656097.0	5535436.0				
LC454	656279.0	5535857.0	2U	1.2		
LC454	656279.0	5535857.0	2L	4.4		
LC454	656279.0	5535857.0	3UB	0.6		
LC454	656279.0	5535857.0	3UA	0.7		
LC454	656279.0	5535857.0	3LB	4.2		
LC454	656279.0	5535857.0	3LA	1.7		
LC454	656279.0	5535857.0	4U	3.6		
LC455	655935.0	5535465.0	A	0.6		
LC455	655935.0	5535465.0	1U	0.7		
LC455	655935.0	5535465.0	2U	8.5		
LC455	655935.0	5535465.0	3UB	1.0		
LC455	655935.0	5535465.0	3UA	1.0		
LC455	655935.0	5535465.0	3LB	5.1		
LC455	655935.0	5535465.0	3LA	1.4		
LC455A	655850.0	5535405.0	3LA	3.0		
LC455A	655850.0	5535405.0	4U	4.1	9.08	
LC456	656032.0	5535045.0	A	4.3		
LC456	656032.0	5535045.0	2L	1.3		
LC456	656032.0	5535045.0	3UB	4.4		
LC456	656032.0	5535045.0	3UA	1.0		
LC456A	656127.0	5535082.0	3UB	5.0		
LC456A	656127.0	5535082.0	3UA	3.2		
LC456A	656127.0	5535082.0	3LB	2.4		
LC456A	656127.0	5535082.0	3LA	0.9		
LC456A	656127.0	5535082.0	4U	1.9	26.72	
LC456A	656127.0	5535082.0	4L	3.7	19.50	
LC457	656061.0	5535703.0	2L	2.2		
LC457	656061.0	5535703.0	3UB	2.0		
LC457	656061.0	5535703.0	3UA	2.0		
LC457	656061.0	5535703.0	3LB	8.0	17.80	
LC457	656061.0	5535703.0	3LA	3.1	33.20	

well name	palinspastic x	palinspastic y	Coal Seam	Seam Thickness	Ash (%)	Sulphur (%)
LC475	653760.0	5534295.0	7B	12.2		
LC475	653760.0	5534295.0	7A	2.2		0.29
LC475	653760.0	5534295.0	8M	2.6	29.40	
LC475A	653878.0	5534320.0	8U	3.5	21.70	0.22
LC475A	653878.0	5534320.0	8L	1.4		
LC475A	653878.0	5534320.0	8R	2.2		
LC475A	653878.0	5534320.0	9U	0.8		
LC475A	653878.0	5534320.0	9L	2.5	38.70	0.35
LC475B	654190.0	5534485.0	9U	0.3		
LC475B	654190.0	5534485.0	9L	2.5		
LC476	653905.0	5534280.0	7C	6.5		
LC476	653905.0	5534280.0	7B	9.4		
LC476	653905.0	5534280.0	7A	12.0		
LC476	653905.0	5534280.0	8M	7.8	29.40	
LC476	653905.0	5534280.0	8U	6.0		
LC476A	654210.0	5534435.0	8U	22.8		
LC476A	654210.0	5534435.0	9U	3.0		
LC476A	654210.0	5534435.0	9L	1.2		
LC476A	654210.0	5534435.0	10B	4.1	30.60	0.38
LC476A	654210.0	5534435.0	10A	7.7	32.70	0.35
LC478	653800.0	5534217.0	7C	4.4	42.60	
LC478	653800.0	5534217.0	7B	3.0	29.00	
LC478	653800.0	5534217.0	7A	7.7		
LC478A	653921.0	5534195.0	7C	3.0	27.30	
LC478A	653921.0	5534195.0	7B	14.0	53.80	
LC478A	653921.0	5534195.0	7A	1.7		
LC478B	654280.0	5534315.0	7B	13.3		
LC478B	654280.0	5534315.0	7A	10.0		
LC478B	654280.0	5534315.0	8M	3.1		
LC478B	654280.0	5534315.0	8U	18.3	24.70	0.67
LC478B	654280.0	5534315.0	8L	9.7	22.80	
LC9201	656130.0	5535699.0	2U	8.3	13.20	0.39
LC9201	656130.0	5535699.0	3UB	0.9	38.80	0.85
LC9201	656130.0	5535699.0	3UA	0.7		
LC9201	656130.0	5535699.0	3LB	2.2	43.20	
LC9201	656130.0	5535699.0	3LA	3.7	11.00	
LC9202	653571.4	5534144.6	1U	0.9		
LC9202	653571.4	5534144.6	1L	0.6		
LC9202	653571.4	5534144.6	2U	2.0		
LC9202	653571.4	5534144.6	2L	0.6		
LC9202	653571.4	5534144.6	3UB	0.6	10.40	
LC9202	653571.4	5534144.6	3UA	0.5		
LC9202	653571.4	5534144.6	3LB	0.9	19.60	0.46
LC9202	653571.4	5534144.6	3LA	2.7		0.36
LC9202A	653665.3	5534178.8	3LB	2.2		0.75
LC9202A	653665.3	5534178.8	3LA	3.5		0.44
MSAN891	661259.1	5537006.1	10B	16.1	15.30	0.40
MSAN891	661259.1	5537006.1	10A	0.6	67.00	
MSAN891A	661311.1	5537015.2	10B	12.0	21.00	
MSAN891A	661311.1	5537015.2	10A	1.0	28.00	
MSAN892	661346.4	5536987.4	10C	2.7		

well name	palinspastic x	palinspastic y	Coal Seam	Seam Thickness	Ash (%)	Sulphur (%)
MSAN893	661331.0	5536980.3	10C	5.1	14.20	0.40
MSAN893	661331.0	5536980.3	10B	11.1	15.80	0.40
MSAN893	661331.0	5536980.3	10A	0.7		
MSAN893A	661385.0	5536989.8	10A	5.3	14.70	
MSAN894	661199.7	5536944.4	8L	2.2	35.00	
MSAN894	661199.7	5536944.4	8R	16.0	25.30	
MSAN894	661199.7	5536944.4	10C	7.8	17.10	
MSAN894	661199.7	5536944.4	10B	14.5	17.20	
MSAN894	661199.7	5536944.4	10A	1.2		
MSAN894A	661221.7	5536948.3	10A	0.6		
MSAN9201	661131.8	5538091.0	9U	7.5		
MSAN9201	661131.8	5538091.0	9L	8.9		
MSAN9201	661131.8	5538091.0	10B	10.2		
MSAN9201	661131.8	5538091.0	10A	4.5		
MSAN9201A	661095.8	5538085.0				
MSAN9202	662010.1	5538110.5	7B	5.2		
MSAN9202	662010.1	5538110.5	7A	3.7		
MSAN9202	662010.1	5538110.5	8U	5.3		
MSAW9203	657883.6	5534425.5	9	5.0		
MSAW9203	657883.6	5534425.5	10C	13.4		
MSAW9203	657883.6	5534425.5	10B	21.0		
MSAW9203	657883.6	5534425.5	10A	6.5		
MSAW9204	657870.0	5534714.4	7A	4.5		
MSAW9204	657870.0	5534714.4	8U	5.1		
MSAW9204	657870.0	5534714.4	8L	6.9		
MSAW9204	657870.0	5534714.4	9	1.2		
MSAW9204	657870.0	5534714.4	10B	5.6		
MSAW9204	657870.0	5534714.4	10A	10.0		

NOTE: Location of the palinspastic drill holes are given in UTM co-ordinates. This allows easy comparison with original location of the drill holes, but the palinspastic drill holes do not exist in reality.

Appendix B

Maceral Composition

Appendix B

MACERAL COMPOSITION

Seam	Sample No. or Drillhole	Vitrinite (%)			Inertinite (%)				Liptinite (%)	TPI	GI
		Telo.	Detro.	Total	Macrinite	Fusinite	Semifus.	Total			
3LA	SV96 -23-279	0.3	76.0	76.3	0.0	2.6	21.0	23.6	0.0	0.31	3.23
4U	SV96-23-272	0.0	63.4	63.4	0.0	1.3	35.4	36.7	0.0	0.58	1.73
4U	SV96-23-273	0.3	43.1	43.4	0.3	1.6	54.4	56.3	0.3	1.31	0.78
4U	SV96-23-274A	0.3	61.1	61.4	0.0	5.0	33.7	38.7	0.0	0.64	1.59
4L	SV96-23-263	3.3	50.0	53.3	1.3	15.6	29.6	46.5	0.2	0.97	1.21
4L	SV96-23-265	0.6	50.2	50.8	0.0	6.0	43.5	49.5	0.0	1.00	1.03
4L	SV96-23-270	0.6	39.1	39.7	2.3	20.4	37.7	60.4	0.0	1.50	0.72
4L	SV96-23-268	0.0	42.0	42.0	0.0	1.0	57.0	58.0	0.0	1.38	0.72
4L	SV96-23-268A	2.3	48.3	50.6	0.3	8.0	41.0	49.3	0.0	1.06	1.04
6U	SV96-23-289	2.6	51.6	54.2	0.0	2.4	43.8	46.2	0.0	0.95	1.17
6U	SV96-23-290	2.0	37.8	39.8	0.4	1.2	58.7	60.3	0.0	1.64	0.67
6U	SV96-23-292	1.5	38.8	40.3	0.0	1.2	58.7	59.9	0.0	1.58	0.67
6U	SV96-23-293	0.3	43.5	43.8	0.0	2.6	53.9	56.5	0.0	1.31	0.78
6U	SV96-28-346	2.6	42.3	44.9	1.0	18.0	36.0	55.0	0.1	1.34	0.85
6U	SV96-28-347	1.3	46.0	47.3	0.3	8.0	44.0	52.3	0.3	1.16	0.92
7A	SV97-01-007	3.0	47.6	50.6	0.0	7.3	42.5	49.8	0.0	1.11	1.02
7A	SV97-01-013	2.3	51.3	53.6	0.3	5.6	40.5	46.4	0.3	0.94	1.17
7A	SV97-01-021	1.3	65.7	67.0	0.0	4.0	29.5	33.5	0.0	0.53	2.00
7A	SV97-05-034	2.0	21.5	23.5	0.0	0.0	76.6	76.6	0.0	3.66	0.31
7A	SV97-05-76	10.5	51.5	62.0	0.0	3.0	35.0	38.0	0.0	0.94	1.63
7A	SV97-05-80	7.2	63.6	70.8	0.0	3.7	25.0	28.7	0.5	0.56	2.47
7A	SV97-05-84	8.2	60.6	68.8	0.0	2.5	28.7	31.2	0.0	0.65	2.21
7A	SV97-05-90	4.0	53.2	57.2	0.0	7.2	35.8	43.0	0.0	0.88	1.33
7A	SV97-05-94	5.2	54.6	59.8	0.0	3.2	37.0	40.2	0.0	0.83	1.49

Seam	Sample No. or Drillhole	Vitrinite (%)			Inertinite (%)				Liptinite (%)	TPI	GI
		Telo.	Detro.	Total	Macrinite	Fusinite	Semifus.	Total			
7A	LC475	-	-	49.8	0.2	16.7	33.3	50.2	0.0	-	-
8M	LC478	-	-	53.0	0.7	20.1	26.2	47.0	0.0	-	-
8U	LC475	-	-	29.6	1.1	16.1	53.2	70.4	0.0	-	-
8U	SV96-08-067	10.2	50.8	61.0	0.0	2.0	37.0	39.0	0.3	0.97	1.56
8U	SV96-08-068	17.2	42.3	59.5	0.0	3.0	37.5	40.5	0.0	1.36	1.47
8U	SV96-08-069	17.4	41.6	59.0	0.0	3.0	34.0	37.0	0.0	1.31	1.59
8U	SV96-08-071	21.9	40.1	62.0	0.0	4.0	34.0	38.0	0.0	1.49	1.63
8U	SV97-08-072	9.5	38.0	47.5	1.0	3.0	48.6	52.6	0.0	1.61	0.94
8U	SV97-03-026	2.3	46.6	48.9	0.6	10.0	40.0	50.6	0.3	1.12	0.99
8U	SV97-03-027	6.6	47.0	53.6	2.0	10.3	34.0	46.3	0.0	1.08	1.26
8U	SV97-03-028	3.6	54.6	58.2	0.0	7.6	33.6	41.2	0.0	0.82	1.41
8U	SV98-01-002	1.6	47.0	48.6	0.6	9.3	41.0	50.9	0.3	1.10	0.98
8U	SV98-01-003	0.6	27.0	27.6	1.6	14.0	56.6	72.2	0.0	2.64	0.41
8U	SV98-01-004	3.0	47.0	50.0	0.3	11.6	38.0	49.9	0.0	1.12	1.01
9	SV96-12-127	15.9	41.0	56.9	0.6	15.9	26.3	42.8	0.3	1.42	1.36
9	LC475	-	-	40.4	0.2	26.4	33.0	59.6	0.0	-	-
9	msan893	-	-	31.6	2.3	8.2	57.7	68.2	0.2	-	-
9	msan894	-	-	47.6	3.9	7.7	40.5	52.1	0.3	-	-
10B	LC476	-	-	35.5	0.4	20.8	43.3	64.5	0.0	-	-
10B	msan89-1	-	-	37.6	1.0	8.9	52.4	62.3	0.1	-	-
10B	msan893	-	-	33.8	2.1	8.1	56.0	66.2	0.0	-	-
10A	LC476	-	-	29.6	0.2	22.2	48.0	70.4	0.0	-	-
10A	SV97-06-040	0.0	78.1	78.1	0.1	2.6	19.3	22.0	0.0	0.28	3.57
10A	SV97-06-046	2.6	51.4	54.0	0.0	10.0	36.0	46.0	0.0	0.95	1.17
10A	SV97-06-052	2.3	33.3	35.6	0.0	14.3	50.1	64.4	0.0	2.00	0.55
10A	SV97-06-058	0.3	26.6	26.9	0.0	13.3	59.7	73.0	0.0	2.76	0.37
10A	SV97-07-064	1.0	47.1	48.1	0.0	14.6	37.0	51.6	0.3	1.12	0.93
10A	SV97-07-068	1.6	44.3	45.9	0.3	4.6	49.3	54.2	0.0	1.25	0.86
10A	SV97-07-072	1.0	51.4	52.4	0.0	6.0	41.7	47.7	0.0	0.95	1.10

Seam	Sample No. or Drillhole	Vitrinite (%)			Inertinite (%)				Liptinite (%)	TPI	GI
		Telo.	Detro.	Total	Macrinite	Fusinite	Semifus.	Total			
M2	SV96-12-117	8.4	46.4	54.8	3.0	6.6	35.4	45.0	0.2	1.09	1.38
M1	SV96-12-118	5.8	46.8	52.6	1.6	9.6	36.5	47.7	0.0	1.11	1.18
-	SV98-01-001	22.0	62.5	84.5	0.0	2.5	13.0	15.5	0.0	0.60	5.45

Appendix C

Adsorption Isotherm Data

Appendix C

ADSORPTION ISOTHERM DATA

SAMPLE	PRESSURE (MPa)	ADSORBED METHANE (cc/g)
SV97-29-346	0.53	4.45
	1.88	10.00
ASH = 43.06%	3.38	13.11
EQM = 3.02%	4.27	14.39
Vm = 24.2 MPa	5.88	16.16
	7.54	17.47
	8.49	18.36
	9.51	19.09
	10.35	19.55
SV97-29-347	0.68	2.20
	1.92	4.83
ASH = 36.84%	3.37	6.54
EQM = 2.5%	4.85	7.80
Vm =13.0 MPa	6.32	8.66
	7.71	9.19
	8.88	9.54
	9.80	9.55
	10.29	9.88
SV97-06-038	0.81	5.81
	1.64	8.65
ASH = 18.05%	2.66	10.79
EQM = 2.02%	4.32	12.95
Vm = 20.6 MPa	5.63	14.15
	7.04	15.20
	8.31	16.05
	9.56	16.65
	10.41	17.09
SV97-06-039	0.70	5.61
	1.79	9.54
ASH = 15.72%	2.95	11.86
EQM = 2.16%	4.42	13.79
Vm = 21.8 MPa	5.96	15.16
	7.38	16.27
	8.61	16.98
	9.50	17.59
	10.42	18.16
SV97-07-074	0.86	7.01
	1.64	9.82
ASH = 44.34%	2.60	12.15
EQM = 2.71%	3.88	14.27
Vm = 25.2 MPa	5.32	16.26
	6.67	17.55
	8.26	18.80
	9.36	19.85
	10.19	20.52

SAMPLE	PRESSURE (MPa)	ADSORBED METHANE (cc/g)
SV97-07-075	0.55	4.93
	1.69	9.63
ASH = 38.66%	2.77	12.00
EQM = 2.08%	4.25	14.00
Vm = 21.1MPa	5.94	15.37
	7.04	16.41
	8.32	16.95
	9.29	17.43
	10.37	17.85
SV97-23-268	0.68	1.45
	1.79	3.19
ASH = 13.84%	2.72	4.17
EQM =8.09%	4.76	5.62
Vm = 11.5 MPa	6.34	6.46
	7.81	7.14
	8.67	7.49
	9.88	7.75
	10.61	7.98
SV96-23-268A	0.55	1.73
	1.65	4.17
ASH = 5.67%	2.64	5.43
EQM = 6.27%	3.99	6.67
Vm = 13.5 MPa	5.70	7.66
	7.21	8.66
	8.58	8.94
	9.31	9.73
	10.24	10.10
SV97-03-026	0.55	1.74
	1.57	3.58
ASH = 35.05%	2.66	4.83
EQM = 2.3%	3.97	5.83
Vm = 17.77 Mpa	5.52	6.66
	6.81	7.29
	8.20	7.82
	9.43	8.33
	10.33	8.59
SV97-03-027	0.46	2.37
	1.45	5.27
ASH = 6.81%	2.64	7.36
EQM = 3.37%	4.01	9.09
Vm = 18.3 MPa	5.31	10.44
	7.06	11.89
	8.41	12.73
	9.49	13.32
	10.42	13.81

SAMPLE	PRESSURE (MPa)	ADSORBED METHANE (cc/g)
SV97-03-028	0.53	2.79
	1.63	5.73
ASH = 5.69%	2.58	7.40
EQM = 4.35%	3.96	9.26
Vm = 18.8 MPa	5.53	10.79
	7.02	12.03
	8.26	12.91
	9.20	13.60
	10.35	14.24
SV98-01-002	0.85	5.31
	2.15	11.03
ASH = 5.1%	3.24	13.62
EQM = 1.17%	4.77	15.95
Vm = 25.7 MPa	6.02	17.31
	7.68	18.55
	9.17	19.22
	9.62	19.55
	10.39	19.94
SV98-01-003	0.79	4.77
	2.09	9.72
ASH = 20.68%	3.39	12.43
EQM = 1.06%	4.83	14.31
Vm = 23.0 MPa	6.32	15.71
	7.91	16.66
	9.25	17.32
	10.21	17.65
	10.66	17.96
SV98-01-004	0.53	3.48
	1.85	10.17
ASH = 7.52%	3.09	13.23
EQM = 1.46%	4.12	15.01
Vm = 27.0 MPa	5.33	16.53
	7.26	18.32
	8.31	19.17
	9.25	19.78
	10.41	20.33
SV98-01-001	0.31	4.52
	1.71	13.90
ASH = 4.32%	3.12	18.21
EQM = 2.16%	4.73	20.99
Vm = 30.3 MPa	6.25	22.88
	7.73	24.17
	8.91	25.06
	9.60	25.59
	10.42	26.00

EQM = Equilibrium Moisture
Vm = Monolayer Volume

Appendix D

Measured Sections

Appendix D – Measured Sections

SECTION 1: NORTH LINE CREEK

Base of unit (m)	Top of unit (m)	Thickness (m)	Lithology	Description
-	0	1+	Coal - 10 Seam	
0	2	2	Siltstone/Sandstone	interbedded siltstone and fine grained sandstone; massive
2	5.4	3.4	Coal/Shale	interbedded coal and black carbonaceous shale
5.4	14.5	9.1	Coal - 9 Seam	
14.5	30.5	16	Siltstone	dark grey; massive with coaly bands
30.5	32	1.5	Coal - 8L Seam	argillaceous coal
32	35.5	3.5	Siltstone	dark grey; massive with coaly bands
35.5	37	1.5	Coal - 8L Seam	
37	44	7	Siltstone	dark grey; massive with coaly bands
44	45.4	1.4	Sandstone	fine grained; dark grey; massive; rare cross bedding and coalspar
45.4	47.9	2.5	Siltstone	dark grey; massive with coaly bands
47.9	50.9	3	Sandstone	fine to very fine grained; dark grey; massive; rare cross bedding and coalspar
50.9	56.4	5.5	Coal - 8L Seam	
56.4	59.4	3	Sandstone	very fine grained; dark grey; cross bedded
59.4	65.6	6.2	Coal - 8U Seam	
65.6	98.6	33	Sandstone	very fine grained; dark grey; cross bedded
98.6	105	6.4	Siltstone/Sandstone	interbedded siltstone and very fine grained sandstone; cross laminated
105	116.6	11.6	Sandstone	fine grained; dark grey; massive; rare cross bedding and coalspar
116.6	117.7	1.1	Coal/Shale	interbedded coal and black carbonaceous shale
117.7	120.2	2.5	Sandstone	medium to fine grained; dark grey; massive; rare cross bedding
120.2	127.5	7.3	Coal/Mudstone	interbedded coal, coaly shale, mudstone and rare fine sandstone; dark grey;
127.5	129.2	1.7	Siltstone/Sandstone	interbedded very fine sandstone and siltstone; dark grey; cross laminated
129.2	135.5	6.3	Coal/Mudstone	interbedded coal, coaly shale, mudstone and siltstone; dark grey;
135.5	137	1.5	Mudstone	dark grey; massive to parallel laminated
137	138.5	1.5	Sandstone	fine to very fine grained; dark grey; massive to cross bedded
138.5	142.7	4.2	Mudstone	dark grey; massive; coarsens up to cross laminated mudstone and siltstone
142.7	145	2.3	Coal/Mudstone	interbedded coal, coaly shale and mudstone; dark grey
145	146.5	1.5	Coal	
146.5	156.5	10	Siltstone	dark grey; cross laminated; coalspar
156.5	157.2	0.7	Coal/Siltstone	interbedded coal and dark grey siltstone
157.2	169.7	12.5	Sandstone	fine to very fine grained; massive to cross bedded; coalspar;

Base of unit (m)	Top of unit (m)	Thickness (m)	Lithology	Description
169.7	171.5	1.8	Siltstone/Sandstone	flaser bedded fine sandstone and siltstone; dark grey
171.5	174	2.5	Carbonaceous Shale	black; massive to wavy laminated
174	175.9	1.9	Coal - 7A Seam	
175.9	179.5	3.6	Siltstone	dark grey; massive
179.5	183.1	3.6	Coal/Siltstone	interbedded coal and sparry siltstone
183.1	185	1.9	Coal - 7B Seam	
185	186.2	1.2	Coal/Siltstone	interbedded coal and sparry siltstone
186.2	187.6	1.4	Coal - 7C Seam	
187.6	188.7	1.1	Carbonaceous Shale	black; massive
188.7	200.2	11.5	Mudstone	dark grey; massive to cross laminated
			Break in Section	
-	210	8+	Mudstone	
210	212.2	2.2	Coal - 6 Seam	
212.2	213.2	1	Carbonaceous Shale	grey-black; massive
213.2	225.9	12.7	Sandstone	fine-medium grained; cross bedded and laminated
225.9	227.9	2	Mudstone	dark grey; massive
227.9	229.5	1.6	Sandstone	fine-medium grained; cross bedded and laminated
229.5	233.5	4	Coal/Mudstone	interbedded coal and dark grey mudstone
233.5	237.2	3.7	Mudstone	dark grey; massive
237.2	238.3	1.1	Sandstone	fine grained; dark grey; cross laminated
238.3	244.4	6.1	Sandstone/Mudstone	interbedded mudstone and fine sandstone; dark grey; cross laminated
244.4	251.4	7	Coal/Siltstone	interbedded coal and dark grey sparry siltstone
251.4	264.3	12.9	Sandstone	fine grained; light grey; cross laminated
264.3	272.1	7.8	Siltstone	dark grey; massive with rare coal and sandstone bands
272.1	273.7	1.6	Coal - 5 Seam	
273.7	278.9	5.2	Siltstone	dark grey; massive with rare coal bands
278.9	294.8	15.9	Sandstone	medium grained; dark grey; massive to cross bedded; coalspar
294.8	296.1	1.3	Siltstone	dark grey; massive
296.1	296.5	0.4	Coal	
296.5	300.2	3.7	Sandstone/Mudstone	interbedded fine sandstone and sparry mudstone; dark grey; cross laminated
300.2	301.2	1	Coal/Mudstone	interbedded coal and grey-black massive mudstone
301.2	306.1	4.9	Sandstone/Mudstone	interbedded very fine sandstone and mudstone; dark grey; cross laminated
306.1	306.5	0.4	Coal	
306.5	309.3	2.8	Mudstone	dark grey; massive
309.3	311.9	2.6	Sandstone	fine grained; dark grey; massive; base is load casted
311.9	312.6	0.7	Coal	
312.6	315	2.4	Mudstone	dark grey; massive
315	317.1	2.1	Sandstone/Mudstone	fine grained sandstone fines up to mudstone; dark grey; cross laminated
317.1	321.1	4	Mudstone	dark grey; massive
321.1	322.8	1.7	Coal/Mudstone	interbedded coal and massive mudstone
322.8	328.8	6	Mudstone	dark grey; massive to cross laminated
328.8	330	1.2	Carbonaceous Shale	black; massive

Base of unit (m)	Top of unit (m)	Thickness (m)	Lithology	Description
330	351	21	Mudstone	dark grey to black; massive; varying carbon content
351	353.8	2.8	Coal	
353.8	356.8	3	Sandstone	fine grained; parallel laminated
356.8	367.1	10.3	Sandstone/Siltstone	cross laminated siltstone and fine sandstone; dark grey
367.1	367.6	0.5	Coal	
367.6	370.6	3	Siltstone	dark grey; massive
370.6	371.5	0.9	Coal	
371.5	373	1.5	Siltstone	dark grey; massive
373	393.3	20.3	Sandstone/Mudstone	interbedded mudstone and fine sandstone; dark grey; cross laminated
393.3	393.8	0.5	Coal/Mudstone	interbedded coal and dark grey massive mudstone
393.8	395	1.2	Siltstone	dark grey; massive
395	442	47	Sandstone	medium grained; salt and pepper; parallel to cross laminated
442	442.5	0.5	Coal	
442.5	-	5+	Sandstone/Mudstone	interbedded mudstone and fine sandstone; dark grey; cross laminated

SECTION 2: MSA WEST

Base of unit (m)	Top of unit (m)	Thickness (m)	Lithology	Description
-	0	2+	10 Seam Coal	Removed during mining
0	2	2	Sandstone	medium-course grained; light grey; massive
2	9	7	Sandstone/siltstone	interbedded very fine light grey sandstone and dark grey siltstone
9	15	6	Sandstone	fine grained; dark grey; ripple cross laminated to cross bedded
15	18.2	3.2	Mudstone	dark grey; parallel to wavy laminated
18.2	21	2.8	Sandstone	fine to very fine grained; moderate grey; ripple cross laminated
21	26	5	Sandstone/siltstone	interbedded very fine light grey sandstone and brown-grey siltstone +-mudstone; coalspar; ripple
26	35.7	9.7	Sandstone	fine to very fine grained; moderate grey; fines upward; ripple cross laminated
35.7	38.4	2.7	Mudstone/Siltstone	interbedded dark grey siltstone and mudstone; ripple cross laminated
38.4	40.1	1.7	Sandstone	fine grained; dark grey; massive to ripple cross laminated
40.1	43.4	3.3	Coal/Shale	interbedded argillaceous coal and black carbonaceous shale
43.4	62.4	19	Sandstone	fine to course grained; salt and pepper; massive to cross bedded; fines upward
62.4	67	4.6	Mudstone	black; massive
67	71.7	4.7	Coal/Shale	interbedded coal and black massive, carbonaceous shale
71.7	80.7	9	Sandstone	medium grained; salt and pepper; cross bedded; coal spar; rip-up clasts at base
80.7	81.3	0.6	Siltstone	dark grey; wavy laminated
81.3	104.6	23.3	Sandstone	fine to medium grained; massive to cross bedded and cross laminated;
104.6	112.4	7.8	Coal/Shale	interbedded coal and black massive, carbonaceous shale
112.4	116.9	4.5	Sandstone	fine to medium grained; massive to cross bedded and cross laminated;
116.9	122.9	6	Coal/Shale	interbedded coal and black massive, carbonaceous shale
122.9	142.4	19.5	Sandstone	fine to medium grained; massive to cross bedded and cross laminated;
142.4	145.7	3.3	Mudstone	dark grey; massive to parallel laminated
145.7	159.2	13.5	Sandstone	fine to medium grained; massive to cross bedded and cross laminated;
159.2	168	8.8	Mudstone	dark grey; massive to parallel laminated
168	171.5	3.5	Siltstone	dark grey; parallel to wavy laminated
171.5	174.5	3	Sandstone	fine to medium grained; massive to cross bedded and cross laminated;
174.5	177.5	3	Mudstone	dark grey; massive to parallel laminated
177.5	182.1	4.6	Coal/Shale	interbedded coal and black massive, carbonaceous shale
182.1	192.3	10.2	Mudstone/Siltstone	interbedded dark grey siltstone and mudstone; ripple cross laminated to massive
192.3	199.8	7.5	Siltstone/Sandstone	interbedded light grey fine sandstone and dark grey siltstone; parallel laminated to massive

Base of unit (m)	Top of unit (m)	Thickness (m)	Lithology	Description
199.8	203.4	3.6	Mudstone	dark grey; massive to parallel laminated
203.4	207.1	3.7	8L Seam Coal	
207.1	209.1	2	Carbonaceous Shale	black; massive
209.1	215.6	6.5	8L Seam Coal	
215.6	217.6	2	Sandstone	fine to very fine grained; moderate grey; ripple cross laminated
217.6	220.8	3.2	8U Seam Coal	
220.8	223+	2.2+	Mudstone	dark grey; massive to parallel laminated

SECTION 3: HORSESHOE RIDGE

Base of unit (m)	Top of unit (m)	Thickness (m)	Lithology	Description
-	0	3+	Sandstone	medium to course grained; light grey; massive to cross bedded and laminated
0	3.2	3.2	Coal - M1 Seam	
3.2	10.7	7.5	Siltstone	dark grey; massive
10.7	20	9.3	Siltstone/Sandstone	interbedded fine sandstone and siltstone; dark grey; massive to flaser bedded and cross laminated;
20	23.3	3.3	Sandstone	fine grained; dark grey; cross laminated
23.3	26.2	2.9	Siltstone/Sandstone	interbedded fine sandstone and siltstone; dark grey; massive to cross laminated; coalspar and coaly bedding planes
26.2	26.7	0.5	Coal - M2 Seam	
26.7	31.9	5.2	Sandstone	medium to fine grained; light grey; cross bedded; coalspar
31.9	36.4	4.5	Siltstone	dark grey; massive; rare coalspar and coaly beds
36.4	52.7	16.3	Sandstone	fine to medium grained; massive to cross bedded; coalspar
52.7	77.7	25	Siltstone	dark grey; massive
77.7	78.6	0.9	Coal - 10A Seam	argillaceous coal grading up-section to coal
78.6	79.1	0.5	Siltstone	dark grey; massive
79.1	82.1	3	Coal - 10B Seam	
82.1	85.9	3.8	Coal/Siltstone	interbedded coaly shale and dark grey siltstone
85.9	88.6	2.7	Coal - 10C Seam	
88.6	110.8	22.2	Siltstone	Grey-brown siltstone with coal bands throughout
110.8	112.2	1.4	Coal/Siltstone	interbedded coaly shale and dark grey siltstone
112.2	120.2	8	Sandstone	fine grained; light grey; parallel bedded; gradational upper contact
120.2	123.7	3.5	Siltstone	dark grey; massive
123.7	128.8	5.1	Sandstone	fine grained; light grey; parallel to cross bedded
128.8	134.8	6	Siltstone	dark grey; massive
134.8	143.1	8.3	Sandstone	fine grained; light grey; cross bedded
143.1	149.1	6	Coal - 9 Seam	
149.1	161.1	12	Sandstone	fine grained; dark grey; cross laminated
161.1	167.1	6	Siltstone/Sandstone	interbedded fine sandstone and siltstone; dark grey; massive to cross laminated
167.1	176.1	9	Sandstone	fine to medium grained; massive to cross bedded; coalspar
176.1	206.1	30	Covered	
206.1	228.6	22.5	Siltstone	dark grey; massive with rare 10 cm bands of cross laminated siltstone
228.6	273.9	45.3	Siltstone/Sandstone	interbedded massive siltstone and ripple cross laminated siltstone and very fine sandstone; dark grey; coaly bands
273.9	275.1	1.2	Coal - 8L Seam	argillaceous coal
275.1	277.1	2	Siltstone	brown grey; massive
277.1	290+	13+	Coal - 8U Seam	
-	-	-	Break in Section	
300	334.4	34.4	Sandstone	medium grained; light grey; massive to cross bedded and laminated

Base of unit (m)	Top of unit (m)	Thickness (m)	Lithology	Description
334.4	337.5	3.1	Siltstone	dark grey; massive with coaly bedding planes
337.5	338.5	1	Sandstone	very fine grained; dark grey; massive
338.5	339.5	1	Coal/Shale	interbedded coal and black carbonaceous shale, plant remains on bedding planes
339.5	341	1.5	Siltstone/Sandstone	interbedded fine sandstone and siltstone; dark grey; cross laminated; bands carbonaceous shale throughout
341	342.7	1.7	Sandstone	fine grained; light grey; massive
342.7	345.9	3.2	Siltstone/Sandstone	interbedded fine sandstone and siltstone; dark grey; cross laminated;
345.9	347.6	1.7	Coal - 7A Seam	
347.6	350.7	3.1	Siltstone/Sandstone	interbedded fine sandstone and siltstone; dark grey; cross laminated;
350.7	352.1	1.4	Coal/Shale	interbedded coal and black carbonaceous shale, plant remains on bedding planes
352.1	360.6	8.5	Siltstone/Sandstone	interbedded fine sandstone and siltstone; dark grey; cross laminated
360.6	363.2	2.6	Coal - 7B Seam	
363.2	-	7.5+	Sandstone	Very fine grained; dark grey; cross bedded to laminated

SECTION 4: NORTH LINE CREEK

Base of unit (m)	Top of unit (m)	Thickness (m)	Lithology	Description
-	0	2+	Sandstone	medium to fine grained; light grey; massive to cross bedded
0	3	3	Coal - 10A Seam	
3	6.3	3.3	Siltstone	dark grey; massive
6.3	13.8	7.5	Sandstone	light grey; massive; coalspar; fines up to siltstone
13.8	18.3	4.5	Coal - 10B Seam	
18.3	20.7	2.4	Coal/Siltstone	interbedded coal and dark grey massive siltstone
20.7	32.7	12	Sandstone	fine grained; dark grey; parallel to cross bedded
32.7	35.4	2.7	Coal/Shale	interbedded coal and grey-black shale
35.4	39.9	4.5	Coal - 9 Seam	
39.9	41.2	1.3	Mudstone	dark grey; massive
41.2	52.2	11	Siltstone/Sandstone	interbedded fine to medium grained sandstone and siltstone; coalspar; parallel bedded
52.2	67.7	15.5	Sandstone	fine to course grained; rip-up clasts; massive to parallel bedded
67.7	68.9	1.2	Siltstone/Sandstone	interbedded fine grained sandstone and siltstone; coalspar massive
68.9	70.6	1.7	Sandstone	fine grained; dark grey; massive; coalspar
70.6	75.8	5.2	Siltstone/Sandstone	interbedded fine grained sandstone and siltstone; coalspar massive
75.8	79.3	3.5	Sandstone	fine grained; dark grey; massive
79.3	82.9	3.6	Siltstone/Sandstone	interbedded fine grained sandstone and siltstone; coalspar massive
82.9	83.5	0.6	Coal/Shale	interbedded coal and grey-black shale
		-	Break in Section	
-	99	14+	Coal - 8U Seam	
99	109	10	Carbonaceous Shale	black; massive; coaly bedding planes
109	131.7	22.7	Mudstone	grey-black; massive to cross laminated; rare siltstone beds
131.7	133.4	1.7	Coal - 8M Seam	
133.4	142.4	9	Siltstone/Sandstone	dark grey; massive to cross laminated
142.4	175.7	33.3	Sandstone	light grey; cross laminated; coaly bands
175.7	193.7	18	Mudstone	grey-black; massive
193.7	203.7	10	Coal - 7A Seam	
203.7	206.4	2.7	Covered	
206.4	218	11.6	Carbonaceous Shale	black; massive; coaly bedding planes
218	219.5	1.5	Coal/Shale	interbedded coal and black carbonaceous shale
219.5	227.9	8.4	Carbonaceous Shale	black; massive; coaly bedding planes
227.9	230.5	2.6	Coal - 7B Seam	
230.5	247	16.5	Mudstone	grey-black; massive to cross laminated
247	247.3	0.3	Coal	
247.3	262.3	15	Mudstone	grey-black; massive to cross laminated
262.3	270.9	8.6	Coal - 6 Seam	
270.9	-	2+	Mudstone	black; massive; coaly bedding planes
			Break in Section	
-	290	2+	Siltstone	dark grey; massive
290	292.8	2.8	Coal/Shale	interbedded coal and black carbonaceous shale

Base of unit (m)	Top of unit (m)	Thickness (m)	Lithology	Description
292.8	297.8	5	Coal -4L Seam	
297.8	299.2	1.4	Coal/Shale	interbedded coal and black carbonaceous shale
299.2	301.3	2.1	Siltstone/Coal	interbedded coal and dark grey cross laminated siltstone
301.3	306.3	5	Coal - 4U Seam	
306.3	316.6	10.3	Siltstone	dark grey; cross laminated; coaly bedding planes
316.6	320.3	3.7	Coal - 3LA Seam	
320.3	324.3	4	Siltstone	dark grey; massive to cross laminated; coalspar
324.3	325.6	1.3	Coal - 3LA Seam	
325.6	334.1	8.5	Siltstone/Coal	interbedded coal and dark grey cross laminated siltstone
334.1	335.3	1.2	Mudstone	grey-black; massive; coalspar
335.3	338.7	3.4	Coal/Shale	interbedded coal and parallel laminated black shale
338.7	346	7.3	Mudstone	dark grey; massive to cross laminated; coalspar
346	349	3+	Coal - 3LB Seam	
349	350.1	1.1	Mudstone	dark grey; cross laminated
350.1	351.5	1.4	Coal/Shale	interbedded black carbonaceous shale and argillaceous coal
351.5	357	5.5	Mudstone	dark grey; massive
357	391.5	34.5	Siltstone/Sandstone	dark grey; cross laminated siltstone and fine sandstone
391.5	393	1.5	Coal/Shale	interbedded black carbonaceous shale and argillaceous coal
393	393.9	0.9	Coal - 3UA Seam	
393.9	395.4	1.5	Coal/Shale	interbedded black carbonaceous shale and argillaceous coal
395.4	396.6	1.2	Coal - 3UB Seam	
396.6	407.6	11	Coal/Shale	interbedded black carbonaceous shale and argillaceous coal
407.6	409.1	1.5	Coal - 2L Seam	
409.1	414.4	5.3	Mudstone	grey-black; massive
414.4	417.4	3	Coal - 2U Seam	
417.4	431.4	14	Coal/Shale	interbedded black shale and argillaceous coal; carbon content of shale increases up-section
431.4	432.2	0.8	Coal	
432.2	433.9	1.7	Sandstone	fine grained; dark grey; cross laminated
433.9	436.3	2.4	Coal/Shale - 1 Seam	
436.3	-	3+	Siltstone	dark grey; massive

SECTION 5: ELKVIEW COAL MINE

Base of unit (m)	Top of unit (m)	Thickness (m)	Lithology	Description
-	20	20+	Sandstone	medium to course grained; salt and pepper; massive
20	22.2	2.2	Coal/Shale - M1 Seam	interbedded coal and carbonaceous shale
22.2	29.7	7.5	Mudstone	grey-black; massive
29.7	31.3	1.6	Coal/Shale - M2 Seam	interbedded coal and carbonaceous shale
31.3	39.5	8.2	Mudstone	grey-black; massive
39.5	42.8	3.3	Sandstone	fine grained; light grey; cross laminated
42.8	44.9	2.1	Carbonaceous Shale	black; massive
44.9	46	1.1	Sandstone	fine grained; light grey; cross laminated
46	49	3	Mudstone	grey-black; massive
49	-	2+	Coal - 10 Seam	
			Break in Section	
-	60	10+	Coal - 10 Seam	
60	68	8	Carbonaceous Shale	black; massive with coalspar and coaly bedding planes
68	80.4	12.4	Siltstone/Mudstone	interbedded massive grey-black mudstone and cross laminated grey-black mudstone and dark grey siltstone
80.4	84.4	4	Covered	
84.4	88	3.6	Conglomerate	pebbles to granules of mudstone, chert and quartz in limited silty matrix
88	88.8	0.8	Siltstone/Mudstone	interbedded dark grey siltstone and mudstone
88.8	94	5.2	Sandstone	course to fine grained; salt and pepper; fines up;
94	94.9	0.9	Siltstone	dark grey; massive
94.9	113.9	19	Sandstone	fine grained; light grey; cross laminated with coalspar
113.9	114.4	0.5	Conglomerate	pebbles to granules of mudstone, chert and quartz in limited silty matrix
114.4	115	0.6	Carbonaceous Shale	black; massive
115	134.5	19.5	Sandstone	fine to medium grained; cross laminated; gradational upper contact
134.5	149.9	15.4	Siltstone/Mudstone	interbedded mudstone and cross laminated mudstone and siltstone; dark grey
149.9	150.4	0.5	Conglomerate	pebbles to granules of mudstone, chert and quartz in limited silty matrix
150.4	159.4	9	Sandstone	medium grained; cross laminated
159.4	163.3	3.9	Sandstone	course grained; chaotically bedded; coalspar
163.3	180.1	16.8	Mudstone	dark grey; massive; rare siltstone beds
180.1	181	0.9	Conglomerate	pebbles to granules of mudstone, chert and quartz in limited silty matrix
181	210	29	Covered	
210	214.3	4.3	Mudstone	dark grey; massive
214.3	222.6	8.3	Siltstone/Sandstone	dark grey siltstone coarsening up to fine sandstone
222.6	224	1.4	Sandstone	medium grained; cross laminated
224	225.8	1.8	Mudstone	dark grey; massive
225.8	227.7	1.9	Sandstone	medium grained; cross laminated

Base of unit (m)	Top of unit (m)	Thickness (m)	Lithology	Description
227.7	229.5	1.8	Mudstone	dark grey; massive
229.5	249	19.5	Sandstone	fine grained coarsening up to medium grained; light grey; cross bedded
249	260.4	11.4	Siltstone	dark grey; massive with rare mudstone beds
260.4	260.8	0.4	Coal	
260.8	262.6	1.8	Carbonaceous Shale	black; massive
262.6	263.7	1.1	Coal	
263.7	264.8	1.1	Sandstone	medium grained; coalspar
264.8	271.9	7.1	Mudstone	dark grey, massive with coaly bedding planes
271.9	278.9	7	Sandstone	fine grained; dark grey; coalspar
278.9	279.1	0.2	Coal	
279.1	289.6	10.5	Mudstone	dark grey; massive
289.6	290.5	0.9	Sandstone	fine grained; dark grey; cross laminated
290.5	292.2	1.7	Carbonaceous Shale	black; massive
292.2	292.7	0.5	Coal	
292.7	311.2	18.5	Carbonaceous Shale	black; coalspar and coaly bands throughout
311.2	311.7	0.5	Coal - 8L Seam	
311.7	314.5	2.8	Carbonaceous Shale	black; coalspar and coaly bands throughout
314.5	317.8	3.3	Coal/Shale	interbedded coal and carbonaceous shale
317.8	318.5	0.7	Coal - 8L Seam	
318.5	319.8	1.3	Coal/Shale	interbedded coal and carbonaceous shale
319.8	325.3	5.5	Coal - 8U Seam	
325.3	328.5	3.2	Carbonaceous Shale	black; coalspar and coaly bands throughout
328.5	329.4	0.9	Coal - 8U Seam	
329.4	341.5	12.1	Carbonaceous Shale	black; coalspar and coaly bands throughout
341.5	343.9	2.4	Coal - 8M Seam	
343.9	345.6	1.7	Carbonaceous Shale	black; coalspar and coaly bands throughout
345.6	346.6	1	Coal - 8M Seam	
346.6	352.6	6	Carbonaceous Shale	
352.6	354.7	2.1	Coal/Shale	interbedded coal and carbonaceous shale
354.7	356.5	1.8	Carbonaceous Shale	black; coalspar and coaly bands throughout
356.5	357.5	1	Coal - 7A Seam	
357.5	378.5	21	Carbonaceous Shale	black; coalspar and coaly bands throughout
378.5	-	5+	Coal - 7B Seam	
			Break in Section	
-	394.5	15.9	Coal - 7B Seam	
394.5	395.8	1.3	Carbonaceous Shale	black; massive
395.8	396.9	1.1	Siltstone	dark grey; massive
396.9	397.2	0.3	Coal	
397.2	399.2	2	Carbonaceous Shale	black; massive
399.2	402.4	3.2	Coal/Shale	interbedded coal and carbonaceous shale
402.4	403.8	1.4	Mudstone	grey-black; massive
403.8	411.7	7.9	Coal/Shale	interbedded coal and carbonaceous shale
411.7	418	6.3	Mudstone	grey-black; massive; carbon content increasing up-section
418	424	6	Coal/Shale	interbedded coal and carbonaceous shale
424	434.9	10.9	Mudstone	grey-black; massive; carbon content increasing up-section
434.9	440.2	5.3	Coal - 6 Seam	
440.2	442.8	2.6	Carbonaceous Shale	black; massive
442.8	446	3.2	Mudstone	grey-black; massive
446	447.8	1.8	Carbonaceous Shale	black; massive

Base of unit (m)	Top of unit (m)	Thickness (m)	Lithology	Description
447.8	453.2	5.4	Mudstone	grey-black; massive; carbon content increasing up-section
453.2	461	7.8	Carbonaceous Shale	black; massive
461	462.5	1.5	Mudstone	grey-black; massive
462.5	484.6	22.1	Coal/Shale - 5 Zone	interbedded coal; coaly shale and carbonaceous shale
484.6	499.2	14.6	Siltstone	dark grey; parallel to cross laminated; gradational upper contact
499.2	505.1	5.9	Mudstone	dark grey; parallel to cross laminated;
505.1	506.3	1.2	Coal - 3 Seam	
506.3	518.3	12	Mudstone	grey-black; massive
518.3	520.5	2.2	Conglomerate	pebbles of mudstone, chert and quartz in course sandstone matrix
520.5	522.2	1.7	Sandstone	fine-medium grained; light grey
522.2	524.4	2.2	Conglomerate/Sandstone	conglomerate fining up to fine sandstone
524.4	526.7	2.3	Conglomerate/Sandstone	conglomerate fining up to fine sandstone
526.7	527.5	0.8	Conglomerate	pebbles of mudstone, chert and quartz in course sandstone matrix
527.5	529	1.5	Siltstone	dark grey; massive
529	529.9	0.9	Sandstone	medium to course grained; salt and pepper; parallel to cross laminated
529.9	559.3	29.4	Covered	
559.3	560.3	1	Carbonaceous Shale	black; massive
560.3	563.6	3.3	Coal - A Seam	
563.6	565.3	1.7	Carbonaceous Shale	black; massive
565.3	580.3	15	Mudstone	interbedded grey-black mudstone and black carbonaceous shale
580.3	583.5	3.2	Coal/Shale	interbedded coal and carbonaceous shale
583.5	-	2+	Mudstone	grey-black; massive

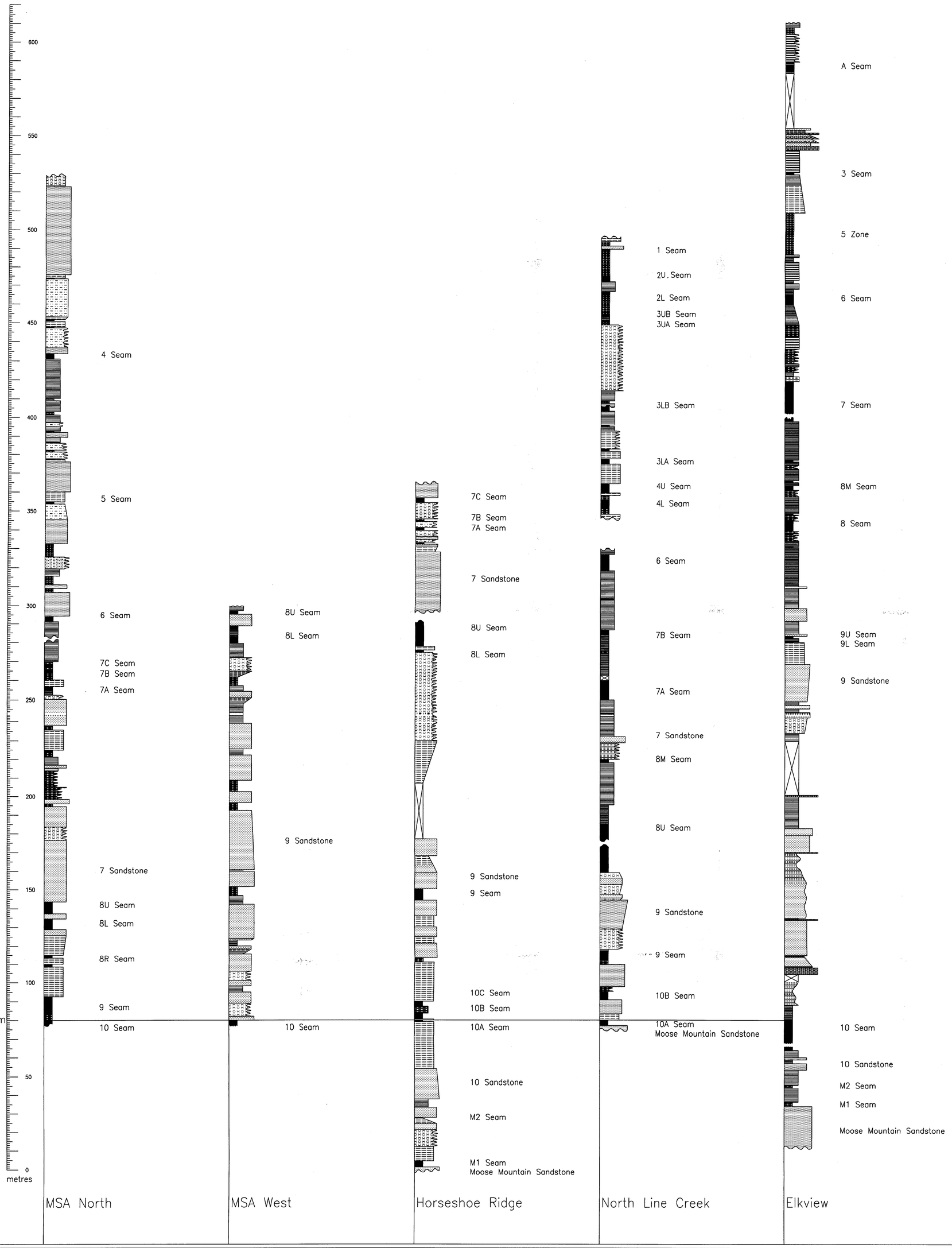

APPENDIX E

Measured Sections from the Line Creek and Elkview Coal Mines.

See Appendix D for Descriptions of Units.